RESEARCH REPORT

StopOx

Utilization Of Industrial Residuals For Prevention Of Sulfide Oxidation In Mine Waste

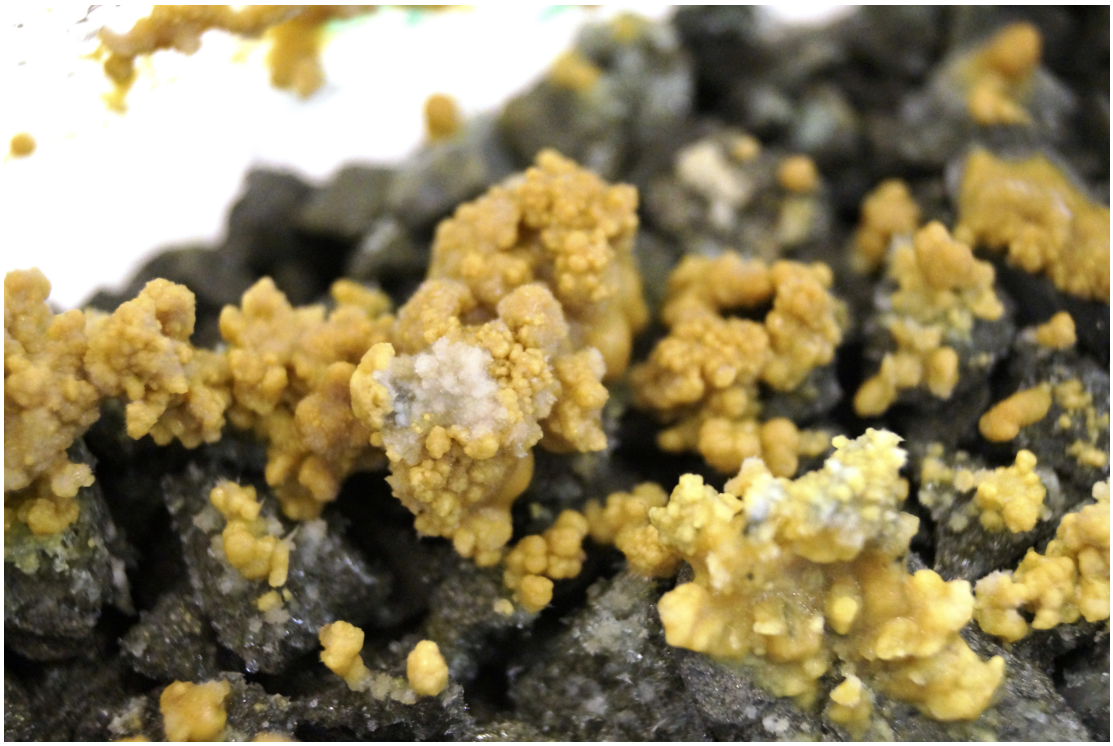

Lena Alakangas
Hanna Kaasalainen
Christian Maurice
Elsa Nyström
Susanne Nigéus

LULEÅ UNIVERSITY OF TECHNOLOGY

LULEÅ
UNIVERSITY
OF TECHNOLOGY

StopOx

Utilization Of Industrial Residuals For Prevention Of Sulfide Oxidation In Mine Waste

Lena Alakangas
Hanna Kaasalainen
Christian Maurice
Elsa Nyström
Susanne Nigéus

Luleå University of Technology
Department of Civil, Environmental and Natural Resources Engineering
Division of Geosciences and Environmental Engineering
Division of Mining and Geotechnical Engineering

Printed by Luleå University of Technology, Graphic Production 2019

Cover picture by Elsa Nyström

ISSN 1402-1528
ISBN 978-91-7790-448-9 (print)
ISBN 978-91-7790-449-6 (pdf)

Luleå 2019

www.ltu.se

PREFACE

This report is the outcome of the SIP STRIM project *StopOx-Utilization of industrial residuals for prevention of sulfide oxidation in mine waste* implemented at Applied geochemistry, Luleå University of Technology running from 2015 to 2018. Boliden Mineral has been partner and co-funder of the project. Other partners in the project were Cementa, Dragon Mining, MEROX, Nordkalk, and SP Processum. The overall aim of the project was to develop prevention technologies to reduce the sulfide oxidation in mine waste, during and after operation, and thereby reduce the generation of acid mine drainage. The StopOx project has been focusing on sulfidic mine waste from the Boliden area which were disposed of and are causing acid mine drainage or have the potential. Industrial residues/products were supplied by BillerudKorsnäs, Cementa, MEROX, and Nordkalk. The report consists of chapters based on three subprojects.

Chapter 1. Introduction

Chapter 2. Inhibition technology with aim to minimize waste rock oxidation during operations by using residues from other industries (passivation of sulfidic surfaces by the formation of secondary minerals)

Chapter 3. The suitability of green liquor dregs as substitutes for or additives to till in a sealing layer as part of a cover system

Chapter 4. Weathering of waste rock under changing chemical conditions

The research described in chapters 2 and 3 was performed by Ph.D. students and will continue until 2021, while the subproject in chapter 2 ended in 2018.

We want to thank all partners that have been involved and engaged in the project

Alakangas, Lena	Coordinator
Kaasalainen, Hanna	Post Doc
Maurice, Christian	Deputy coordinator
Nyström, Elsa	PhD student
Nigéus, Susanne	PhD student

Applied geochemistry at Luleå University of Technology, August 2019, Luleå

TABLE OF CONTENTS

1. INTRODUCTION

The global demand for metals and minerals is growing rapidly, driven by growth industries in Asia and China. Europe has a huge trade deficit in metallic minerals and therefore needs to extract more of its resources to reduce this dependence. Minerals and metals are essential for modern living, and mining is still the primary method of their extraction, but these operations are generally associated with a range of environmental impacts that adversely affect local communities and necessitate costly site remediation efforts. Given the non-renewable nature of mined resources, the sustainability of this industry and the efficient use of its resources for development remain crucial. Mining can be more sustainable by developing practices that minimize the environmental impact of mining operations during the planning of a mine. Future sustainable mining activities will require a holistic approach to the environmental consequences that could emerge during the mine's life, and the application of the best available techniques to prevent or mitigate these consequences. Because all mine sites are unique, knowledge of one site's characteristics and processing, extraction, and remediation measures are crucial, and prevention methods cannot be directly applied to other sites without adaptions. In the long term, more efficient and holistic view of exploration, ore separation and extraction, and waste disposal can dramatically prevent environmental impacts.

The two most common types of mine wastes are tailings and waste rock. Tailings are residues resulting from milling and processing ores into metal concentrates, while waste rock is rock removed to access the ore. Waste rock is generally a very heterogeneous material containing particles ranging from clays to boulder-sized fragments. Waste rock is commonly stored in mined-out voids or in heaps close to the mine workings. Many waste deposits from base metal mines have high content of Fe-sulfides such as pyrite and pyrrhotite that oxidize when exposed to air and water, forming so-called Acid Rock Drainage (ARD), which contains elevated concentrations of undesirable elements.

Sulfide minerals are unstable under oxidizing conditions. Although ARD can form naturally, anthropogenic activities such as mining can accelerate its generation because blasting, crushing, and milling increase the surface area of sulfides exposed to the atmosphere. Pyrite is the most abundant Fe-sulfide, and its oxidation proceeds via the following reactions (Singer and Stumm, 1970):

$$FeS_2 + 7/2\ O_2(aq) + H_2O \leftrightarrow\ Fe^{2+} + 2\ SO_4^{2-} + 2\ H^+ \quad (2.1)$$

$$Fe^{2+} + 1/4\ O_2 + H^+ \leftrightarrow\ \ Fe^{3+} +\ 1/2\ H_2O \quad (2.2)$$

$$Fe^{3+} + 2H_2O\ \leftrightarrow\ Fe(OH)_3 + 4H^+ \quad (2.3)$$

The overall reaction is:

$$FeS_{2(s)} + 15/4\ O_{2(g)} + 7/2\ H_2O_{(l)} \leftrightarrow Fe(OH)_{3(s)} + 2\ SO_{4(aq)}^{2-} + 4\ H^+ \quad (2.4)$$

In reality, pyrite oxidation involves several reactions occurring in separate steps with the movement of a few electrons at a time, and oxygen is not the only oxidant capable of oxidizing pyrite – ferric iron can also act in this way (reaction 2.5) (Nordstrom and Alpers, 1999):

$$FeS_2 + 14\,Fe^{3+} + 8\,H_2O \leftrightarrow 15\,Fe^{2+} + 2\,SO_4^{2-} + 16\,H^+ \qquad (2.5)$$

At low pH (<3.5), the rate of Fe^{3+} hydrolysis is very low, and the presence of Fe-oxidizing bacteria accelerates the oxidation of Fe^{2+}into Fe^{3+} by a factor of 10^6, making Fe^{3+} the most important oxidant under such conditions, which is very important in ARD formation (Singer and Stumm, 1970). Pyrite oxidation releases Fe, $SO_4^{2,}$ and acidity into solution, but also releases other trace elements associated with pyrite and other sulfides. Other gangue minerals, such as silicates, dissolve under the acidic conditions, and thus also contribute to the chemistry of the ARD.

ARD formation may occur over hundreds of years in a waste deposit and is difficult to stop once started (INAP, 2015 and references therein). Mine wastes with high contents of carbonates and small quantities of sulfides such as skarn tailings can also be important sources of hazardous elements in the drainage (Hallstrom et al., 2018).

1.1. Control of sulfide oxidation

Liming of ARD is a way of treating the problem rather than preventing it. A more viable and environmentally sustainable solution would be to stop ARD generation by preventing sulfide oxidation at the source (Johnson and Hallberg, 2005; Evangelou 1995). Several strategies have been developed to prevent sulfide oxidation and subsequent ARD formation. According to Sahoo et al., (2013), these strategies can be divided into five categories: bacterial inhibition, desulfurization, electrochemical cover, and physical and chemical barriers (Figure 1.1).

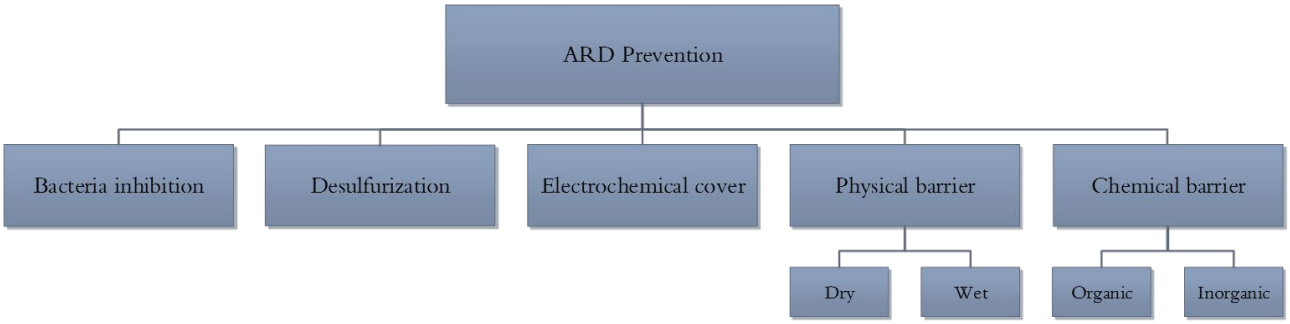

Figure 1.1. Types of strategies for preventing acid rock drainage (ARD). Adapted from the work of Sahoo et al. (2013).

Bacteria inhibition strategies use bactericides to inhibit Fe- and S-oxidizing bacteria by either removing the protective coating that allows them to function in acidic environments or by disrupting their contact with the mineral surface. Since bactericides are harmful to bacteria, they can also harm other living organisms.

Desulfurization strategies involve separating sulfide minerals from gangue minerals. They rely on froth flotation, which is commonly used to separate valuable minerals from tailings. Their success depends partly on how well the sulfide minerals are isolated from the non-sulfidic ones. The advantage of desulfurization is, if successful, it can limit the amount of mine waste needing treatment.

Electrochemical covers introduce an electrical current that polarizes the tailings-electrolyte interface and the overburden, making them into a cathode and an anode, respectively, reducing dissolved oxygen at the tailings surface.

Physical barrier strategies are the approaches most commonly used to control ARD generation in Sweden. A wet or a dry cover encapsulate the mine waste to limit oxygen ingress and thus sulfide oxidation. Dry covers, are commonly constructed of till of varying quality in Sweden.

1.2. Reference

Hallstrom, L., Alakangas, L., Martinsson, O. (2018) Geochemical characterization of W, Cu and F skarn tailings at Yxsjöberg, Sweden. Journal of Geochemical Exploration, 194, 266-279. doi.org/10.1016/j.gexplo.2018.09.001

Singer, P.C., Stumm, W. (1970). Acidic mine drainage: The rate-determining step. Science, 167(3921), 1121-1123.

Nordstrom, D.K., Alpers, C.N. (1999). Negative pH, efflorescent mineralogy, and consequences for environmental restoration at the iron mountain superfund site, California. Proceedings of the National Academy of Sciences of the United States of America, 96(7), 3455-3462. doi:10.1073/pnas.96.7.3455

Johnson, D.B., & Hallberg, K.B. (2005). Acid mine drainage remediation options: A review. Science of the Total Environment, 338(1-2 SPEC. ISS.), 3-14. doi:10.1016/j.scitotenv.2004.09.002

Evangelou, V.P. (1995). Potential microencapsulation of pyrite by artificial inducement of ferric phosphate coatings. Journal of Environmental Quality, 24(3), 535-542.

Sahoo, P.K., Kim, K., Equeenuddin, S.M., Powell, M.A. (2013). Current approaches for mitigating acid mine drainage. Reviews of Environmental Contamination and Toxicology, 226, 1-32. doi:10.1007/978-1-4614-6898-1_1

2. INHIBITION

ELSA NYSTRÖM

2.1. Background

The total annual production of waste rock during non-ferrous mining in Sweden alone amounts to as much as 38 million tons, of which a substantial part is sulfide-bearing (SGU, 2017). This waste rock is commonly stored underground or in heaps close to the mine workings, thus becoming a part of the hydrological system with water being transported to, through, and from the storage (Amos et al., 2015). The waste rock is typically left under ambient conditions until remediation is initiated, which usually occurs during decommissioning of the mine. Consequently, waste rock may be stored for tens of years before any measures are taken to prevent sulfide oxidation. Acid rock drainage (ARD) formation is characterized by low pH and elevated concentrations of metals and metalloids due to sulfide oxidation. It can have severe detrimental effects on the receiving environment and may endanger both water resources and organisms. The application of preventative measures during mining operations could potentially reduce or eliminate the need to treat ARD, which is a costly procedure that requires large volumes of virgin natural resources such as lime and also creates a gypsum and metal-rich sludge that itself requires further treatment.

Several ARD management strategies have been developed. The most common involves active treatment by adding an alkaline substance such as hydrated lime, $Ca(OH)_2$, to neutralize the drainage. The dissolution of hydrated lime liberates hydroxide ions that react with dissolved metal ions in the drainage, leading to their precipitation as metal hydroxides that can subsequently be removed using settling and filtration systems (Brown et al., 2002; Younger et al., 2002). These approaches form sludges that typically have high contents of gypsum and Me-hydroxides requiring further treatment.

Quicklime and hydrated lime are considered to be the most efficient neutralizing substances and are therefore the most widely used for ARD treatment (Johnson and Hallberg 2005; Brown et al., 2002; Younger et al., 2002). The use of industrial residues (such as by-products and wastes) instead of virgin materials is an essential part of the circular economy strategy. Laboratory studies on the substitution of virgin natural resources with industrial residues such as cement kiln dust (Sulaymon et al., 2015; Mackie and Walsh, 2012; Doye and Duchesne, 2003), lime kiln dust (Tolonen et al., 2014), coal fly ash (Jones and Cetin, 2017; Madzivire et al., 2014), blast furnace slag (Golab et al., 2006), and paper mill residues (Alakangas et al., 2013; Pérez-López et al., 2011) have yielded promising results but their sustainability and efficiency will have to be evaluated on larger scales before they can be used in practice.

Chemical barriers

Sulfide passivation or microencapsulation is an alternative inhibition technique (i.e., an alternative to cover systems, desulfurization, bacterial inhibition, etc.) for controlling ARD formation. It involves the formation of a chemically inert coating on the sulfidic surface that protects the sulfidic core from attack by O_2 and Fe^{3+}. Several organic and inorganic additives with the potential to enhance surface coatings have been studied. The most commonly studied additives for this purpose are silica (Fan et al., 2017; Kang et al., 2016; Kollias et al., 2015; Bessho et al., 2011; Evangelou, 1996), phosphate (Kang et al., 2016; Kollias et al., 2015; Evangelou, 1995), and permanganate solutions (Ji et al., 2012; Misra et al., 2006; De Vries, 1996). Passivation is considered to be an inexpensive prevention technique, especially

compared to traditional mine drainage treatments using alkaline additives (Sahoo et al., 2013a). However, most of the materials studied for passivation are either too expensive or potentially harmful to the environment (Sahoo et al., 2013b). Consequently, there is a need to find cost-effective materials capable of passivating sulfide surfaces for extended periods.

During the last decade, alternative materials such as alkaline industrial residues have been studied based on the assumption that passivation can be achieved by maintaining a near-neutral pH in the sulfidic mine waste. This theory is based on the results of Huminicki and Rimstidt (2009), who found that sulfide oxidation at near-neutral pH in the presence of sufficient alkalinity promotes precipitation of secondary minerals such as hydrous ferric oxides (HFO) on the sulfide surface. This precipitate layer grows thicker over time; when sufficiently thick, it protects the underlying sulfide from further oxidation. Unlike other methods, this creates a self-healing system that should be independent of additives in the long term. One of the most extensively studied materials for this purpose is fly ash from coal combustion (Sahoo et al., 2013b; Yeheyis et al., 2009; Pérez-López et al., 2007, 2009). However, most approaches involving this material use a relatively high proportion of alkaline industrial residues compared to mine waste. Consequently, these approaches are most applicable when the alkaline industrial residue is generated near the mine or when the mine can use its own residue. Unfortunately, the scope for applying this design in Sweden is limited by transportation costs, which are the major expense of such treatments. Furthermore, the mining industry's goal is to limit the total amount of wastes to be stored at mine sites. Consequently, alternative passivating materials that are effective when added in small quantities (≤5wt.%) are needed to achieve acceptable cost- and space-efficiency.

2.2. Materials

Sulfidic waste rock

The sulfidic waste rock originated from one of Boliden Mineral AB's currently operating Zn-Cu-Au-Ag mines in northern Sweden. The mine is a volcanic-associated massive sulfide ore belonging to the so-called Skellefte group, a collection of volcanic rocks in the Skellefte field (northern Sweden) deposited at the bottom of the sea approximately 1.89 billion years ago. The host rock is quartz-feldspar porphyritic rhyolite, which also occurs as isolated bodies scattered throughout greater parts of the mining area (Montelius, 2005). Since it opened in 2000, the mine has generated 9.9 million tons of waste rock; it is expected to have generated 10 million tons of waste rock by the end of its life, of which 9.3 million tons is predicted to be potentially acid-producing. At the end of the mine's life, the waste rock will be backfilled into the open pit followed by flooding. The remaining waste rock will be covered with a till and bentonite mixture. It is expected that leachate from the waste rock heap and pit lake will have to be collected and treated for at least 20-30 years before it can be diverted to the recipient (Löfgren and Karlsson, 2018).

For this study, waste rock was chosen selectively based on its sulfur content. Partially oxidized waste rocks of varying sizes (<30cm) were screened using a handheld X-ray Fluorescence (XRF) instrument (Olympus Innov-x systems, USA), and waste rock samples were collected from a pile at the site with high sulfur content. Alakangas et al. (2013) characterized the elemental composition of the waste rock, showing that its average sulfur content is 30%.

Industrial residues

Industrial residue is a collective term for materials whose common denominator is that their production is not the primary objective of the industry within which they are produced. Therefore, industrial residues can range from wastes to commercially established (by)-products.

Each plant generates unique industrial residues due to differences in process layout, raw material, and fuel. All industrial residues are expected to exhibit change over time, particularly in terms of their chemical composition but also in terms of their mineralogy. These changes should be less pronounced in commercially established (by)-products than in wastes.

Residues for testing were chosen based on the results of a preliminary study by Alakangas et al. (2014) that mapped various industrial residues in Sweden in terms of their availability, characteristics, and yearly yield. The industrial residues discussed here are divided into two groups:

Blast furnace slag (BFS) originates from the manufacturing of crude iron in a blast furnace. Iron ore is added to the furnace together with coke as a reducing agent and limestone as a slag former whose purpose is to remove impurities. Residues, mainly coke ash and non-metallic components, are removed from the crude iron by chemically combining them into a liquid slag that can be air-cooled to form a predominantly crystalline material (BFS) or water-granulated, resulting in an amorphous sand-like material (0-4mm) known as Granulated Blast Furnace Slag (GBFS). The air-cooled BFS may need further crushing to achieve the desired particle size; the BFS used in this work had been crushed to a particle size of 0-4mm. Both BFS and GBFS are known to have excellent geotechnical properties such as low density and cementing properties. Consequently, BFS is often used in road construction while ground GBFS is mostly used as a supplementary cementing material that is blended with cement for the production of concrete. MEROX AB supplied the BFS and GBFS used in this work, both of which are commercially established (by)-products, REACH registered, and CE-classified as ballast.

Cement Kiln Dust (CKD) originates from cement manufacturing, in which $CaCO_3$ and Si-, Al- and Fe oxides are added to a rotary kiln and heated to a temperature of 1450℃ to form alite, the main mineral in Portland cement (Hökfors, 2014). Cement kiln dust is primarily used as a component in cement. The CKD used in this work was distributed by Cementa AB.

Bark Ash (BA) originates from the manufacturing of wood pulp, a principal component of paper. Wood is washed and debarked before being chopped into wood chips and digested in the Kraft process. The bark is combusted for energy, leaving a residue in the form of fly ash, which is typically landfilled. The BA used in this work was fresh dry material supplied by BillerudKorsnäs.

Lime Kiln Dust (LKD) originates from the manufacturing of quicklime (CaO), in which limestone is added to a rotary kiln and heated to 1200-1300 ℃. Some quicklime manufacturers make briquettes out of the LKD while others deposit it in piles/silos on site. Sometimes the LKD is mixed with varying amounts of crushed limestone to produce niche products. Nordkalk distributed the LKD used in this work, which was a mixture of partially calcined material and finely crushed limestone (too fine for the kiln). The LKD had been stored in piles outdoors.

2.3. Methods

Geochemical characterization of materials

Mineralogy

Multiple methods were used for mineralogical characterization of the waste rock and industrial residues.

The waste rock's mineralogy was determined by:

- Optical examination of polished thin sections in reflected and transmitted light using a conventional petrographic microscope (Nikon Eclipse E600POL) to gather basic information on the waste rock prior to automated quantitative mineralogical characterization using a QEMSCAN® 650 instrument with two Bruker EDX detectors. The step size was set to 6 μm as a compromise between the number of analysis points and the time required for analysis (approximately 7 h/thin section). Four thin sections were analyzed, with each thin section representing at least seven waste rock samples.

The mineralogy of the industrial residues was determined by:

- X-ray powder diffraction (XRPD), recorded using a PANalytical Empyrean diffractometer operating in the Bragg-Brentano geometry with CuKα radiation (λ=1.5406Å). The samples were scanned over a 2θ range of 5-90° with a step size of 0.0130° and a scan time of 47 min.
- Thermogravimetric measurements using a NETZSCH STA 409 C/CD with heating up to 1000°C in inert Ar gas for quantitative mineralogical characterization of the LKD. The quicklime content was estimated using the "sugar rapid method" specified in ASTM C25-11.

Chemical composition

The total chemical composition of the waste rock was determined by several laboratories:

- One sample was screened for over 70 elements using Inductively Coupled Plasma Mass Spectroscopy (ICP-MS) by the SWEDAC-accredited ALS Scandinavia laboratory in Luleå, Sweden. Total element concentrations were analyzed after lithium borate fusion and three acid digestions (nitric acid, hydrochloric acid, and hydrofluoric acid).
- ALS Brisbane (Australia) analyzed three waste rock samples, two of which were analyzed with XRF after lithium borate fusion containing 20% sodium nitrate as an oxidizing agent. One sample was analyzed by Inductively Coupled Plasma Atomic Emission Spectroscopy (ICP-AES) after being fused with sodium peroxide and dissolved in diluted hydrochloric acid.
- ALS Loughrea (Ireland) analyzed one waste rock sample using ICP-MS or ICP-AES. Total element concentrations were analyzed after lithium borate fusion and two acid digestions (nitric acid and hydrochloric acid).
- Sulfidic sulfur was determined on three samples using a 25% HCl leach followed by a leco furnace melt. ALS Vancouver (Canada) analyzed the samples by inductively coupled plasma optical emission spectroscopy (ICP-OES).

The total chemical composition of the industrial residues was also characterized, and the results were compared to those reported by the suppliers.

Two samples of each industrial residue were screened for over 70 elements using ICP-MS by the SWEDAC-accredited ALS Scandinavia laboratory in Luleå, Sweden. Total element concentrations were analyzed after lithium borate fusion and three acid digestions (nitric acid, hydrochloric acid, and hydrofluoric acid).

Readily soluble elements in the industrial residues

The industrial residues were batch tested using a modification of the SIS protocol (2003) for determination of readily soluble elements. The batch test was extended to 72 h (3 days, L/S 12) and 600 h (25 days, L/S 14) rather than conducting a two-stage batch test (L/S 2 and 10). After 24 h rotation on an end-over-end rotating device, the samples were decanted, and 20% of their volume was replaced with MilliQ water. The procedure was repeated at 72 h (L/S 12) and 600 h (L/S 14). The procedure is described in more detail by Nyström et al. (2019) and in section 2.3 of this report. The chemical composition of the leachates was analyzed as described below under the heading "Analysis of dissolved elements in leachates".

Leaching of waste rock covered with industrial residues

Kinetic testing was conducted in high-density polyethylene small-scale test cells with a surface area of 513 cm^2 (total volume of 10 L) lined with geotextile at the bottom to avoid clogging the tap system at the bottom front of the cell (Figure 2.1). Four cells were set up with 5-30 mm and 30-60 mm size fractions (Table 2.1).

The waste rock was irrigated with 600 ml of MilliQ water on a weekly basis, corresponding to the average annual precipitation in the mine area. Waste rock from all eight test cells was leached for 4-8 weeks before adding industrial residues on top of the waste rock. The smallest waste rock fraction (5-30 mm) was re-sieved after three weeks of leaching due to clogging in the system. Various quantities of industrial residues were added on top of the waste rock (Table 2.1). A geotextile liner was placed between the larger waste rock (30-60 mm) and industrial residue to avoid downward movement of the industrial residue. Leachates from the test cells were collected every week. All water samples were measured for pH and electrical conductivity (EC) in closed containers to avoid exposure to air using a WTW Multi 3420 multimeter equipped with either Sentix® 940 (pH) or TetraCon® 925 (EC) electrodes. Water samples were filtered (using a 0.22 µm nitrocellulose membrane

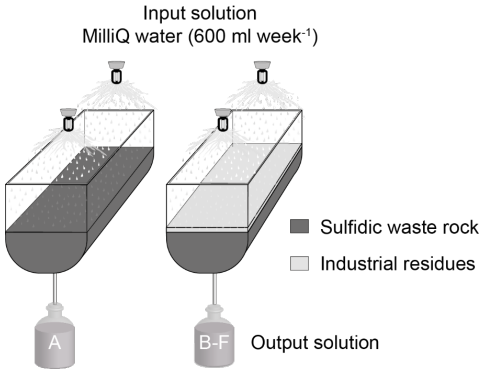

Figure 2.1 Experimental design of small-scale test cells filled with A: sulfidic waste rock, B: sulfidic waste rock with 1-5wt.% industrial residue.

filter) into high-density polyethylene bottles using vacuum filtration. Samples were acidified with 1 ml nitric acid (suprapur) per 100 ml sample and stored cold (4 °C) in darkness until analysis.

Table 2.1 Differences in leaching conditions in the eight small-scale test cells with varying additions of lime kiln dust (LKD), blast furnace slag (BFS), granulated blast furnace slag (GBFS), cement kiln dust (CKD), and bark ash (BA).

Cell	Waste rock		Addition	LKD	BFS	GBFS	CKD	BA
	5-30 mm	30-60 mm	week	wt.%	wt.%	wt.%	wt.%	wt.%
A	7.75 kg		8	No addition of industrial residues				
B	7.75 kg		8	5				
C	7.75 kg		8		4		1	
D	7.75 kg		8			4	1	
E		11 kg	4			5		
F		11 kg	6					1
G		11 kg	Only background leaching measured					
H		11 kg						

Analysis of dissolved elements in leachates

Selected samples were analyzed for major and trace element composition using ICP-AES and Inductively Coupled Plasma Sector Field Mass Spectrometry (ICP-SFMS) at the SVEDAC-accredited laboratory ALS Scandinavia in Luleå. The analysis was either performed according to US EPA Methods 200.7 (modified) and 200.8 (modified) or by quantitative screening analysis for over 70 elements. Analysis of Cl was performed by GBA (Germany) using ion chromatography.

Solid phases

Solid waste rock samples were collected prior to leaching (initially) and from cells A and B (Table 2.1) on separate occasions after 1 and 2 years (weeks 52 and 103). The samples were taken approximately halfway down the waste rock profile and were oven-dried at <40°C for five hours before subjected to small amounts of high pressured air to remove excess material. Sequential extraction was performed by SGS Canada Inc. Mineral Services using the protocol of Dold (2003) to evaluate the element distribution in the different phases as leaching proceeded.

2.4. Results

Waste rock characteristics

Quantitative mineralogical studies of the waste rock showed that it mainly consisted of sulfides with an average pyrite content of 66% (Table 2.2). Other sulfide minerals such as arsenopyrite, chalcopyrite, and sphalerite were also found but at much lower concentrations. The complex sulfide (sulfosalt) bournonite was found in the waste rock, and the presence of other complex sulfides such as tetrahedrite, gudmundite, pyrargyrite, and various Pb-Sb-sulfosalts has been suggested (Nyström, 2018).

Table 2.2 Quantitative mineralogical composition of waste rock and lime kiln dust (LKD) as determined by QEMSCAN and thermogravimetry, respectively. The mineralogical composition of cement kiln dust (CKD) and bark ash (BA) was determined by X-Ray powder diffraction (XRPD). A similar method was used for the blast furnace slag (BFS) and granulated blast furnace slag (GBFS), but these results were supplied by MEROX (2015).

Waste rock	%	**LKD**	%	**BFS**	**GBFS**	**CKD**	**BA**
Calcite	1	Anhydrite		[1]Monticellite	[1]Glass	Akermanite	Anhydrite
Chlorite	4	Calcite	73	[1]Akermanite	[1]Hercynite	Alite	Anorthite
Dravite	0.4	Gypsum	2			Anhydrite	Arcanite
Kaolinite	0.3	Mg-rich calcite	7			Anorthite	Calcite
Muscovite	6	Quicklime	1			Arcanite	Ettringite
Pyrite	66	Slaked lime	2			Calcite	Gehlenite
Quartz	20	Sylvine				Gehlenite	Halite
						Gypsum	Quartz
						Larnite	Quicklime
						Quartz	Slaked lime
						Quicklime	Sylvine
						Slaked lime	
						Sylvine	

[1]unpublished results, MEROX (2015)

The waste rock had a low content of carbonate minerals (1% calcite) and other buffering minerals, suggesting a limited neutralizing capacity. Indeed, static tests such as acid-base accounting indicated that the waste rock would require an almost 1:1 calcite addition to neutralize its total acid production. Although the waste rock was rich in S (because of its pyrite content), its contents of elements other than Fe and Si were relatively low (Table 2.3). Overall, the composition of the waste rock suggests that it has the potential to generate highly acidic leachate with elevated concentrations of Fe and S but comparatively low concentrations of trace elements due to their limited abundance in the waste rock.

Table 2.3 Abundance of selected elements in lime kiln dust (LKD), blast furnace slag (BFS), granulated blast furnace slag (GBFS), cement kiln dust (CKD), bark ash (BA) and waste rock. Waste rock data obtained from Alakangas et al. (2013). Elements in the industrial residues are classified according to their enrichment relative to the waste rock and whether they exceed recommended levels for the use of waste materials in landfill constructions above a sealing layer (SEPA, 2010). SEPA classifications of solids are based on the levels of As, Cr, Cu, Hg, Ni, Pb and Zn. **Bold** typeface indicates values that are >3 times the average level of the corresponding element in the Earth's crust (Krauskopf and Bird, 1995).

Element	LKD	BFS	GBFS	CKD	BA	Waste rock[a]
			%			
Al	0.3	7	7	2	4	3
Ca	46	28	25	38	15	0.9
Cl	<0.1	<0.1	<0.1	5	0.4	0.009
Fe	0.4	1	1	2	3	12
K	0.02	0.5	0.6	7	4	0.5
Mg	0.7	10	11	1	2	0.6
Mn	0.02	0.3	0.5	0.05	0.8	0.02
Na	0.02	0.5	0.5	0.5	2	0.3
P	0.003	0.004	0.002	0.02	1	0.01
S	0.4	1	2	4	1	**31**
Si	0.7	15	16	7	21	13
Ti	0.02	2	2	0.2	0.2	0.1
			mg/kg			
As	0.8	0.3	0.7	9	3	**191**
Ba	22	495	524	179	1398	91
Cd	0.1	0.01	0.01	46	7	0.1
Co	0.9	0.7	0.9	6	10	2
Cr	7	43	74	41	176	57
Cu	2	7	12	54	80	15
F	70	675	440	730	285	1320
Hg	0.1	0.1	0.1	0.1	0.2	**12**
Ni	3	4	5.3	16	75	1
Pb	3	0.2	0.8	861	51	20
Sb	0.1	0.1	0.2	5	1.6	**21**
Sc	0.8	30	32	4	4	6
Sr	168	496	425	249	583	42
U	1	13	14	2	1	2
V	31	654	560	71	46	8
Y	5	56	59	14	7	11
Zn	25	16	13	568	1257	75
Zr	9	280	294	65	38	67

[a]Alakangas et al. (2013)

> 1 times	Increased concentration compared to waste rock.
> 20 times	Enriched when 5 wt.% is added to waste rock.
> 25 times	Enriched when 4 wt.% is added to waste rock.
> 100 times	Enriched when 1 wt.% is added to waste rock.

Exceed levels for landfill above a sealing layer (SEPA, 2010)

Quality of the acid rock drainage

Leaching of the waste rock in small-scale laboratory test cells showed that the leachate was initially dominated by high concentrations of Al, Ca, Fe, Mg, and S, in keeping with the results obtained for the water-soluble phase during the sequential extraction (Figure 2.2). Elevated element concentrations due to the dissolution of soluble salts during the early stages of leaching are often called the "initial flush" by analogy to the effects of heavy rain after a period of drought (Nordstrom, 2009). The dissolution of soluble salts increased the leachate's content of acid solutes (Maest and Nordstrom, 2017); when the waste rock was re-sieved after three weeks of leaching, the leachate's pH started to increase, presumably because of the removal of water-soluble phases and acid solutes. It took approximately 29 weeks of leaching before the leachate started showing signs of accelerated sulfide oxidation in the waste rock, which is a long time given the waste rock's high sulfide content. Once sulfide oxidation was established, the leachate was characterized by a low pH (around 1.5), high EC, and elevated concentrations of metals and metalloids. Despite the waste rock's low overall content of trace elements, the leachate exhibited high concentrations of elements such as As, Cu, Mn, Pb, Sb and Zn, and surprisingly high leachability, with up to 80% elemental depletion after only three years of leaching. This high leachability was due to a combination of low pH, high ferric iron concentrations, and high exposure of the sulfide surfaces. This suggests that forced oxidation to extract valuable minerals and metalloids may be preferable to treating the waste rock and trying to prevent sulfide oxidation.

Characteristics of the industrial residues

As described in section 3.1, the treatment strategy for the waste rock involves covering some of it with a till and bentonite mixture to prevent oxidation. That means that during the mine's operation, the waste rock will be left under ambient conditions, allowing sulfide oxidation to accelerate. This can have negative long-term environmental effects.

An alternative method is to treat the waste rock with industrial residues to reduce sulfide oxidation and subsequent ARD generation. The waste rock's mineralogy, chemistry and leaching behavior (see section 5.1) suggest that any industrial residue used to prevent sulfide oxidation acceleration and achieve long-term passivation of the sulfide surface will have to satisfy a number of challenging criteria. A geochemical investigation of selected industrial residues was therefore performed to identify promising candidates.

The two slags (BFS and GBFS) used in the study had similar chemical compositions because they originate from the same liquid slag. Both slags mainly consist of silicates but are cooled in different ways and thus have differing degrees of crystallization, with GBFS having a large amorphous (glass) fraction (Table 2.2). Batch testing of the two slags showed that they can both generate alkaline conditions but that their content of highly water-soluble minerals is low, suggesting that their solubility is limited (Table 2.4). In extended batch tests, the pH of solutions exposed to GBFS increased with the volume of water used in the test (Figure 2.3). This is probably because the dissolution of GBFS increases with increasing pH (Hooton, 2000), whereas that of BFS decreases (Engström et al., 2013). The results imply that the two slags, despite their limited dissolution, could be effective at preventing ARD generation. However, their divergent behaviors suggest that the chemical conditions can

profoundly impact their dissolution rates, which must be accounted for when selecting neutralization materials.

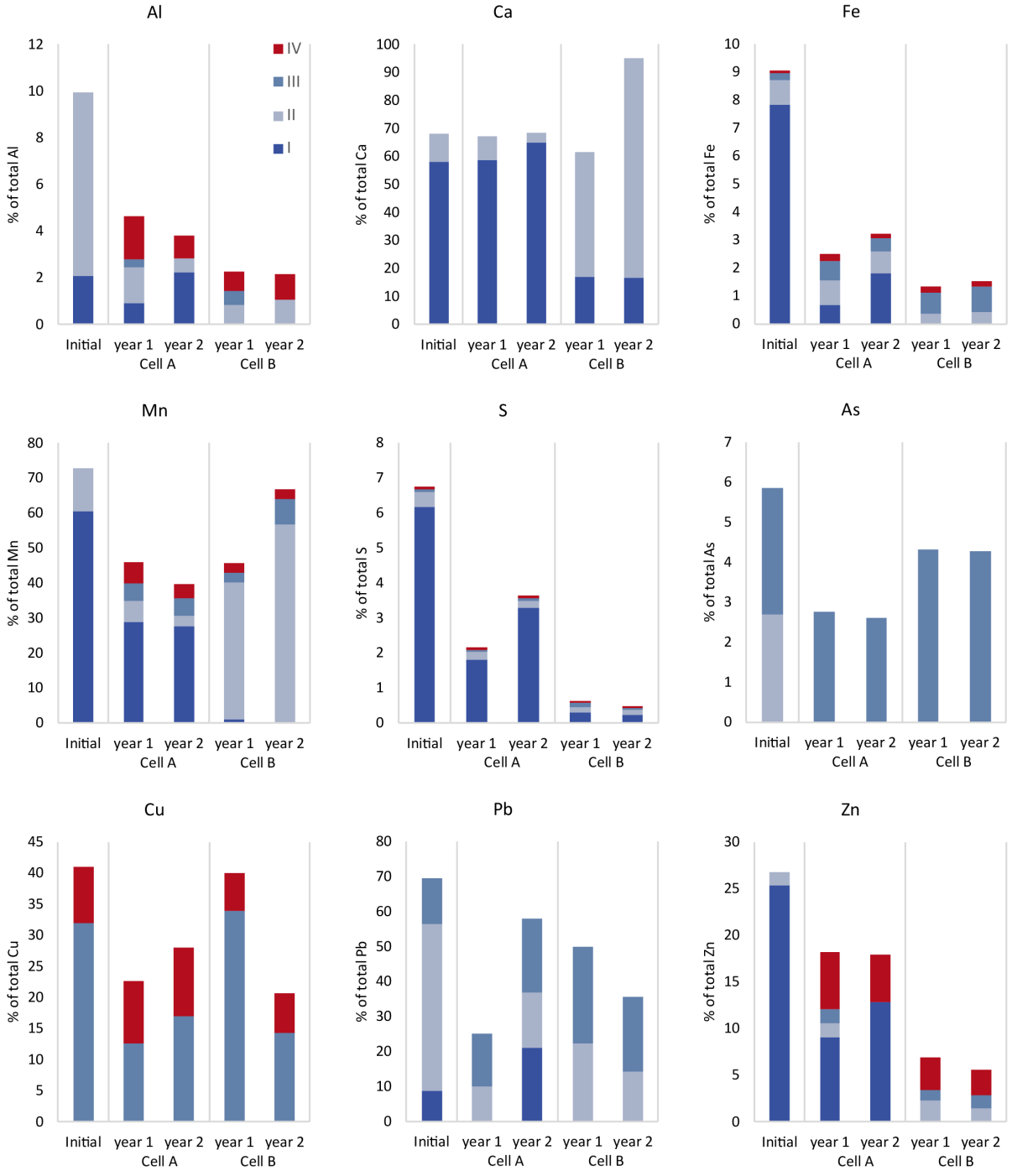

Figure 2.2 Concentrations of extracted elements in the leachate, expressed as percentages of the contents in the starting waste rock, during the initial flush ("initial") and in cells A (waste rock) and B (waste rock with 5wt.% lime kiln dust) after 1 and 2 years (in weeks 52 and 103 of the experiment). Detectable concentrations are shown for each of the sequential extraction steps I-IV as described by Dold (2003): the water-soluble fraction (I), exchangeable fraction (II), Fe(III) oxy-hydroxide fraction (III), and Fe(III) oxide fraction (IV). Concentrations below the detection limit are not shown.

Like the slags, both the BA and CKD contained silicates whereas the LKD consisted mainly of carbonates. The BA, CKD, and LKD all included various amounts of easily soluble minerals such as quicklime and slaked lime. The BA and CKD also contained various salts such as anhydrite, arcanite, and sylvine (Table 2.2), whereas the LKD only contained sylvine. Minerals such as quicklime and slaked lime are more reactive than natural silicates, which is consistent with the batch testing results: upon mixing with water, BA, CKD, and LKD generated higher pH values than the slags. The BA and CKD generated slightly higher pH values and much higher EC values than the LKD, suggesting a greater content of easily water-soluble minerals; this may be due to salt dissolution (Duchesne and Reardon, 1998). Whereas the CKD had the highest concentrations of easily soluble elements such as Cl, Na, and K, the LKD exhibited no substantial dissolution of the only salt identified in the material, namely sylvine, which also explains the low EC observed with LKD. The short- and long-term release of neutralizing minerals from the BA, CKD, and LKD suggests that they could be more effective at preventing ARD generation than the slags. If the quicklime content of the ash is high, its dissolution could be slowed down by hardening the material (Bulusu et al., 2007). However, it should be noted that the dissolution of salts can generate an "initial flush" similar to that seen for the waste rock but with a relatively high content of other elements such as Cl that can form complexes with metal ions, making them difficult to remove from the drainage and also potentially posing a risk to the receiving environment.

Table 2.4 Concentrations of selected elements in leachates from batch testing (L/S 10) of the industrial residues (SIS, 2003). The element concentrations are classified according to whether they exceed recommended levels for the use of waste materials in landfill construction above a sealing layer (SEPA, 2010). The classification of the soluble fraction is based on the elements As, Cl, Cr, Cu, Hg, Ni, Pb, S, and Zn.

	BFS		**GBFS**		**CKD**		**BA**		**LKD**	
	pH	EC mS/cm	pH	EC mS/cm	pH	EC mS/cm	pH	EC mS/cm	pH	EC mS/cm
24 h	11.5	0.896	9.88	0.125	12.9	31.2	12.9	27.9	12	12
72 h	11.4	0.87	10.3	0.13	12.8	27.5	12.9	25.7	11.9	11.9
600 h	11.6	1.36	11.7	1.09	12.7	25.5	12.8	24	11.9	11.9
					mg/L					
Al	4		0.1		0.04		0.04		4	
Ca	110		9		1562		299		338	
Cl	0.1		0.1		8737		728		0.5	
Fe	<0.002		<0.002		0.004		0.01		<0.002	
K	16		2		5738		3354		5.4	
Mg	0.1		3		0.1		<0.01		0.02	
Mn	0.002		0.001		0.0002		0.001		0.0005	
Na	4		0.002		377		465		0.3	
P	0.01		0.004		0.1		<0.005		0.01	
S	271		5		891.6		26		2	
Si	3		7		1		0.4		1	
Ti	<0.002		<0.002		0.002		<0.002		<0.02	
					µg/L					
As	<0.05		0.1		0.1		0.07		0.08	
Ba	355		2		585		2250		34	
Cd	<0.025		<0.025		0.5		0.3		<0.025	
Co	<0.05		<0.05		0.1		<0.05		<0.05	
Cr	1		<0.5		145		477		6	
Cu	<0.5		<0.2		2		2		<0.5	
F	229		233		2600		<200		<200	
Hg	<0.05		<0.05		0.8		0.1		<0.05	
Ni	<0.5		<0.5		<0.5		<0.5		<0.5	
Pb	<0.05		<0.05		986		102		0.1	
Sb	<0.05		<0.05		0.5		0.1		0.08	
Sc	<0.02		<0.02		0.3		<0.02		0.03	
Sr	275		24		7535		5904		438	
U	<0.01		0.01		0.1		0.01		0.01	
V	156		25		1		<0.5		2	
Y	<0.02		<0.02		<0.05		0.03		<0.02	
Zn	<2		<2		10		897		<2	
Zr	<0.05		<0.05		<0.05		0.1		<0.05	

Exceed recommended values for landfill above a sealing layer (SEPA, 2010)

Quality of the leachates from industrial residues

Like waste rock, industrial residues can contain a wide variety of elements that can be released from the material. The release of elements during the leaching of the waste rock is discussed in section 5.1 above. The most suitable way of assessing the potential release of specific elements from industrial residues would be to compare it to the release from the waste rock. A comparison of the chemical compositions of the industrial residues and the waste rock (Table 2.3) revealed that adding small amounts (<5wt.%) of any residue to the rock would increase the amount of potentially harmful elements and that all of the industrial residues were enriched in trace elements. Both BFS and GBFS were highly enriched in V, the CKD was enriched in Cd, Cl, and Pb, and the BA was enriched in Cd, Cl, and Ni.

Because the industrial residues range from wastes to commercially established (by)-products, it is difficult to compare their properties to environmental quality standards (or similar criteria), and such comparisons may be inappropriate without considering the receiving environment. The elemental contents of the solid phase residues (Table 2.3) and the leachates from the batch tests (Table 2.4) were compared to values recommended for waste materials to be placed above a sealing layer in landfill sites (SEPA, 2010).

Based on the SEPA's recommended values (2010) and the solid phase measurements (Table 2.3), the trace element concentrations of the LKD were acceptable but those in the CKD and BA exceeded the recommended limits. The SEPA recommendations only apply to As, Cr, Cu, Hg, Ni, Pb, and Zn. However, exceeding the recommended levels for some elements does not necessarily preclude the use of a material. Instead, a "case-by-case" suitability assessment must be performed.

A comparison of the measured elemental composition of the leachates (L/S 10) and the SEPA recommendations for the soluble fraction (SEPA, 2010) revealed that GBFS was the additive material whose leachate had the lowest trace element concentrations, although they were not consistently lower than those for LKD. The concentrations of Cr and Pb in the CKD and BA leachates exceeded the recommended levels (Table 2.4), as did the concentrations of Cl and S in the CKD leachate and Zn in the BA leachate. It should be noted that the S concentration of the BFS leachate was slightly below the range recommended by the SEPA (2010). The enrichment and leachability of Pb in the CKD, and those of Cr and Zn in the BA, indicate that these materials contain elements of potential concern that may restrict their use. The potential harm resulting from the addition of an industrial residue must be evaluated with respect to the environment in which it is to be used and the properties of the waste rock.

Storage of industrial residues

Because of the calcination process by which it is formed, LKD typically has a high content of quicklime (Bulusu et al., 2007; Miller and Callaghan, 2004). However, the LKD used in this work contained only small amounts of quicklime – less than $1/10^{th}$ of the value reported by the supplier. Conversely, the material was rich in calcite (Table 2.2), suggesting that its composition changed during storage in piles under ambient conditions. This may be because hydration and re-carbonation during storage depleted the levels of water-soluble minerals (i.e., quicklime and slaked lime) in the LKD. Storage may also have depleted the salt content of the LKD, explaining why it contained only a small amount of sylvine.

Compared to the other industrial residues, the LKD exhibited considerable variation in chemical composition and leachate composition between samples, suggesting that it may be more heterogeneous than the other studied residues. This may be because storage did not affect the bulk material in the same way and to the same extent between samples. Based on these observations, we cannot exclude the possibility that storing residues such as BA, CKD, and LKD before applying them to waste rock could have positive effects on their geochemistry as long as reactive minerals such as quicklime are not depleted (which would substantially reduce their short-term neutralizing capacity). The use of industrial residues to treat mine waste would inevitably necessitate the storage of large quantities of material, possibly leading to changes in the material's physicochemical properties during storage.

The ability of industrial residues to prevent acid rock drainage generation

Geochemical tests alone cannot determine an industrial residue's suitability for preventing ARD formation. Although batch tests can provide valuable information about a residue's content of easily water-soluble phases, they cannot be used to assess the long-term dissolution rate of minerals under ambient conditions. Kinetic leaching experiments conducted under ambient conditions are therefore needed to fully assess a material's potential to prevent ARD generation.

The quantity of industrial residue used in the leaching experiments was limited to a maximum of 5 wt.% because of the need to minimize costs and difficulties associated with residue transportation, as discussed by Alakangas et al. (2014). Active treatment of ARD generated from the waste rock would require an almost 1:1 ratio of carbonate material to waste rock. For comparative purposes, the addition of 5wt.% of an industrial residue such as LKD would provide approximately 4% of the total neutralizing potential needed for active treatment (assuming complete oxidation of all the pyrite in the waste rock).

Leaching experiments using waste rock samples with small amounts of industrial residues added on top showed that all of the residues could raise the pH of the leachate (Figure 2.3). However, not all of the residues were capable of maintaining a circumneutral leachate pH throughout the leaching period.

Mixtures of (granulated) blast furnace slag and cement kiln dust

CKD (1wt.%) was added to BFS (4wt.%) and GBFS (4wt.%), respectively, under the assumption that the quicklime in the CKD would hydrate the slags and enable stabilization/solidification of the waste rock as described by Tariq and Yanful (2013). These residues (especially the CKD) contain minerals with cementing properties. To avoid cementation of the materials, the quantity of added CKD was lower than that used by Chaunsali and Peethamparan (2013) and the GBFS was not ground.

Both mixtures initially increased the leachate pH to circumneutral levels, but none of them maintained these conditions for an extended period. Shortly after the addition of the industrial residue to the waste rock, these mixtures showed signs of hardening; this was probably due to the CKD because the cementation rates of slag are generally low (Tariq and Yanful, 2013). Moreover, Merox (2015) reported that the cementation of BFS only occurs when its content of fine particles is high, and the GBS was not ground, which would have limited its hydration. The hardening is assumed to be the reason why these mixtures failed to maintain a circumneutral pH. Because of this failure, experiments using these test-cells were terminated after 22 weeks of leaching. However, it should be noted that addition of these mixtures to the waste rock had positive effects on metal and metalloid release because elements such as Cr and Pb were elevated in the leachate from batch testing of the CKD but not in the test cell leachate. Moreover, the addition of the BFS/CKD and GBFS/CKD mixtures reduced the

concentrations of metals and metalloids such as and Zn in the test cell leachate. This suggests that CKD addition can have positive effects on leachate chemistry. However, these effects may not persist because hardening appears to prevent the neutralizing effect from being sustained.

Granulated blast furnace slag

Addition of GBFS alone (5 wt.%) had similar effects on the leachates to those observed with the GBFS/CKD mixture: the pH initially increased to circumneutral but then fell. Huijgen and Comans (2005) reported that under ambient conditions, ground GBFS can sequester CO_2 via $CaCO_3$ formation, and that the rate of this process depends on the release of Ca during GBFS leaching. It is not clear whether the slightly higher pH observed upon adding GBFS instead of the GBFS/CKD mixture was due to hardening of the CKD, dissolution of $CaCO_3$ resulting from carbonation of the GBFS, or a combination of both. Another explanation is that carbonation may partly hinder dissolution of the GBFS or that the experimental leaching setup was not optimal for dissolution of the material. Despite the possibly beneficial effects of carbonation on the leachate, GBFS was not able to maintain a circumneutral pH throughout the leaching period. Consequently, these experiments were terminated after 14 weeks.

Adding GBFS reduced the metal and metalloid concentrations of the leachate relative to those seen for waste rock alone. Additionally, the leachate in cells containing GBFS with larger waste rock sizes initially had lower concentrations of As and Zn than that from cells containing LKD or a GBFS/CKD mixture. However, as the experiment progressed, the concentrations of these elements in the GBFS leachate eventually exceeded those in the LKD and GBFS/CKD leachates.

Bark ash

Adding BA to the waste rock resulted in a circumneutral pH that was maintained over 38 weeks of leaching. The leaching of waste rock covered with BA or GBFS could not be directly compared to that of waste rock alone due to differences in particle size. Moreover, the limited number of leachate samples analyzed made comparisons even more difficult.

The concentration of Cr in the leachate initially rose after adding BA but then declined over time. The initial increase could thus have been due to the dissolution of easily water-soluble minerals. The leachability of Cr (2.7%) from BA during the batch tests supports this suggestion. The Pb and Zn concentrations in the leachate were lower when BA was applied on top of the waste rock despite the elevated concentrations of these elements observed during batch testing. BA is produced all over Sweden as a byproduct of the Kraft process and is available in greater quantities than CKD and LKD. Therefore, the test cell with BA was not terminated despite the uncertain ability of BA to maintain a circumneutral pH in the long-term. The results presented here are based on the addition of only 1wt.% BA; the use of larger amounts could potentially improve this material's long-term neutralization capacity.

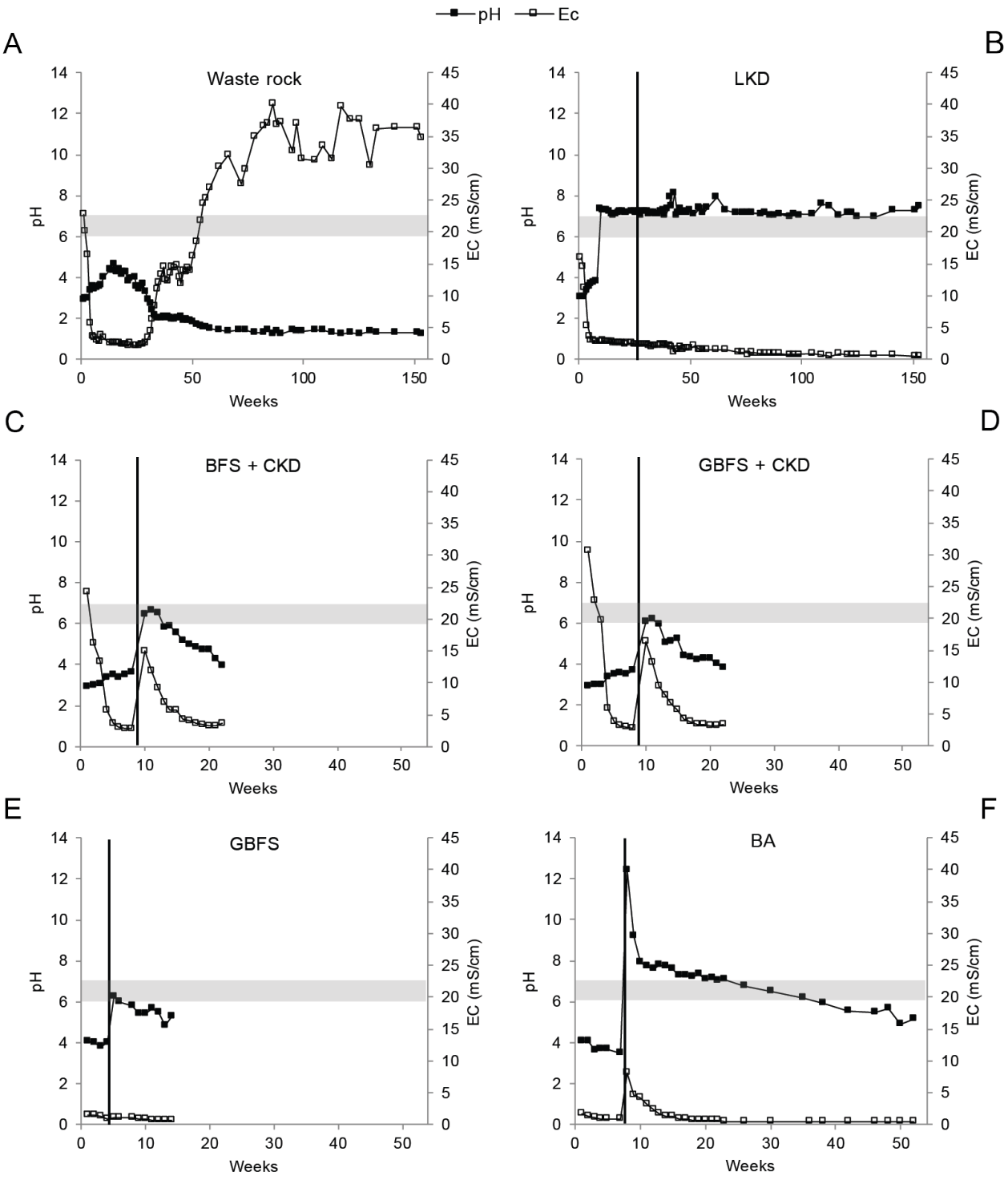

Figure 2.3 Changes in the pH and EC of leachates from highly sulfidic waste rock covered with industrial residues: A: waste rock (reference), B: lime kiln dust (5 wt.%), C: blast furnace slag (4 wt.%) and cement kiln dust (1 wt.%), D: granulated blast furnace slag (4 wt.%) and cement kiln dust (1 wt.%), E: granulated blast furnace slag (5 wt.%), F: bark ash (1 wt.%). Circumneutral pH as defined by Moses and Herman (1991) is indicated by a horizontal band. The time of addition of the industrial residues is indicated by a vertical band.

Lime kiln dust

Addition of LKD (5wt.%) on top of the waste rock increased the pH to slightly above circumneutral without increasing the EC (Figure 2.3). At the time of writing, this pH had been maintained for over three years of leaching, and the experiment was ongoing. The maintenance of a neural pH during sulfide oxidation caused metal ions to precipitate as or associate with secondary minerals, causing them to be largely immobilized. Secondary minerals can precipitate either on the reactive mineral surface or in between minerals. To prevent sulfide oxidation, secondary minerals such as HFO must grow on the sulfide surface for an extended period, forming a coating that is thick enough to hinder oxygen ingress (Huminicki and Rimstidt, 2009). Therefore, the low metal and metalloid concentrations in the leachate of LKD-covered waste rock are not necessarily due to reduced sulfide oxidation.

The extracts obtained in the first four steps of the sequential extraction process were assumed to correspond to the dominant secondary phases in the waste rock. The sequential extraction results indicated that adding LKD to the waste rock changed the sulfide oxidation rate and promoted secondary mineral precipitation on the sulfide surfaces. The waste rock (cell A) was dominated by water-soluble phases such as melanterite. In the case of cell A, the first sequential extraction fraction contained both dissolved water-soluble minerals and oxidation products that had been dissolved in the pore water. This explains why the trace element content of the first fraction increased over time (Figure 2.2). Conversely, the presence of LKD in cell B resulted in the formation of stable secondary phases due to precipitation of and co-precipitation with HFO.

The sequential extraction results also indicate that considerably more gypsum formation occurred in cell A than in cell B. The saturation index values for the cells suggest that gypsum formation in cells A and B was controlled by the concentrations of Ca and S, respectively. The saturation index also indicates that extensive gypsum dissolution occurred in cell B after one year of leaching. Together with the observed decrease in S concentrations, this suggests that the release of S due to sulfide oxidation was suppressed in cell B. Time-series of element leaching revealed that the overall concentrations of Ca, Mg, and Si in the cell B leachates decreased over time, in keeping with the hypothesized reduction in sulfide oxidation. One element of potential concern is As, which was more abundant in cell B than in cell A even though the extent of HFO formation was lower in cell B. This implies that As is associated with other phases in cell B, and suggests that if the environment becomes more reducing (for example, as a result of remediation efforts), these secondary phases may dissolve, releasing accumulated As.

One potential drawback of adding neutralizing minerals is that an excess of secondary minerals may form. In Sweden, waste rock will either be backfilled and flooded in an open pit or dry covered, independently of whether inhibition and passivation of the sulfide surfaces are achieved. If an excess of secondary minerals accumulates, latent acidity will be stored over time and may be released if the environment becomes more reducing, for example during remediation. This can cause drainage from pit lakes or heaps, necessitating extended treatment before the drainage can be released to a recipient. The results presented here suggest that adding LKD effectively prevents sulfide oxidation and subsequent release of metals and metalloids from waste rock into the leachate. Moreover, it appears that LKD addition causes relatively small amounts of secondary mineral precipitation. However, we cannot exclude the possible formation of secondary phases inside the test cell, for example on the geotextile at the cell's bottom. Future research will focus on identifying the secondary minerals formed in this system and determining their trace element distributions.

2.5. Conclusion

- All of the industrial residues generated a circumneutral pH when applied on top of the waste rock, but only LKD and BA were able to maintain it for more than 15 weeks of leaching.
- BA is a very interesting material for preventing ARD generation, partially due to its availability but also because of its promising ability to maintain a circumneutral leachate pH when applied on top of waste rock. However, studies using larger quantities of BA are needed to fully evaluate its potential.
- All of the studied industrial residues reduced the metal ion concentrations in the leachates. However, some metals and metalloids (notably, As and Cr) did not exhibit such reductions following BA addition. The mechanism of their retention needs further study
- Increasing the amount of added industrial residue will not necessarily increase the quality of the leachate. For example, the dissolution of salts from BA adversely affected leachate quality. The release of ions such as Cl^- can result in metal ion complexation, which may adversely affect the downstream environment. The presence of these salts means that only the minimum necessary amount of BA should be added, or that BA should be pre-treated (e.g., during storage) to remove undesirable and highly water-soluble elements. One drawback of storage is that it may reduce the residue's neutralization potential.
- Out of the tested industrial residues, LKD exhibited highly promising results in terms of maintaining a long-term stable pH and creating an optimal environment for precipitation of Me-carbonates and hydroxides.
- The amount of LKD added corresponded to approximately 4% of the amount of $CaCO_3$ required to neutralize the sulfide content of the waste rock.
- The addition of LKD to the waste rock reduced the S concentration of the leachate by reducing the rate of sulfide oxidation, which subsequently led to gypsum dissolution.
- The addition of LKD to the waste rock led to precipitation of more stable secondary phases than those that formed without addition.
- The addition of LKD seemingly reduced the amount of secondary mineral formation. However, since the leaching is still ongoing, we cannot exclude the possibility that secondary mineral formation may occur elsewhere in the test cell, for example, on the geotextile at the bottom of the cell.

Future perspective

The leaching of the LKD-waste rock system will continue to determine whether the neutralization capacity of the LKD is likely to be exhausted in the foreseeable future. Future investigations will focus on identifying and characterizing the secondary minerals formed on the sulfide surface in the presence of LKD, and on assessing the stability of these secondary minerals. The purpose of these studies will be to estimate the long-term stability of LKD-treated waste rock in response to changes in chemical conditions (such as those caused by backfilling or covering the waste rock). Future studies will also examine the trace element content of the waste rock minerals and the secondary minerals formed during waste rock leaching in the presence of LKD.

2.6. References

Alakangas, L., Andersson, E., & Mueller, S. (2013). Neutralization/prevention of acid rock drainage using mixtures of alkaline by-products and sulfidic mine wastes. Environmental Science and Pollution Research, 20(11), 7907-7916. doi:10.1007/s11356-013-1838-z

Alakangas, L., Maurice, C., Macsik, J., Nyström, E., Sandström, N., Andersson-Wikström, A., & Hällström, L. (2014). Kartläggning av restprodukter för efterbehandling och inhibering av gruvavfall: Funktion tillgång och logistik. Luleå: Luleå University of Technology. (In Swedish)

Amos, R.T., Blowes, D.W., Bailey, B.L., Sego, D.C., Smith, L., & Ritchie, A. I. M. (2015). Waste-rock hydrogeology and geochemistry. Applied Geochemistry, 57, 140-156. doi:10.1016/j.apgeochem.2014.06.020

Bessho, M., Wajima, T., Ida, T., & Nishiyama, T. (2011). Experimental study on prevention of acid mine drainage by silica coating of pyrite waste rocks with amorphous silica solution. Environmental Earth Sciences, 64(2), 311-318.

Brown, M., Barley, B., & Wood, H. (2002). Minewater treatment: Technology, application and policy. London: IWA Publishing.

Bulusu, S., Aydilek, A.H., & Rustagi, N. (2007). CCB-based encapsulation of pyrite for remediation of acid mine drainage doi:https://doi.org/10.1016/j.jhazmat.2007.01.035

Chaunsali, P., & Peethamparan, S. (2013). Novel cementitious binder incorporating cement kiln dust: Strength and durability. ACI Materials Journal, 110(3), 297-304.

De Vries, N.H.C. (1996). Process for treating iron-containing sulfide rocks and ores. US Patent: 5,587,001.

Dold, B. (2003). Speciation of the most soluble phases in a sequential extraction procedure adapted for geochemical studies of copper sulfide mine waste. Journal of Geochemical Exploration, 80(1), 55-68. doi:10.1016/S0375-6742(03)00182-1

Doye, I., & Duchesne, J. (2005). Column leaching test to evaluate the use of alkaline industrial wastes to neutralize acid mine tailings. Journal of Environmental Engineering, 131(8), 1221-1229. doi:10.1061/(ASCE)0733-9372(2005)131:8(1221)

Duchesne, J., & Reardon, E. J. (1998). Determining controls on element concentrations in cement kiln dust leachate. Waste Management, 18(5), 339-350. doi:10.1016/S0956-053X(98)00078-6

Engström, F., Adolfsson, D., Samuelsson, C., Sandström, Å., & Björkman, B. (2013). A study of the solubility of pure slag minerals. Minerals Engineering, 41, 46-52. doi:10.1016/j.mineng.2012.10.004

Evangelou, V.P. (1995). Potential microencapsulation of pyrite by artificial inducement of ferric phosphate coatings. Journal of Environmental Quality, 24(3), 535-542.

Evangelou, V.P. (1996). Oxidation proof silica surface coating iron sulfides. US Patent: 5,494,703.

Fan, R., Short, M.D., Zeng, S., Qian, G., Li, J., Schumann, R.C., Gerson, A.R. (2017). The formation of silicate-stabilized passivating layers on pyrite for reduced acid rock drainage. Environmental Science and Technology, 51(19), 11317-11325. doi:10.1021/acs.est.7b03232

Golab, A.N., Peterson, M.A., & Indraratna, B. (2006). Selection of potential reactive materials for a permeable reactive barrier for remediating acidic groundwater in acid sulphate soil

terrains. Quarterly Journal of Engineering Geology and Hydrogeology, 39(2), 209-223. doi:10.1144/1470-9236/05-037

Hallberg, R.O., Granhagen, J.R., & Liljemark, A. (2005). A fly ash/biosludge dry cover for the mitigation of AMD at the Falun mine. Chemie Der Erde, 65(SUPPL. 1), 43-63. doi:10.1016/j.chemer.2005.06.008

Hökfors, B. (2014). Phase chemistry in process models for cement clinker and lime production (Doctoral thesis). Retrieved from http://urn.kb.se/resolve?urn=urn:nbn:se:umu:diva-86004

Hooton, R.D. (2000). Canadian use of ground granulated blast-furnace slag as a supplementary cementing material for enhanced performance of concrete. Canadian Journal of Civil Engineering, 27(4), 754-760.

Huijgen, W.J.J., & Comans, R.N.J. (2005). Mineral CO_2 sequestration by steel slag carbonation. Environmental Science and Technology, 39(24), 9676-9682. doi:10.1021/es050795f

Huminicki, D.M.C., & Rimstidt, J.D. (2009). Iron oxyhydroxide coating of pyrite for acid mine drainage control. Applied Geochemistry, 24(9), 1626-1634. doi:10.1016/j.apgeochem.2009.04.032

Ji, M., Gee, E., Yun, H., Lee, W., Park, Y., Khan, M.A., Choi, J. (2012). Inhibition of sulfide mineral oxidation by surface coating agents: Batch and field studies. Journal of Hazardous Materials, 229-230, 298-306. doi:10.1016/j.jhazmat.2012.06.003

Johnson, D.B., & Hallberg, K.B. (2005). Acid mine drainage remediation options: A review. Science of the Total Environment, 338(1-2 SPEC. ISS.), 3-14. doi:10.1016/j.scitotenv.2004.09.002

Jones, S. N., & Cetin, B. (2017). Evaluation of waste materials for acid mine drainage remediation doi:https://doi-org.proxy.lib.ltu.se/10.1016/j.fuel.2016.10.018

Kang, C., Jeon, B., Park, S., Kang, J., Kim, K., Kim, D., Kim, S. (2016). Inhibition of pyrite oxidation by surface coating: A long-term field study. Environmental Geochemistry and Health, 38(5), 1137-1146. doi:10.1007/s10653-015-9778-9

Kollias, K., Mylona, E., Papassiopi, N., Xenidis, A. (2015). Conditions favoring the formation of iron phosphate coatings on the pyrite surface. Desalination and Water Treatment, 56(5), 1274-1281. doi:10.1080/19443994.2014.958537

Krauskopf, K.B., Bird, D.K. (1995). Introduction to Geochemistry (3. ed.). New York: McGraw-Hill.

Löfgren, A., Karlsson, E. (2018). Reviderad avfallshanteringsplan, maurlidengruvan och maurliden östra. Boliden Mineral AB. (In Swedish)

Lottermoser, B.G. (2010). Mine wastes (third edition): Characterization, treatment and environmental impacts. Mine wastes (third edition): Characterization, treatment and environmental impacts (pp. 1-400) doi:10.1007/978-3-642-12419-8

Lu, J., Alakangas, L., Wanhainen, C. (2014). Metal mobilization under alkaline conditions in ash-covered tailings. Journal of Environmental Management, 139, 38-49.

Mackie, A. L., & Walsh, M. E. (2012). Bench-scale study of active mine water treatment using cement kiln dust (CKD) as a neutralization agent. Water Research, 46(2), 327-334. doi:10.1016/j.watres.2011.10.030

Madzivire, G., Maleka, P.P., Vadapalli, V.R.K., Gitari, W.M., Lindsay, R., Petrik, L.F. (2014). Fate of the naturally occurring radioactive materials during treatment of acid mine drainage

with coal fly ash and aluminium hydroxide doi:https://doi-org.proxy.lib.ltu.se/10.1016/j.jenvman.2013.11.041

Maest, A. S., Nordstrom, D. K. (2017). A geochemical examination of humidity cell tests. Applied Geochemistry, 81, 109-131. doi:10.1016/j.apgeochem.2017.03.016

Mäkitalo, M., Lu, J., Maurice, C., Öhlander, B. (2016). Prediction of the long-term performance of green liquor dregs as a sealing layer to prevent the formation of acid mine drainage. Journal of Environmental Chemical Engineering, 4(2), 2121-2127. doi:10.1016/j.jece.2015.10.005

Mäkitalo, M., Mácsik, J., Maurice, C., Öhlander, B. (2015). Improving properties of sealing layers made of till by adding green liquor dregs to reduce oxidation of sulfidic mine waste. Geotechnical and Geological Engineering, 33(4), 1047-1054. doi:10.1007/s10706-015-9886-4

MEROX (2015). Handbok hyttsten typ L väg- och anläggningsarbeten. Retrieved from http://www.merox.se/uploads/images/1020/Handbok_Hyttsten_typ_L__A4_Ver_4_Slutlig.pdf (In Swedish)

Miller, M.M., Callaghan, R.M. (2004). Lime kiln dust as a potential raw material in portland cement manufacturing. (No. 2004-1336).U.S. GEOLOGICAL SURVEY. Retrieved from https://pubs.usgs.gov/of/2004/1336/2004-1336.pdf

Misra, M., Chen, S., Fuerstenau, M.C. (2006). Passivation of acid mine tailings. Paper presented at the IMPC 2006 - Proceedings of 23rd International Mineral Processing Congress, 2388-2393.

Montelius, C. (2005). The genetic relationship between rhyolitic volcanism and Zn-Cu-Au deposits in the Maurliden volcanic centre, Skellefte district, Sweden: Volcanic facies, lithogeochemistry and geochronology (Doctoral thesis). Retrieved from http://ltu.diva-portal.org/smash/record.jsf?pid=diva2%3A999019&dswid=-3423

Nason, P., Alakangas, L., Öhlander, B. (2013). Using sewage sludge as a sealing layer to remediate sulphidic mine tailings: A pilot-scale experiment, northern Sweden. Environmental Earth Sciences, 70(7), 3093-3105. doi:10.1007/s12665-013-2369-0

Nyström, E. (2018) Suitability of Industrial Residues for Preventing Acid Rock Drainage Generation from Waste Rock (licentiate thesis), Luleå, Sweden. Retrieved from http://ltu.diva-portal.org/smash/record.jsf?pid=diva2%3A1200782&dswid=7226

Nyström, E., Kaasalainen, H., Alakangas, L. (2019) Suitability study of secondary raw materials for prevention of acid rock drainage generation from waste rock. J Clean Prod. https://doi.org/10.1016/j.jclepro.2019.05.130

Nordstrom, D.K. (2009). Acid rock drainage and climate change. Journal of Geochemical Exploration, 100(2-3), 97-104. doi:10.1016/j.gexplo.2008.08.002

Nordstrom, D.K., Alpers, C.N. (1999). Negative pH, efflorescent mineralogy, and consequences for environmental restoration at the iron mountain superfund site, California. Proceedings of the National Academy of Sciences of the United States of America, 96(7), 3455-3462. doi:10.1073/pnas.96.7.3455

Pérez-López, R., Cama, J., Miguel Nieto, J., Ayora, C., Saaltink, M.W. (2009). Attenuation of pyrite oxidation with a fly ash pre-barrier: Reactive transport modelling of column experiments. Applied Geochemistry, 24(9), 1712-1723.

Pérez-López, R., Nieto, J.M., de Almodóvar, G.R. (2007). Immobilization of toxic elements in mine residues derived from mining activities in the Iberian pyrite belt (SW Spain):

Laboratory experiments. Applied Geochemistry, 22(9), 1919-1935. doi:10.1016/j.apgeochem.2007.03.055

Pérez-López, R., Quispe, D., Castillo, J., Nieto, J.M. (2011). Acid neutralization by dissolution of alkaline paper mill wastes and implications for treatment of sulfide-mine drainage. American Mineralogist, 96(5-6), 781-791. doi:10.2138/am.2011.3685

Sahoo, P.K., Kim, K., Equeenuddin, S.M., Powell, M.A. (2013). Current approaches for mitigating acid mine drainage. Reviews of Environmental Contamination and Toxicology, 226, 1-32. doi:10.1007/978-1-4614-6898-1_1

Sahoo, P.K., Tripathy, S., Panigrahi, M.K., Md Equeenuddin, S. (2013). Inhibition of acid mine drainage from a pyrite-rich mining waste using industrial by-products: Role of neo-formed phases. Water, Air, and Soil Pollution, 224(11) doi:10.1007/s11270-013-1757-0

SEPA (Swedish Environmental Protection Agency). (2010). Återvinning av avfall i anläggningsarbeten. (No. 2010:1). Retrieved from http://www.naturvardsverket.se/Documents/publikationer/978-91-620-0164-3.pdf

SGU (Swedish Geological Survey). (2017). Statistics of the Swedish mining industry 2016. (No. 2017:1). http://resource.sgu.se/produkter/pp/pp2017-1-rapport.pdf: (In Swedish)

Singer, P.C., Stumm, W. (1970). Acidic mine drainage: The rate-determining step. Science, 167(3921), 1121-1123.

Sirén, S., Maurice, C., Alakangas, L. (2016). (2016). Green liquor dregs in mine waste remediation, from laboratory investigations to field application. Paper presented at the 12th International Mine Water Association Congress – "Mining Meets Water – Conflicts and Solutions", Leipzig, Germany, 11-15 July 2016. 706-713.

SIS (2003) Characterization of waste – Leaching - Compliance test for leaching of granular waste materials and sludges, Part 2: One stage batch test at liquid solid ratio of 10l/kg for materials with particle size below 4 mm (without or with size reduction). Swedish standard SS-EN 12457-2. Swedish Standard Institute, Stockholm, Sweden.

Sulaymon, A.H., Faisal, A.A.H., Khaliefa, Q.M. (2015). Cement kiln dust (CKD)-filter sand permeable reactive barrier for the removal of Cu(II) and Zn(II) from simulated acidic groundwater. Journal of Hazardous Materials, 297, 160-172. doi:10.1016/j.jhazmat.2015.04.061

Tariq, A., Yanful, E.K. (2013). A review of binders used in cemented paste tailings for underground and surface disposal practices. Journal of Environmental Management, 131, 138-149. doi:10.1016/j.jenvman.2013.09.039

Tolonen, E., Sarpola, A., Hu, T., Rämö, J., Lassi, U. (2014). Acid mine drainage treatment using by-products from quicklime manufacturing as neutralization chemicals. Chemosphere, 117(1), 419-424. doi:10.1016/j.chemosphere.2014.07.090

Yeheyis, M.B., Shang, J.Q., Yanful, E.K. (2009). Long-term evaluation of coal fly ash and mine tailings co-placement: A site-specific study doi:https://doi-org.proxy.lib.ltu.se/10.1016/j.jenvman.2009.08.010

Younger, P.L., Banwart, S.A., Hedin, R.S. (2002). Mine water: Hydrology, pollution, remediation. Dordrecht: Kluwer Academic.

Younger, P.L., Wolkerdorfer, C.H., Bowell, R.J., Diels, L. (2006). Partnership for acid drainage remediation in Europe (PADRE): Building a better future founded on research and best practice. Paper presented at the 7th International Conference on Acid Rock Drainage

2006, ICARD – also Serves as the 23rd Annual Meetings of the American Society of Mining and Reclamation, 3 2571-2574

3. COVER SYSTEM SUSANNE NIGÉUS

3.1. Background

Massive amounts of mine wastes are created all over the world. Sweden alone generated 139-million-ton mine waste in 2014, accounting for 83 % of all waste produced during that year (Swedish EPA, 2016). These wastes need to be managed in an environmentally-, technically- and economically sustainable way. A considerable amount of the mine waste generated contains sulfides. If sulfidic mine waste is left unattended and in contact with oxygen and humidity the sulfides oxidize and have the potential to produce acid rock drainage (ARD). ARD is a major long-term threat to the environment as metals and metalloids may become mobile (Saria et al., 2006). A typical method in Sweden to stop sulfide oxidation from mine waste is to apply a dry cover on top of the waste. The dry cover usually consists of a sealing layer placed on top of the mine waste and above this, a protective layer. In multilayer covers, oxygen diffusion is controlled by the sealing layer (or moisture retaining layer). The sealing layer is typically placed between two coarser grain layers, which will develop capillary barrier effects, and prevent water loss by drainage and evaporation. The main objective of the sealing layer is usually to limit water transport and remain close to saturation, using materials with low saturated hydraulic conductivity (HC). Several factors control the HC, for example, compaction degree (Watabe et al., 2000; Leroueil et al., 2002) and the molding water content of the material (Leroueil et al. 2002; Benson and Trast 1995). The presence of fine-grained material is another important factor that influences the HC. An increasing amount of fines in the material decreases the HC (Leroueil et al., 2002; Benson and Trast, 1995; Benson et al., 1994), as the porosity of the material decreases.

Soil cover solution

If sulfidic mine waste is left unattended and in contact with oxygen and humidity the sulfides oxidize and have potential to produce acid rock drainage (ARD). There are several ways to prevent ARD both in situ while the mine is still operating and after mine closure (Figure 3.1). The most common way to prevent ARD from mine waste in Sweden is a soil cover that consists of a sealing layer made of a compacted fine-grained material with a low saturated HC. On top of the sealing layer, you have an uncompacted protection layer, usually made of till. The purpose of the protection layer is to protect the sealing layer from erosion and penetration of roots and frost. Above the protection layer, a nutrient-rich vegetation layer is usually placed, to easier reestablishment of vegetation (Figure 3.2).

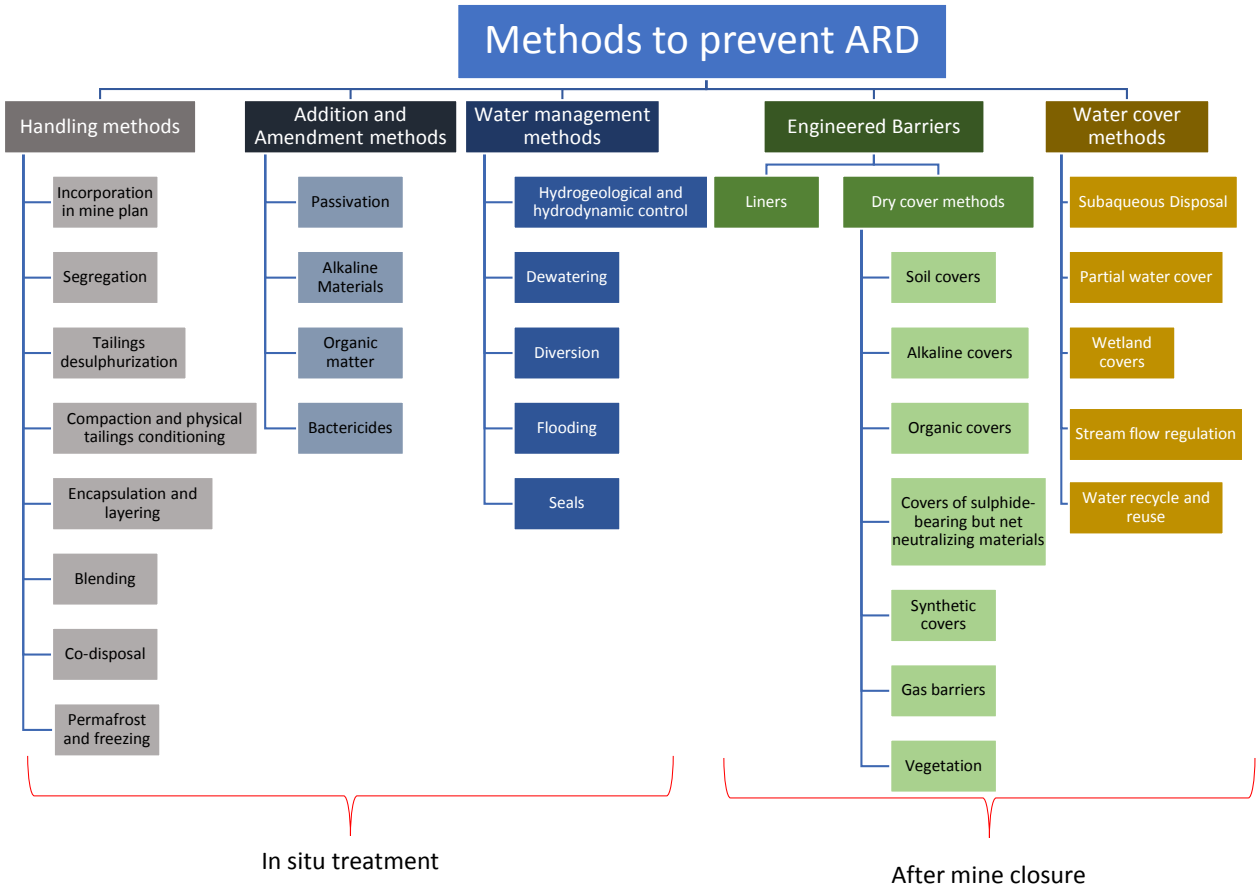

Figure 3.1. Different methods to prevent ARD from mine waste.

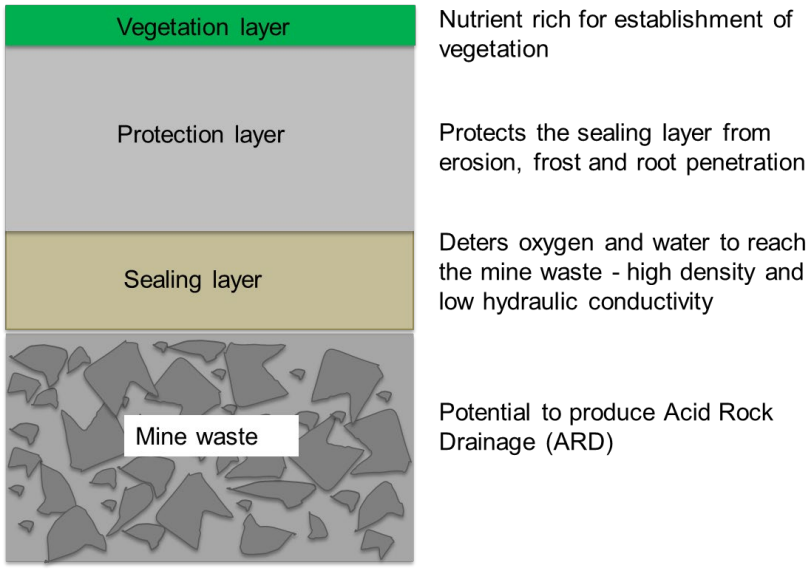

Figure 2.2. A describing figure of a typical dry cover system in Sweden.

A sealing layer in Sweden is usually made of a clayey till. The availability of a clayey till nearby a mine is however often limited, and there is a great need for alternative materials. A suitable alternative material to the clayey till can be an industrial residue. Sweden produces 28 million

ton wastes, excluding mine waste, of which about 26 million ton is classified as a non-hazardous waste by the Swedish EPA and of that 6 million ton is residues from industrial production (Swedish EPA 2016). Most of these residues are deposited and only a small amount recycled. Using an industrial residue in a mine remediation program is useful for both the mining industry and the industry providing the residue and a large benefit for the environment. The system serves as a circular economy as the industries aim towards reducing waste deposition. Some examples of industrial residues that previously have been used as a mine waste cover are sewage sludge, fly ash, desulfurized tailings, coal combustion by-products (CCB) and steel slag (Hallberg et al., 2005; Bäckström et al., 2009; Dobchuk et al., 2013; Lu et al., 2013; Nason et al., 2013; Park et al., 2014; de Almeida et al., 2015; Phanikumar and Shankar, 2016).

Green Liquor Dregs

Previous studies have shown that a residue from pulp production, Green Liquor Dregs (GLD), has properties suitable for a sealing layer i.e. it is fine-grained (d100 < 63μm), commonly has an HC in the range of 10^{-8} and 10^{-9} m/s and a higher water retention capacity (WRC) compared to materials with similar particle size, such as clayey/sandy silt (Mäkitalo et al., 2014). In Sweden, about 200 000 tons of GLD was produced annually, and about 300 000 ton is in depositions (SGI 2003). GLD is an alkaline, inorganic waste originating from the recycling process at sulfate pulp and paper mills. For pictures of GLD and an overview of the generating process see figures 3.3, 3.4. GLD consists of unburned carbon residues, process elements (mainly Al, Si, and $CaCO_3$) and is regarded as an inert material (Mäkelä and Höynälä, 2000). It has the same grain size distribution as silt. Other characteristics of GLD are a high pH (10-11), relatively high porosity (73 - 82 %), a bulk density of 0.44-0.67 g/m^3, a compact density of 2.47 to 2.60 g/cm^3 and consist of up to 75 % of $CaCO_3$ (Mäkitalo et al., 2014). The high $CaCO_3$ is generated in the retrieving process where a pre-coat lime mud filter (a mixture of $CaCO_3$, CaO and $Ca(OH)_2$) is used, leading to various amounts of lime mud mixed with the green liquor. This strongly influences the composition of the GLD and leads to a high buffering capacity. Sequential extraction has been performed on GLD and indicates relatively low bioavailability of metals in general (Nurmesniemi et al., 2005). Batch leaching studies performed on tailings amended with GLD shows a general decrease in metal content in the leachate (Jia et al., 2016; Mäkitalo et al., 2015) and the values did not exceed the limit values for landfills for non-hazardous waste (Jia et al. 2016). The content of As, however, did exceed the limits, which should be taken into consideration when using GLD (Jia et al., 2016; Mäkitalo et al., 2015). Another batch leaching test also shows a general metal removal when adding GLD to AMD, 100 % removal for Al, As, Cr and Cu, 98 % for Fe, 84 % for Cd, 75 % for Ni and 66 % for Zn (Pérez-López et al., 2011).

Figure 3.3. Pictures of GLD by Maria Mäkitalo.

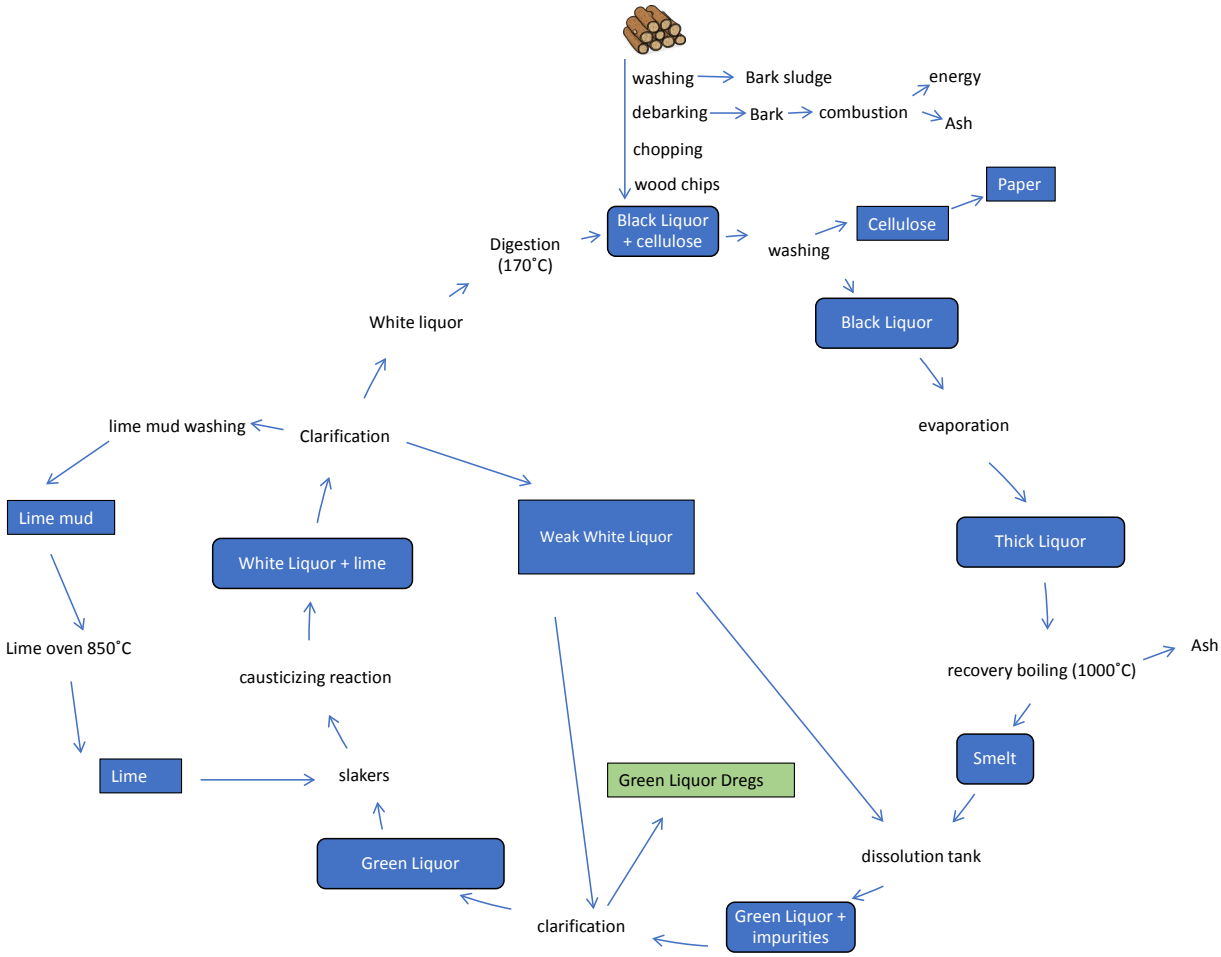

Figure 3.4. Overview of the production process that generates green liquor dregs (Reworked from (Mäkitalo 2015).

GLD has been used in a few sanitary landfill cover applications (Pousette and Mácsik, 2000; Hargelius, 2008). It has also been reported to have a possibility to act as a neutralizing agent for acidic wastewater (Pöykiö et al., 2006) and for sulphidic mine waste (Bäckström et al., 2010; Bellaloui et al., 1999; Lu et al., 2013), as the increase in pH enhances the metal removal (Pérez-López et al., 2011). The possibilities to use GLD as a cover material on top of mine waste have been investigated in several pilot-scale studies (Ragnvaldsson et al., 2014; Chtaini et al., 2001;

Lu et al., 2013). The studies show a reduced effluent volume by 40 % (Ragnvaldsson et al., 2014), a reduction of leaching metals (Chtaini et al., 2001; Lu et al., 2013; Ragnvaldsson et al., 2014) and reduced oxygen diffusion to the mine wastes (Chtaini et al., 2001). The long-term stability of the GLD has been studied by Mäkitalo et al. (2016). The study concluded that aging of GLD mainly depends on the amount of water passing through the material, which is changing its pH and chemical composition, primarily by leaching S and K. The GLD did not show any physical or mineralogical changes in the study that will affect its ability to prevent oxygen diffusion to the underlying mine waste. The WRC observed to be >85 % under field conditions and maintained a high degree of saturation with low HC independently of its age. The shear strength of the GLD increased over time, but not enough to ensure long-term physical stability. The main concern was expected to be the chemical stability of the GLD due to the high content of calcite, which might dissolve and profoundly change its properties. (Mäkitalo et al., 2016) saw from estimations of the density and HC of the GLD as well as their performance in the batch leaching experiments, no evidence that this will occur within the next thousands of years. Considering its lack of long-term physical stability, due to low shear strength, it is not reasonable to solely use GLD in the sealing layer from a geotechnical point of view. Neither is it reasonable from an economic point of view, due to its relatively high transportation costs, which are affected by its high water content (leading to higher weight) and relatively long distances to the mine sites. Previous field studies on mixing GLD with till have shown promising results for the mixtures to be used as a sealing layer, with low HC, high WRC and increased compaction properties (Mäkitalo et al., 2015; Jia et al., 2013; Hargelius, 2008).

Optimal properties for a sealing layer

Considering its lack of long-term physical stability, it is not reasonable to solely use GLD for the construction of sealing layer in slopes. Neither is it reasonable from an economic point of view, due to its relatively high transportation costs, which are affected by its high water content (leading to higher weight) and relatively long distances to the mine sites. Previous field studies on mixing GLD with till have shown promising results for a till-GLD mixture to be used as a sealing layer (Mäkitalo et al., 2015; Jia et al., 20; Hargelius, 2008). The mixture in the studies has a low HC, high WRC and improved compaction properties. Water retention, porosity, HC, particle size distribution and density are properties that are dependent. At the highest density, both the total porosity and the macro-porosity in a well-grade soil are minimum which also reduces the hydraulic conductivity of the material to a minimum. Consequently, as water transport is limited and capillary forces are able to retain water in the porosity, the chance for the material to remain close to saturation even during dry periods increases, providing efficient oxygen barriers. Therefore, even of WRC is the key property for the function of the sealing layer, HC and high compaction degrees are often set as prerequisite to ensure high WRC. However, materials such as GLD have higher WRC despite lower HC and density compared to pure till. Therefore addition of GLD could be beneficial even though traditionally set HC-limits and degree of compaction are not reached.

Nigéus et al. (2018) have studied how the contents of fines and clays affect the HC and compaction degree in mixtures of till and GLD. That study shows that the finer the till is, the lower HC in the mixture. Especially the contents of clay play a major role in determining the

final HC of the mixture. The higher clay-content, the lower HC. However, the initial water content, molding water content and dry density (ρ_d) after compaction effect on the HC of the GLD-till mixtures have not yet been studied. The HC and the compaction degree in a material that is to be used as a sealing layer on top of sulfidic mine waste, are important factors to understand. This as the main objective of the sealing layer is usually to limit water infiltration through the cover and to reach a low HC the sealing layer should be compacted to a high density (Höglund et al., 2004). Studies by Leroueil et al. (2002) and Watabe et al. (2000) on glacial till shows that the HC is highly dependent on the degree of compaction, with significantly decreasing values with decreased void ratio during loading. Another feature connected to compaction that is affecting the HC, is the molding water content of the material (Benson and Trast 1995; Leroueil et al. 2002), i.e. the water content after compaction. A study conducted by Benson and Trast (1995) on thirteen compacted clays shows that the lowest HC was reached at molding water content of 1-2 % wet of the line of optimums. The optimum water content is the molding water content at which the highest dry density (ρ_d) can be reached (Figure 3.5). The presence of fine-grained material is another important factor that influences the HC. An increasing amount of fines in the material decreases the HC (Leroueil et al., 2002; Benson and Trast, 1995; Benson et al., 1994), as the porosity of the material decreases.

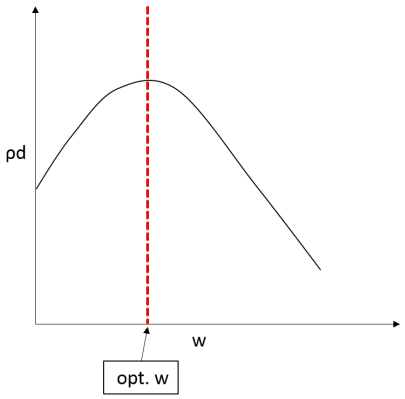

Figure 3.5. Describing figure of the optimal water content. ρ_d = dry density after compaction, w= water content and opt. w = optimal water content.

The objectives and hypothesizes of his study

In this laboratory study 5 to 20 wt. % of GLD were mixed with three sieved (<20 mm) tills with different contents of fines and clays with the main objective to learn if GLD and till mixtures can replace a clayey till in a sealing layer. There is a limitation of how much GLD can be added to the till due to decreased compaction properties and shear strength. A maximum of 20 % of addition of GLD was set as a limit as a mixture with more GLD becomes very difficult to compact. The tills consisted of two silty (~35 % <63 μm) tills with different clay contents (2.6 and 4.3 % <2 μm respectively) and one sandy till (~14 % <63 μm). The specific objectives of the laboratory study were to investigate how the (i) contents of fines and clays-, (ii) initial water content-, (iii) dry density after compaction- and (iv) compaction effort affects the hydraulic conductivity of different till-GLD mixtures.

It is expected that till as a heterogenic material, and a dominant part of the mixture will have a significant impact on especially the HC of the mixtures. The finer the till is, the lower the HC (Leroueil et al., 2002). The dry density after compaction is expected to increase with an increasing amount of fines in the till, as the porosity decreases (Benson and Trast, 1995). The addition of GLD is expected to decrease the dry density after compaction as the GLD has a lower particle density, a higher water content and a low shear strength (Mäkitalo et al., 2014). Regarding HC, the addition of GLD to the tills is expected to decrease the HC to a certain limit, after that limit the high water content and low shear strength of the GLD is expected to decrease the compaction degree and therefore increase the HC. The compaction degree will likely be more influenced by the percentage of GLD added, with an expected decrease in dry density with addition of GLD. This as previous studies have shown that GLD has a low particle density, low shear strength and high water content (Mäkitalo et al., 2014), leading to a lower dry density after compaction. The addition of GLD to the tills is expected to decrease its HC to a limit of around 10 % of addition, after that the high water content and low shear strength of the GLD is expected to decrease the compaction degree and therefore increase the HC. Lower initial water content of till and GLD is expected to decrease the HC with higher amounts of GLD added. An increase in the compaction degree is projected with a lower initial water content of the GLD, as the total water content of the mixture will decrease to a value closer to the optimal water content. With higher amounts of GLD in the mixtures, the HC is expected to increase, due to a decrease in dry density after compaction. However, with lower amounts of GLD, the HC is expected to decrease, even with decreasing dry density after compaction. This as the low HC and high WRC of the GLD is predicted to lead to a decrease in the initial HC of the tills. However, as the amount of GLD increases, other properties of the GLD as its low shear strength and high water content is anticipated to have more influence in the HC of the mixtures. It becomes more difficult to compact with a water content above the optimal water content of the mixture. The mixtures are expected to reach the lowest HC and higher WRC in mixtures a few percent wet of the optimal water content (Leroueil et al., 2002). A decreased compaction effort is expected to decrease the HC. A field study by (Mäkitalo et al., 2015) indicates that the more strain the material is exposed to, the water content and porosity of the till-GLD mixture increases.

3.2. Methods and materials

Materials

Two silty tills and a sandy till was used as the bulk material. The silty tills were collected at two till quarries at the Brännkläppen facility in Boden, Sweden. The sandy till was collected at a quarry at Sunderbyn, Luleå, Sweden. GLD from two different paper mills were used in this study, GLD1 from Smurfit Kappa paper mill in Piteå (northern Sweden) and GLD2 from Billerud Korsnäs paper mill in Kalix (also northern Sweden). The GLD was collected in sealed plastic containers to preserve the water content of the material. The two different GLD were chemically characterized by an accredited commercial laboratory (ALS Scandinavia AB in Luleå, Sweden) for chemical analysis by a semi-quantitative screening analysis by ICP-SMS (HR-ICP-MS).

The tills were air-dried (Figure 3.6) and sieved through a 20-mm sieve and the particles above 20 mm removed. This as particles above 20 mm will affect negatively on the effectiveness of the materials used as a sealing layer. Then it was mixed with 5, 10, 15 and 20 wt. % of GLD. The weight percentage was calculated towards a dry till and a naturally moist GLD. The mixing was carried out by hand with a small shovel until the mixture was visibly estimated as homogenized. An overview of the different mixtures can be seen in Figure 3.7.

Figure 3.6 Air-drying of the till.

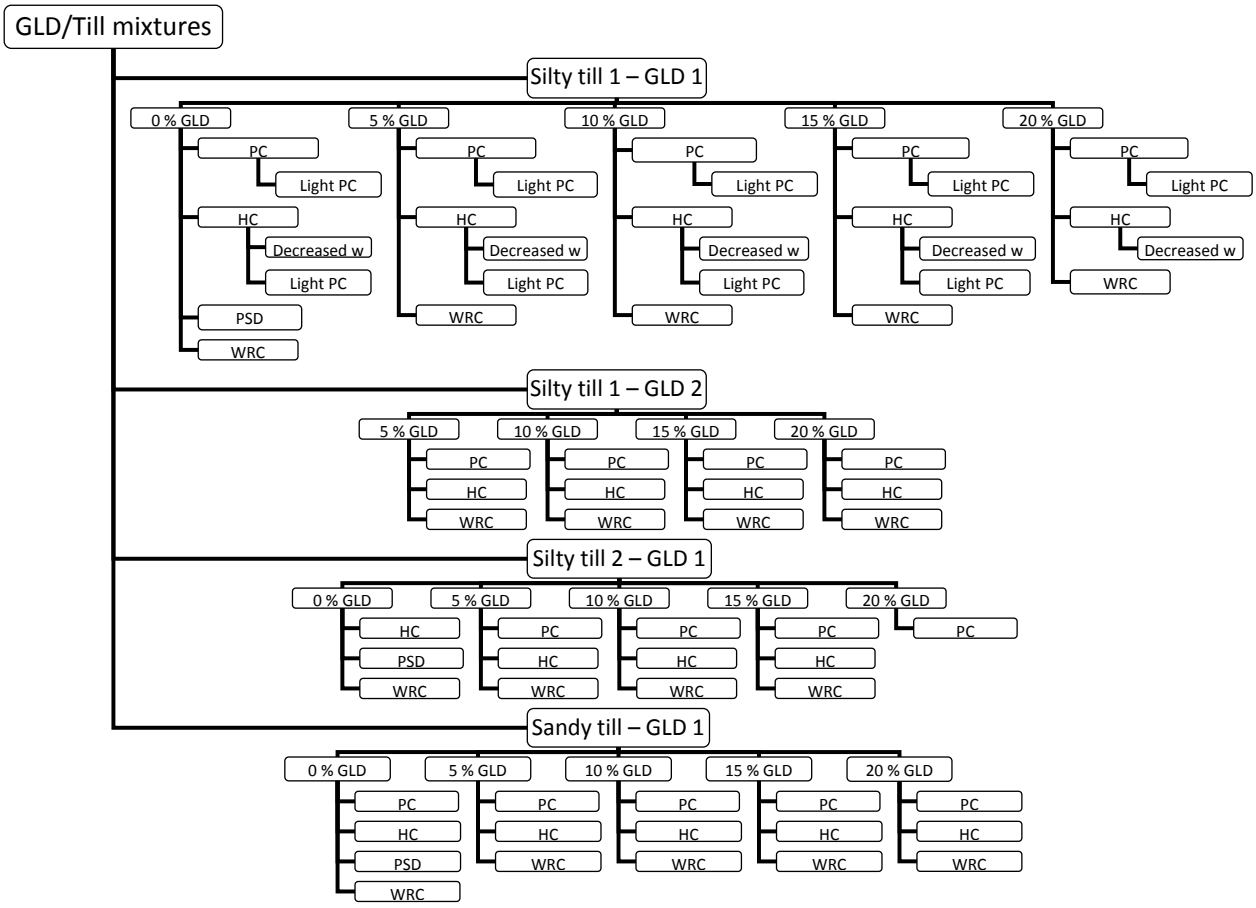

Figure 3.7 An overview of the different mixtures of tills and GLD and the analysis performed on them. PC stands for Proctor compaction, HC for hydraulic conductivity, WRC for water retention capacity, w for water content and PSD for particle size distribution.

Particle size distribution

The tills were washed and dry sieved according to SS-EN 933-1:2012 to obtain the weight percentage of fines. A mechanical sieve tower (Retsch AS 200) with an amplitude of 2.2 mm/"g" was used. The cut-off sizes were 12.5, 10, 8, 5, 4, 2, 1, 0.5, 0.25, 0.125 and 0.063 mm (Figure 3.8).

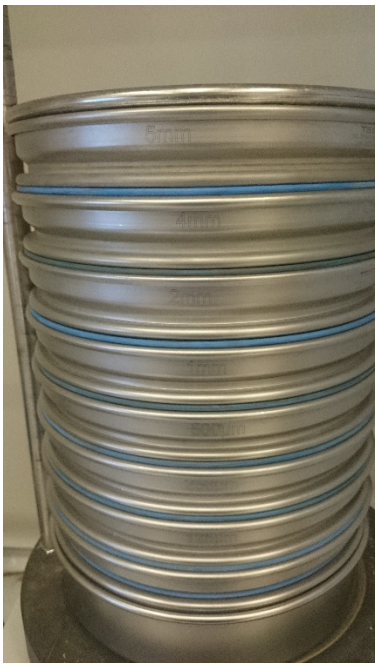

Figure 3.8. Picture of the sieves used for PSD-analysis on the particles >0.063 mm.

PSD for the fines (<0.063 mm) in the tills and GLD were done by laser diffraction analysis on triplicate samples of each material by a CILAS Granulometer 1064 (CILAS, Orléans, France). With a compact cast iron optical bench, the CILAS 1064 integrates 2 sequenced laser sources positioned at 0° and 45°, to produce a diffraction pattern analysed on a 64-channel silicon detector. The PSD is then calculated using the CILAS software.

Particle density

The particle density of the materials was determined using an AccuPyc II 1340 Pycnometer that uses the gas displacement method to measure volume accurately. The samples were sealed in the instrument compartment of known volume, an inert gas was admitted and then expanded into another precision internal volume. The pressures observed upon filling the sample chamber and then discharging it into a second empty chamber allowed computation of the sample solid phase volume.

Proctor compaction

Proctor compaction (PC) was carried out according to standard SS-EN 13286-2:2010. Also, a lighter compaction weight and drop length were used in one test. At that point, a 2.5 kg weight was dropped from a height of 30 cm. The PC-tests were started with triplicates but the need for this was considered unnecessary due to similar results and only one or two repetitions were made after that. The PC was done on air-dried till and naturally moist GLD.

The dry density (ρ_d) and the water content (w) were then calculated with equations 3.1 and 3.2:

$$\rho_d = m/((1+w) +V) \quad (3.1)$$

$$w = (m-m_d)/m_d \quad (3.2)$$

where m is the mass of the moist sample, m_d is the mass of the dry sample and V is the volume.

Hydraulic conductivity

HC measurements were conducted on a moist and a drier till (TSC 91±1 %, n=24 for the moist till and TSC 96 % for the drier till) with 5, 10, 15 and 20 wt. % addition of GLD. The TSC (total solid content) of each material were decided by drying them in an oven (105°C for 24 h) according to the SIS standard SS-EN 14346:2007. The constant head-method was used in airtight cylinders with a volume of 996 cm^3. The walls of the cylinders were coated with a thin layer of bentonite to prevent the preferential wall flow. The mixtures inside the cylinder were compacted with standard PC method in five equally thick layers with a falling weight of 4.54 kg, falling 45 cm 25 times on each layer. Silty till with an addition of 5-20 wt. % of GLD1 was also compacted with a light PC with a 2.45 kg weight, falling 30 cm.
Water was lead to the bottom of the cylinder with a hydraulic gradient of 8.7. The water passing through the cylinders were collected in plastic bottles, sealed from the top to prohibit evaporation. The plastic bottle was weighed regularly, and the time was noted to measure the velocity of the water passing through the sample. HC was calculated using Darcy's law. The analysis was done with three sets of each sample.

WRC?

3.3. Main results

The main constitutes of the two GLD are Ca, Na and Si, followed by Mg, K, Al and S (Table 3.1). None of the metals are above the limits for the material to be classified as hazardous waste according to the Swedish Waste Management Association (Sverige, 2007).

Table 3.1. Chemical characterization of GLD1 from Smurfit Kappa paper mill and GLD2 from Billerud Korsnäs paper mill. The concentrations represent an average of three different samples of the same GLD in mg/kg. The standard deviation of the three samples is presented as a ± value.

mg/kg	GLD1	GLD2	mg/kg	GLD1	GLD2	mg/kg	GLD1	GLD2
Calcium, Ca	73000±6000	200000	Cobalt, Co	3±0	0,7±0	Hafnium, Hf	0,13±0,06	0,03±0
Sodium, Na	20000±600	18000±0	Lanthanum, La	2±1	0,7±0	Erbium, Er	0,1±0,02	0,06±0
Silicon, Si	19000±6000	1030±60	Lithium, Li	2±1	0,7±0	Ytterbium, Yb	0,1±0,0	0,05±0
Magnesium, Mg	8800±600	10300±600	Gallium, Ga	2±1	0,08±0,01	Bismuth, Bi	0,08±0,01	0,01±0
Potassium, K	8500±1700	1270±60	Bromine, Br	2±1	<2	Tantalum, Ta	0,05±0,03	<0.01
Aluminium, Al	7100±1600	850±10	Yttrium, Y	1,3±0,6	1±0	Europium, Eu	0,05±0,01	0,02±0
Sulphur, S	6630±60	4970±60	Silver, Ag	1±0	0,7±0	Holmium, Ho	0,04±0,01	0,02±0
Manganese, Mn	3700±200	2300±0	Neodymium, Nd	1	0,5±0	Terbium, Tb	0,03±0,01	0,01±0
Iron, Fe	2700±500	580±10	Molybdenum, Mo	0,8±0,1	0,3±0	Lutetium, Lu	0,02±0,01	<0.01
Phosphorus, P	1200±173	980±10	Niobium, Nb	0,6±0,3	0,1±0	Thulium, Tm	0,01±0,01	<0.01
Zinc, Zn	720±50	230±0	Tin, Sn	0,6±0,2	0,06±0,01	Selenium, Se	<0.5	<0.5

Barium, Ba	270±50	78±1	Scandium, Sc	0,6±0,1	0,1±0	Germanium, Ge	<0.1	<0.1
Titanium, Ti	210±80	33±1	Arsenic, As	0,4±0,1	0,1±0	Iodine, I	<0.1	<0.1
Strontium, Sr	117±6	160±0	Antimony,Sb	0,4±0,1	0,01±0	Palladium, Pd	<0.02	<0.02
Copper, Cu	60±3	22±0	Praseodymium, Pr	0,3±0,1	0,1±0	Gold, Au	<0.01	<0.01
Chromium, Cr	34±2	25±0	Cesium, Cs	0,3±0,1	0,05±0	Iridium, Ir	<0.01	<0.01
Rubidium, Rb	31±6	6±0	Uranium, U	0,2±0,1	0,4±0	Mercury, Hg	<0.01	<0.01
Nickel, Ni	18±1	11±0	Thorium, Th	0,2±0,1	0,1±0	Osmium, Os	<0.01	<0.01
Boron, B	11±1	4±1	Samarium, Sm	0,2±0,1	0,09±0,01	Platinum, Pt	<0.01	<0.01
Lead, Pb	7±1	1±0	Dysprosium, Dy	0,2±0,1	0,09±0	Rhenium, Re	<0.01	<0.01
Zirconium, Zr	6±3	1±0	Gadolinium, Gd	0,2±0,1	0,08±0	Rhodium, Rh	<0.01	<0.01
Vanadium, V	4±2	2±0	Beryllium, Be	0,2±0,1	0,04±0	Ruthenium, Ru	<0.01	<0.01
Cadmium, Cd	3±1	1±0	Thallium, Tl	0,2±0	0,2±0	Tellurium, Te	<0.01	<0.01
Cerium, Ce	3±1	0,8±0	Tungsten, W	0,2±0	0,04±0			

How the content of fines and clay in till affects the HC of till-GLD mixtures

The PSD of the GLD showed that the majority was finer than 63 μm. 5.4±4.1 % and 9.5±1.6 % were in the clay fraction for GLD1 and GLD2 respectively (Figure 3.9 and Table 3.2). The Silty till 1 consisted of 35 % fines of which 2.6 % was in the clay fraction. Silty till 2 had the same percentage of fines as the silty till-1, but a higher percentage of these were in the clay fraction, 4.3 %. The sandy till had a lower percentage of fines and clays (14 % fines and 0.7 % clays (Figure 3.9**).** and Table 3.2). A summary of the results from the laboratory study is presented in Table 3.3.

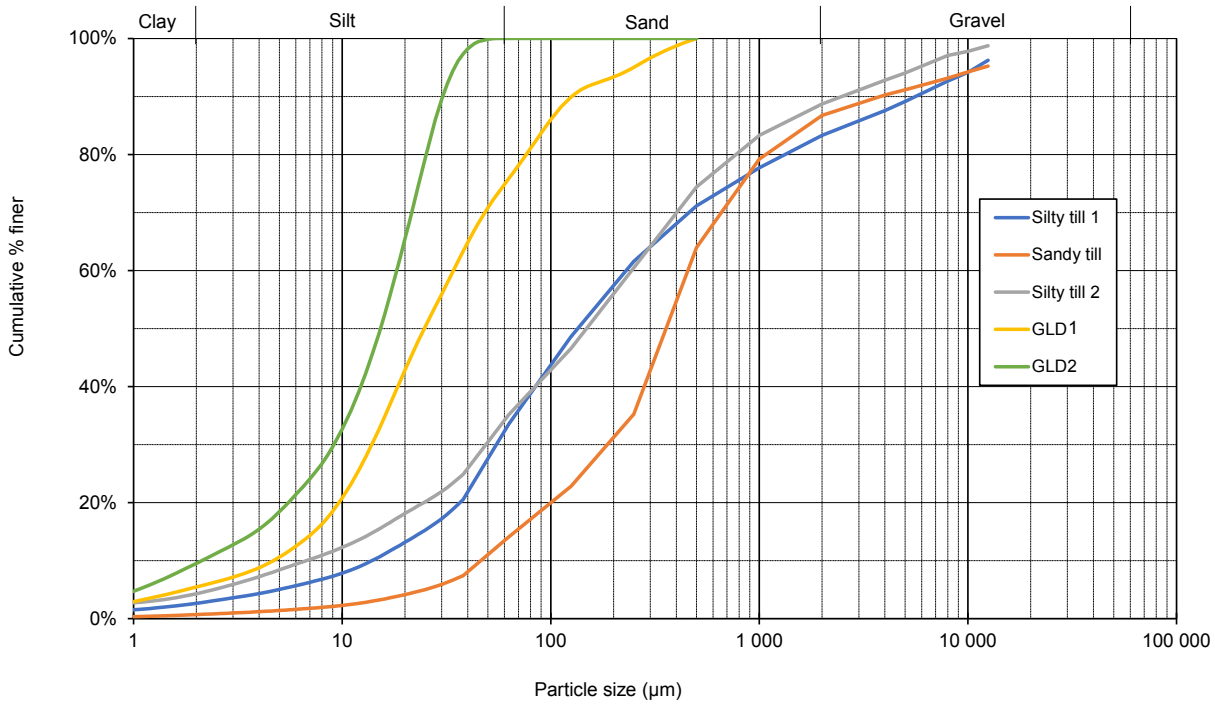

Figure 3.9. PSD of the GLD and tills.

Table 3.2. Particle density (g/cm3), TSC (%) and contents of fines and clays in the tills and GLD.

Material	Particle density (g/cm^3)	TSC (%)	Content of fines (<63µm)	Content of clays (<2µm)
Silty till	2.71	91.5±0.4 (n=9)	34±5 % (n=9)	2.6 % (n=1)
Silty till 2	2.70	91.7±0.4 (n=9)	35±1 % (n=2)	4.3 % (n=1)
Sandy till	2.68	91.1±0.8 (n=6)	14±1 % (n=3)	0.7 % (n=1)
GLD1	2.49	43±4 (n=12)	76±29 % (n=3)	5.4±4.1 % (n=3)
GLD2	2.63	58±0.3 % (n=3)	100±0 % (n=3)	9.5±1.6 % (n=3)

Table 3.3 Summary of the results from the laboratory study conducted in this thesis, i.e. hydraulic conductivity (HC), dry density (ρ_d), water content (w) and fines/clay content.

		HC				Compaction properties		PSD	
	GLD (wt.%)	Average HC (m/s)	Average ρ_d (g/cm³)	Average w (%)	Wet of opt. w (%)	Average max. ρ_d (g/cm³)	Opt. molding w (%)	Fines (%<63µm)	Clays (%<2µm)
Silty till 1 - GLD1	**0%**	3E-08±3E-09 (n=3)	2.01± 0.05 (n=3)	9±0.5 (n=3)	1	2.08±0.01 (n=3)	6	34±5 (n=9)	2.6
	5%	2E-08±5E-09 (n=3)	1.97±0.02 (n=3)	10±0.6 (n=3)	2	2.05±0.01 (n=2)	8		
	10%	4E-08±5E-09 (n=3)	1.88±0.01 (n=3)	14±1.3 (n=3)	5	1.99±0.01 (n=2)	9		
	15%	6E-08±1E-08 (n=3)	1.74±0.05 (n=3)	18±0.4 (n=3)	8	1.95±0.00 (n=2)	10		
	20%	7E-08±1E-08 (n=3)	1.65±0.02 (n=3)	20±0.7 (n=3)					
Sandy till - GLD1	**0%**	7E-08±3-08 (n=3)	2.04±0.02 (n=3)	9±0.6 (n=3)	1	2.03±0.01 (n=3)	8	14±1 (n=3)	0.7
	5%	2E-08±3E-09 (n=3)	1.99±0.03 (n=3)	11±1.0 (n=3)	2	2.01±0.00 (n=3)	9		
	10%	2E-08±3E-09 (n=3)	1.92±0.02 (n=3)	14±0.3 (n=3)	3	1.98±0.02 (n=3)	11		
	15%	3E-08±3E-09 (n=3)	1.78±0.05 (n=3)	18±1.0 (n=3)	6	1.93±0.02 (n=3)	12		
	20%	4E-08±1E-08 (n=3)	1.64±0.04 (n=3)	21±0.4 (n=3)					
Silty till 2 - GLD1	**0%**	3E-10±8E-11 (n=2)	2.12±0.01 (n=2)	10±0.1 (n=2)				35±1 (n=2)	4.3
	5%	8E-10+3E-10 (n=2)	1.95+0.01 (n=2)	14+0.5 (n=2)					
	10%	2E-09±2E-10 (n=2)	1.87±0.03 (n=2)	15±1.0 (n=2)					
	15%	5E-09 (n=1)	1.67 (n=1)	21 (n=1)					
Silty till 1 - GLD1 - drier till	**0%**	1E-07 (n=1)	2,02 (n=1)	5 (n=1)	-1				
	5%	7E-08+2E-09 (n=3)	2.06+0.02 (n=3)	7+0.5 (n=3)	-1				
	10%	5E-08±1E-09 (n=3)	2.03±0.04 (n=3)	10±1.3 (n=3)	2				
	15%	3E-08±1E-08 (n=3)	1.93±0.01 (n=3)	14±0.4 (n=3)	4				
	20%	4E-08 (n=1)	1,66 (n=1)	21 (n=1)					
Silty till 1 - GLD2	**0%**					2.09 (n=1)	6		
	5%	3E-08±4E-09 (n=3)	1.96±0.02 (n=3)	10±0.5 (n=3)	3	2.12 (n=1)	7		
	10%	3E-08±5E-09 (n=3)	1.91±0.02 (n=3)	12±0.3 (n=3)	4	2.05 (n=1)	8		
	15%	3E-08±2E-08 (n=3)	1.74±0.03 (n=3)	14±0.8 (n=3)	4	2.04 (n=1)	10		
	20%					1.99 (n=1)	11		
Silty till 1 - GLD1 - Light compaction	**0%**	4E-08 (n=1)	2.04 (n=1)	9 (n=1)	2	2.1 (n=1)	7		
	5%	4E-08+4E-09 (n=3)	1.95+0.02 (n=3)	11+0.9 (n=3)	1	2.03 (n=1)	10		
	10%	5E-08±5E-09 (n=3)	1.83±0.05 (n=3)	15±0.6 (n=3)	3	1.93 (n=1)	12		
	15%	6E-08±1E-08 (n=3)	1.72±0.02 (n=3)	19±0.4 (n=3)	4	1.81 (n=1)	15		
	20%	9E-08 (n=1)	1.54 (n=1)	25(n=1)					
GLD1								76±2 (n=3)	5.4+4.1 (n=3)
GLD2		1E-08+7E-09 (n=3) *						100+0 (n=3)	9.5+1.6 (n=3)

*(Mäkitalo et al. 2014).

The HC for silty till 1 and sandy till decreases with the addition of GLD1, up to a wt. % of 5-10 (Figure 3.10A). This was expected as the GLD increases the fine-grained material in the mixtures, leading to a decrease in micro-porosity and results in decreasing HC (Benson et al., 1994; Benson and Trast 1995; Leroueil et al., 2002). With more than 10-15 % of GLD, the HC increases. Likely due to a deterioration of the compaction degree with an increase in water content. Unlike the sandy till and the silty till the HC of the more clayey silty till 2, does not decrease at the addition of GLD. This is likely the results of that the increased clay content leaves no space for the GLD in its micropores. This is also the reason for the much lower HC compared to the silty till 1 (Figure 3.10A). In a study on tills conducted by Leroueil (2002) the HC

decreased several orders of magnitude when the clay-size fraction increased from 2 to 12 %. Also, a study on clay conducted by Benson et al., (1994) showed a strong relationship between clay content and HC and a weak relationship between the contents of fines and HC. However, using a drier and fine-grained GLD (GLD2) in the mixture with silty till 1, there is no decrease in HC. The HC stays stable around 3E-08 m/s (Figure 3.10B). The expectation was that the addition of a more fine-grained and drier GLD (Table 3.2) to the till would lead to a more pronounced decrease in HC, and that more GLD could be added to the till. This as the fine-grained material in the mixture increases compared to when using GLD1, and the final water content in the mixture decreases leading to a higher compaction degree. The final water content is in fact lower than when using GLD1 in the mixture (Figure 3.10D), but it is not leading to a higher dry density after compaction (Figure 3.10F). When adding 10-20 wt. % of GLD2 the HC is lower compared to when using GLD1. This is likely due to the decrease in water content and is explained further in section 3.2.

The HC in a material used in a sealing layer should be as low as possible, this way the oxygen diffusion through the material is minimized. In Höglund et al., (2004), it is stated that is reasonable to expect that a well constructed sealing layer in a dry cover can reach a maximum HC of 1E-09 m/s, which should ensure a low enough oxygen diffusion. However, Boliden mining company, has developed different criteria for the HC for sealing layer, depending on site specific conditions, to reach sufficient oxygen diffusion. None of the mixtures studied here meets these requirements, expect from the mixture based on a more clayey till (silty till 2) that had an HC below 1E-09 m/s (Figure 3.10A). The hypothesis was that the addition of GLD would improve the HC of the tills that alone would not reach the requirements. Unfortunately, this was not reached in the mixtures studied here. The initial HC of till, the bulk material, seems to be the driving force in controlling the HC of the final mixture. The HC in the till is in turn affected by the content of fines and especially clay in the till. One reason for the unexpectedly low decrease of HC with the addition of GLD might be the method of compaction that was chosen. In this study, a standardized PC method was chosen to limit the differences between the samples to imitate compaction in the field. One disadvantage with using proctor compaction, is that there is a small margin on the sides of the cylinder that is not compacted as the weight does not reach all the way to the sides. This can lead to a preferential flow along the edges of the cylinder and a higher HC than in the field. However, if and how much the compaction method affects HC needs further investigation.

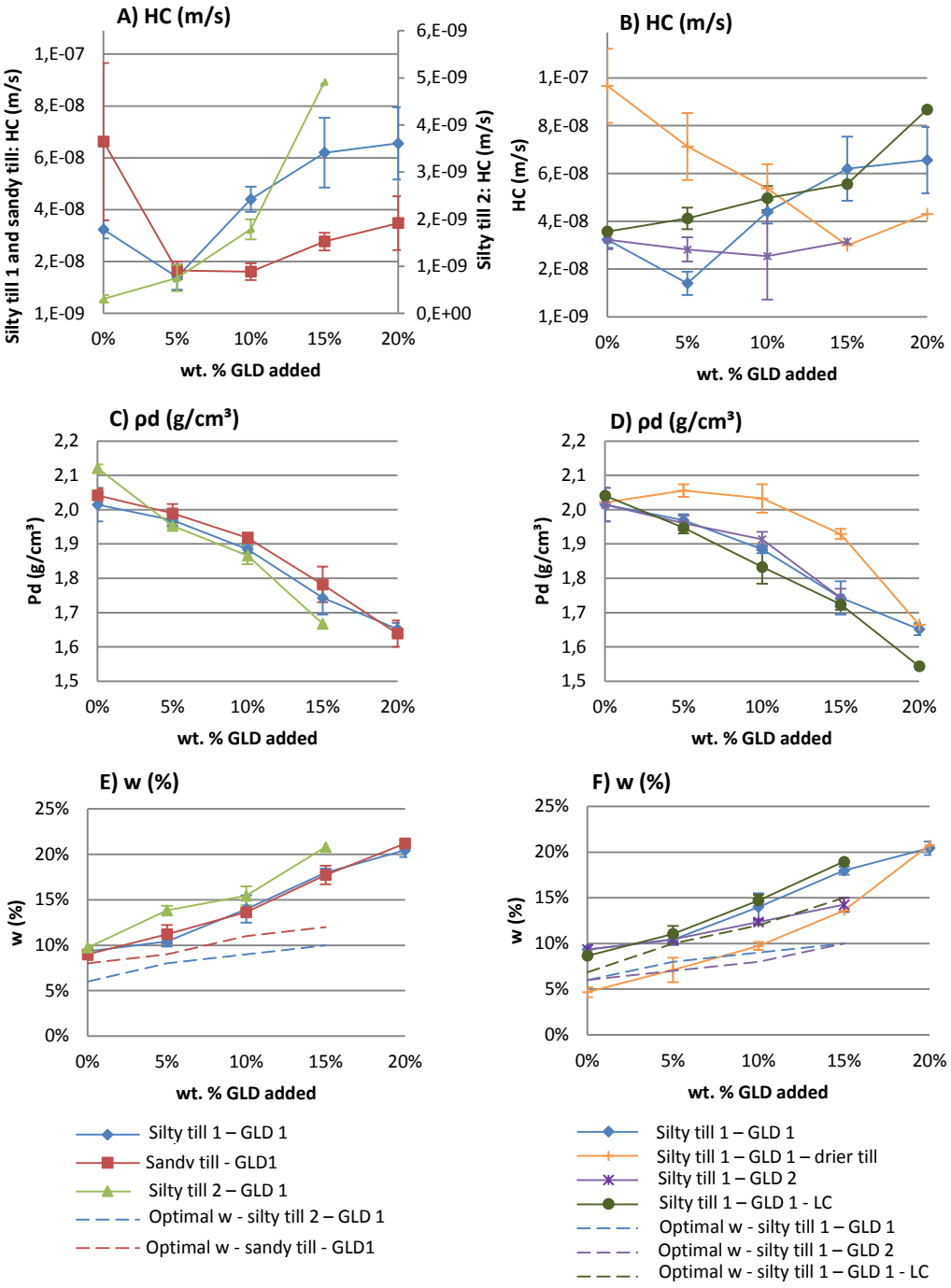

Figure 3.10.3 Hydraulic conductivity (HC), dry density after compaction (ρ_d), water content (w) and optimal water content in the different mixtures of till and GLD. *Silty till 1 – GLD1 - drier till* represents a till with a TSC of 96 % compared to 91 %. *Silty till 1–GLD1-LC* represents the same as *Silty till 1-GLD1* except that is has been compacted with less compaction effort (lower weight and drop height).

How the initial water content of the materials affects the HC in the till-GLD mixtures

When using a drier till and mixing it with GLD1, the HC shows a different trend compared to the mixture with a wetter till. The initial HC is higher in the drier till, 10E-08 compared to 3E-0 m/s. It is only when the GLD percentage reaches over 10 wt. % in the mixture that the HC becomes lower than in the moister mixture (Figure 3.10A). The decrease in HC with a drier till can be explained by the connection between HC and degree of compaction (Benson et al., 1994; Leroueil et al., 2002; Watabe et al., 2000). As the till is drier the mixture also becomes drier and the dry density after compaction is higher compared to when using the wetter till, around 0.1-0.2 g/cm^3 higher (Figure 3.10B). This was expected. However, even if the dry density is higher in the drier till-mixture, the HC is not lower, except with a 15 wt. % of GLD addition. This is likely due to the water content of the mixtures. Adding 15 wt. % to an already moist till increases the water content far beyond the optimal water content (Figure 3.10C), leading to a lower dry density and a higher HC than in a mixture with a drier till. A study conducted by Benson and Trast (1995) on thirteen compacted clays shows that HC is sensitive to molding water content, where the lowest HC was reached at molding water content of 1-2 % wet of the line of optimums. The molding water content of the samples tested for HC is for pure till 1-3 % wet of the optimum molding water content, 2-3 % wet of the optimum for 5 wt. % addition of GLD, 3-5 % wet of optimum for 10 wt. % addition of GLD and for 15 wt. % of GLD addition the water content is 4-8 % wet of the optimum molding water content (Figures 3.10E, F). Around 10 wt. % of GLD seems to be a threshold for tills with a TSC of about 91 % and with increasing amount of GLD above that the water content increases beyond the 1-2 % wet of optimum. A drier till can, therefore, tolerate a higher amount of GLD-addition compare to a wetter till (Figures 3.10B, F). The properties of the GLD discussed previously are likely also contributing to the materials difficulties to be compacted.

When adding GLD2, a drier and more fine-grained GLD (Figure 3.9 and Table 3.2) to the silty till 1, the HC stays around 3E-08 m/s when adding up to 15 wt. % of GLD and does not follow the same trend as when using GLD1, a decrease followed by an increase (Figure 3.10B). As for the mixture with the drier till there seems to be a higher tolerance of how much GLD2 can be added to the silty till compared to GLD1. One explanation for this can be that GLD2 is drier and the deteriorating trend seen in HC with more than 5 wt. % addition of GLD1 due to exceeding water content is therefore not seen. The mixture of GLD2 can keep its relatively low HC even with an addition of up to 15 wt. % of GLD. Support for this argument is found in the molding water content that is lower for the mixtures with 10 and 15 wt. % of GLD2 added compared with the mixture with GLD1 (Figure 3.10C). For 10-15 wt. % addition of GLD the mixture with GLD1 reaches 5-8 % wet of optimum water content after compaction, for GLD2 the corresponding number is 4 % (Figure 3.10C). Another explanation to that a higher amount of GLD2 can be added to the mixture before an increase in HC occurs may be that GLD2 is more fine-grained than GLD1. Even if the compaction degree decreases with more addition of GLD, the increase of fine-grained material levels out the expected increase in HC.

How dry density after compaction affect HC in the till-GLD mixtures

Maximum dry density after compaction decreases with increasing GLD addition to the till (Figure 3.11A). From 2.08 to 1.95 g/cm^3 in the till with GLD1 addition (Figure 3.11A) and

from 2.10 to 1.81 g/cm³ in the till that was lightly compacted (Figure 3.11A). The GLD2-mixture had a higher maximum dry density than the GLD1-mixture, from 2.09 to 1.99 g/cm3 with 5 to 20 wt. % GLD addition (Figure 3.11A). This may be due to the higher contents of fines and clays in GLD2 compared to GLD1 (Table 3.2). A high amount of clay minerals generally corresponds to a decrease in the size of microscale pores (Benson and Trast, 1995) which in turn increases the possibility to reach a higher dry density during compaction. This has also been shown in an earlier study where tills with different contents of fines and clays were used in the till-GLD mixtures (Nigéus et al 2018). Another reason for the higher dry density when adding GLD2 compared to when adding GLD1 to the silty till might be the higher TSC of GLD2 (Table 3.2), which makes the material less sticky and easier to compact due to the decreasing water content.

HC has previously shown to be highly dependent on the degree of compaction, with decreasing HC with increasing degree of compaction (Benson et al., 1994; Leroueil et al., 2002; Watabe et al., 2000). In the mixtures studied here, the HC is decreasing when adding 5-10 wt. % of GLD1 to the silty till 1 and sandy till to then increase with an addition of up to 10-15 wt. % or more GLD1 (Figure 3.10A). The dry density, however, is not following this trend but is decreasing with increasing amount of GLD added, from around 2.0 to 1.6 g/cm^3 when adding up to 20 wt. % of GLD (Figures 3.10C, D). The decrease was expected and can be explained by the properties of the GLD, i.e. its lower particle density and TSC (Table 3.2), together with its high WRC (Mäkitalo et al., 2014). So, even if the dry density decreases with increasing amount of GLD in the mixtures the HC is decreasing due to the increase in fine material. Also, the high WRC of the GLD adds to the decrease of HC in the mixtures. However, when more than 10 wt. % of GLD is added to the till the water content increases above the optimum water content for HC, which as discussed in section 3.2 is 1-2 % wet of the optimum water content (Benson and Trast, 1995).

The more clayey silty till 2, behaves differently and is more connected to dry density after compaction and the final water content, with increasing HC with decreasing dry density and increasing water content (Figures 3.10A, C, E). As discussed in section 3.1, this might be due to that the till already has a fair amount of clayey material that fills up the micro pores and the addition of GLD is not necessary and only leads to a deterioration in HC.

In the mixture with a drier till, the dry density after compaction stays stabile around 2.0 g/cm^3 with up to 10 wt. % GLD added, to then decrease with an addition of 15 or more wt. % GLD (Figure 3.10D). The HC on the other hand decreases steadily with an addition of up to 15 wt. % of GLD and does not seem to be connected to the dry density after compaction (Figure 3.10B). As discussed in section 3.2 the initial water content seems to be the driving force when determining HC in the mixture with the drier till.

For mixtures of tills with high initial HC and GLD the dry density after compaction seems to affect the HC for higher amounts of GLD added but does not seem to be the main driving force with lower percentages HC added.

How compaction effort affects the HC in the till-GLD mixtures

Comparing light compaction to standard compaction, lower dry densities was reached when light PC was used. The difference increases with increasing amount of GLD added (Figure 3.11 A). Generally, a decreased dry density due to a decreased compaction effort is expected (Benson and Trast, 1995). However, the expectation for the materials studied here was that a light compaction might increase the dry density. This as the water retained in the GLD due to its high WRC might be released with more compaction effort used. Previous studies on GLD-till mixtures conducted by Mäkitalo et al., (2015) indicate a decrease in compaction degree with increasing mixing effort. Evidence of this was not detected in this study (Figure 3.11A).

Compaction effort has also shown to have an impact on HC. A study conducted on thirteen compacted clays show a decrease in HC with an increase in compaction effort (Benson and Trast, 1995). However, studies conducted by (Mäkitalo et al., 2015) indicate that mixing time and mixing effort increases the water content and porosity of the till-GLD mixtures used in that study. The suggestion was that standard proctor compactor might not be the best choice when working with GLD, as the effort and contact with the GLD are quite high with a standard compaction method. The hypothesis was that a lower compaction effort might decrease the HC of the till-GLD mixtures. However, the results from this study do not agree with this argumentation, as a decreased compaction effort does not significantly affect the HC, neither positively or negatively. A difference in the mixtures where light compaction was used compared to standard PC is only seen with an addition of 5 wt. % of GLD1, where the HC is higher than when using standard compaction (4E-08 compared to 2E-08 m/s; Figure 3.10A). This can likely be explained by the decrease in compaction effort that, as explained before, has been shown to increase HC (Benson and Trast, 1995). The negative effects that Mäkitalo (2015) found when using a higher compaction degree on GLD cannot be seen with this low percentage of GLD added. However, despite the lack of positive effects on HC when using a lighter compaction effort, it might still be a good choice, as laboratory tests tend to underpredict HC compare to actual values in the field. There is evidence of an underprediction of HC by a factor of 10 and sometimes more (Daniel, 1984). When comparing HC in the lab and in the field, the compaction effort in the field is usually less than in the lab, leading to an increase in optimum water content (Daniel, 1984). Therefore, when compacting in the field, the compaction is made dry of optimum water content instead of at the optimum, resulting in a larger HC than expected. This can be avoided by compacting at the same compaction effort that will be used in the field when compacting in the lab (Daniel, 1984).

In summary, the study shows that the compaction effort does not seem to be the driving factor controlling HC when working with till-GLD mixtures. However, due to the properties of the GLD and the aim to mimic field conditions, a lighter compaction effort than standard PC is still recommended.

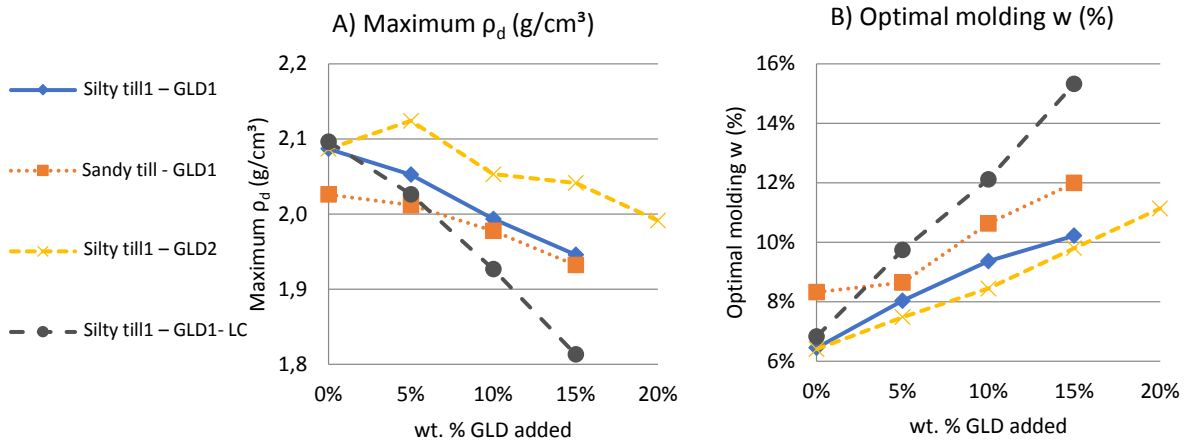

Figure 3.11 Maximum dry density, ρ_d (g/cm³) and optimal water content, *w* (%) of the different till-GLD mixtures.

3.4. Conclusions

Unexpectedly only the mixture based on a more clayey till (silty till 2) had a HC below 1E-09 m/s (Figure 3.10A). The hypothesis was that the addition of GLD would improve the HC of the tills that alone would not reach the requirement. The HC of the mixtures based on the silty till 1, the sandy till did and the drier till did improve (decrease), but not enough to reach below 1E-08 m/s. This study confirms the fact that the initial HC of the till that is used in the mixtures plays a major role in controlling the HC of the final mixture. The HC decreases with addition of GLD to two of tills studied and increases in one of the tills. The HC of the till is in turn affected by the content of fines and especially clay in the till. This study also shows that the initial water content of the materials plays a major role than dry density after compaction in determining the HC of the mixtures. It determines the degree wet of optimum that in this and previous studies has shown to greatly affect the HC (Benson and Trast, 1995; Benson et al., 1994). A drier till and GLD leads to that more GLD can be added to the mixture for reaching the optimal HC. If the till is dry a higher amount of GLD is required, otherwise the HC will be too high. If the GLD is drier, it does not seem to matter if it is 5 or 15 wt. % of GLD that is added to the till.

The hydraulic conductivity reached in this study were above the targeted values of 10^{-8} m/s which implies a risk for water percolation to be large enough to drain the net precipitation reaching the sealing layer. However, results from experiments reported in Nigéus (2018) shows that addition of GLD improves the water retention capacity of the blend. The higher the addition is, the better the WRC was, even though the optimal water content was passed, and the maximum density was not reached. Results from Virolainen (2018) showed that very low oxygen diffusion coefficients are obtained when the GLD-blends but also that desiccation could rapidly alter the oxygen barrier. All together, the results indicate that WRC increases in blends of GLD/till compared to the pure till and that low diffusion coefficient can be obtained, even at higher HC higher than 10^{-8} m/s. Consequently, aiming at HC lower than 10^{-8} m/s and maximum density, may not be necessary to reduce the oxygen diffusion to wanted levels. Insuring regular water supply to the sealing layer and adding enough GLDs to ensure near to saturation condition during dry periods would ensure a satisfactory oxygen barrier. Slope stability issues and cost associated with GLDs supplies are limiting the GLD amendments that are possible.

Future research should focus on defining criteria to decide the quantity of GLDs to be added to reach the requirements regarding oxygen diffusion without having to measure it. In the same way as density has been used as quality criteria for HC, in natural soils, a method is needed to decide how GLDs should be added to obtain a blend with sufficient WRC and sealing layer with the required oxygen diffusion.

3.5. References

Akcil, A. and Kolidas, S. (2006) Acid mine drainage (AMD): causes, treatment and case studies. Journal of Cleaner Production, 14(12), pp. 1139-1145.

Bäckström, M., Karlsson, S. and Sartz, L. (2009) Utvärdering och Demonstration av Efterbehandlingsalternativ för Historiskt Gruvavfall Med Aska och Alkaliska Restprodukter. Värmeforsk report, 1099.

Bäckström, M., Sartz, L., Karlsson, S. and Allard, B. (2010) Prevention of ARD through stabilization of waste rock with alkaline by-products: results from a meso-scale experiment, Mine Water & Innovative Thinking, Sydney 2010, pp. 559-563.

Bellaloui, A., Chtaini, A., Ballivy, G. and Narasiah, S. (1999) Laboratory investigation of the control of acid mine drainage using alkaline paper mill waste. Water, air, and soil pollution, 111(1-4), pp. 57-73.

Benson, C.H., Zhai, H. and Wang, X. (1994) Estimating hydraulic conductivity of compacted clay liners. Journal of Geotechnical Engineering, 120(2), pp. 366-387.

Benson, C.H. and Trast, J.M. (1995) Hydraulic conductivity of thirteen compacted clays. Clays and Clay Minerals, 43(6), pp. 669-681.

Chtaini, A., Bellaloui, A., Ballivy, G. and Narasiah, S. (2001) Field investigation of controlling acid mine drainage using alkaline paper mill waste. Water, air, and soil pollution, 125(1), pp. 357-374.

Daniel, D.E. (1984) Predicting hydraulic conductivity of clay liners. Journal of Geotechnical Engineering, 110(2), pp. 285-300.

De Almeida, R.P., Leite Ado, L. and Borghetti Soares, A. (2015) Reduction of acid rock drainage using steel slag in cover systems over sulfide rock waste piles. Waste management & research : the journal of the International Solid Wastes and Public Cleansing Association, ISWA, 33(4), pp. 353-362.

Dobchuk, B., Nichol, C., Wilson, G.W. and Aubertin, M. (2013) Evaluation of a single-layer desulphurized tailings cover. Canadian Geotechnical Journal, 50(7), pp. 777-792.

Hallberg, R.O., Granhagen, J.R. and Liljemark, A., (2005) A fly ash/biosludge dry cover for the mitigation of AMD at the falun mine. Chemie Der Erde-Geochemistry, 65, pp. 43-63.

Hargelius, K. (2008) Pilotyta med Tätskikt på Ätrans Deponi, Fältförsök-Värö-FAVRAB-Hylte. Ramböll Sverige AB, region väst, Gothenburg (in Swedish), .

Höglund, L.O., Herbert, R., Lövgren, L., Öhlander, B., Neretniks, I., Moreno, L., Malmström, M., Elander, P., Lindvall, M. and Lindström, B. (2004) MiMi-Performance assessment: Main report.

Jia, Y., Maurice, C. and Öhlander, B. (2013) Effect of the alkaline industrial residues fly ash, green liquor dregs, and lime mud on mine tailings oxidation when used as covering material. Environmental Earth Sciences, , pp. 1-16.

Jia, Y., Maurice, C. and Öhlander, B. (2016) Mobility of as, Cu, Cr, and Zn from tailings covered with sealing materials using alkaline industrial residues: a comparison between two leaching methods. Environmental Science and Pollution Research, 23(1), pp. 648-660.

Leroueil, S., Le Bihan, J., Sebaihi, S. and Alicescu, V. (2002) Hydraulic conductivity of compacted tills from northern Quebec. Canadian geotechnical journal, 39(5), pp. 1039-1049.

Lu, J., Alakangas, L., Jia, Y. and Gotthardsson, J. (2013) Evaluation of the application of dry covers over carbonate-rich sulphide tailings. Journal of hazardous materials, 244, pp. 180-194.

Mäkelä, H. and Höynälä, H. (2000) By-products and Recycled Materials in Earth Structures: Materials and Applications. Tekes.

Mäkitalo, M. (2015) Green liquor dregs in sealing layers to prevent the formation of acid mine drainage: from characterization to implementation. Doctoral thesis., Luleå tekniska universitet.

Mäkitalo, M., Maurice, C., Jia, Y. and Öhlander, B. (2014) Characterization of green liquor dregs, potentially useful for prevention of the formation of acid rock drainage. Minerals, 4(2), pp. 330-344.

Mäkitalo, M., Lu, J., Maurice, C. and Öhlander, B. (2016) Prediction of the long-term performance of green liquor dregs as a sealing layer to prevent the formation of acid mine drainage. Journal of Environmental Chemical Engineering, 4(2), pp. 2121-2127.

Mäkitalo, M., Stenman, D., Ikumapayi, F., Maurice, C. and Öhlander, B. (2015) An Evaluation of Using Various Admixtures of Green Liquor Dregs, a Residual Product, as a Sealing Layer on Reactive Mine Tailings. Mine Water and the Environment.

Mäkitalo, M., Macsik, J., Maurice, C. and Öhlander, B. (2015) Improving Properties of Sealing Layers Made of Till by Adding Green Liquor Dregs to Reduce Oxidation of Sulfidic Mine Waste. Geotechnical and Geological Engineering, 33(4), pp. 1047-1054.

Nason, P., Alakangas, L. and Öhlander, B. (2013) Using sewage sludge as a sealing layer to remediate sulphidic mine tailings: a pilot-scale experiment, northern Sweden. Environmental earth sciences, 70(7), pp. 3093-3105.

Nigéus, S. (2018). Green liquor dregs-amended till to cover sulfidic mine waste. Licentiate thesis. Luleå University of Technology.

Nurmesniemi, H., Pöykiö, R., Perämäki, P. and Kuokkanen, T. (2005) The use of a sequential leaching procedure for heavy metal fractionation in green liquor dregs from a causticizing process at a pulp mill. Chemosphere, 61(10), pp. 1475-1484.

Park, J.H., Edraki, M., Mulligan, D. and Jang, H.S. (2014) The application of coal combustion by-products in mine site rehabilitation. Journal of Cleaner Production, 84(0), pp. 761-772.

Pérez-López, R., Quispe, D., Castillo, J. and Nieto, J.M. (2011) Acid neutralization by dissolution of alkaline paper mill wastes and implications for treatment of sulfide-mine drainage. American Mineralogist, 96(5-6), pp. 781-791.

Phanikumar, B. and Shankar, M.U. (2016) Studies on Hydraulic Conductivity of Fly Ash-Stabilised Expansive Clay Liners. Geotechnical and Geological Engineering, 34(2), pp. 449-462.

Pousette, K. and Mácsik, J. (2000) Material-och miljöteknisk undersökning av grönlutsslam, mesa, kalkgrus, flyg-och bottenaska från AssiDomäns fem svenska bruk. Luleå Tekniska Universitet, Institutionen för Väg-och Vattenbyggnad, avdelningen för Geoteknik, förmodligen år, .

Pöykiö, R., Nurmesniemi, H., Kuokkanen, T. and Perämäki, P. (2006) Green liquor dregs as an alternative neutralizing agent at a pulp mill. Environmental Chemistry Letters, 4(1), pp. 37-40.

Ragnvaldsson, D., Bergknut, M., Lewis, J., Drotz, S., Lundkvist, A., Abrahamsson, K. and Fernerud, S. (2014) A novel method for reducing acid mine drainage using green liquor dregs. Environmental Chemistry Letters, .

Saria, L., Shimaoka, T. and Miyawaki, K. (2006) Leaching of heavy metals in acid mine drainage. Waste management & research : the journal of the International Solid Wastes and Public Cleansing Association, ISWA, 24(2), pp. 134-140.

SGI, 2003. In Swedish: Inventering av restprodukter som kan utgöra ersättningsmaterial för naturgrus och bergkross i anläggningsbyggande. 2-0203-0182. SGI.

Sverige, A., 2007. Uppdaterade bedömningsgrunder för förorenade massor. Avfall Sverige Rapport, 1.

Swedish EPA, 2016. In Swedish: Avfall i Sverige 2014. 6727. Bromma, Sweden: Arkitektkopia AB.

Virolainen, A. (2018). Evaluating the effective oxygen diffusion coefficient in blends of till and green liquor dregs (GLD) used as sealing layer in mine waste covers. Master thesis. Luleå University of Technology.

Watabe, Y., Leroueil, S. and Le Bihan, J. (2000) Influence of compaction conditions on pore-size distribution and saturated hydraulic conductivity of a glacial till. Canadian Geotechnical Journal, 37(6), pp. 1184-1194.

4. PARTIALLY OXIDISED WASTE ROCK UNDER CHANGING CHEMICAL CONDITIONS

HANNA KAASALAINEN

4.1. Background

One of the main sources of uncertainty when predicting water quality at mine closure is the unknown long-term stability of secondary minerals and associated contaminants in waste rock dumps, which are characterized by complex mineralogical, geochemical, hydrological, and microbiological interactions. During mining operations, waste rock is typically deposited on the ground surface and is therefore exposed to oxidative weathering over time periods ranging from years to decades prior to the initiation of remediation measures at mine closure. During this time, secondary minerals may accumulate in the waste rock. Many secondary minerals such as ferrihydrite and schwertmannite are effective scavengers of metal(loid)s and may therefore contain significant quantities of potentially harmful elements. A common way of remediating waste rock is to apply a soil cover over the waste surface (Chapter 2) in order to limit oxygen (O_2) ingress and water percolation to the waste, thereby preventing sulfide oxidation by promoting anoxic conditions and limiting contaminant transport. However, there is a concern that the chemical conditions imposed by such covers may lead to the dissolution of secondary minerals and the subsequent release of the associated contaminants.

Only a few studies have explored the behavior of partially oxidized waste rock under changing chemical conditions caused by the application of a cover. Some lessons can be learned from studies on subaqueous disposal of partially oxidized waste rock and remediation of weathered mine tailings. Notably, dissolution of secondary minerals and consequent mobilization of metal(loid)s were found to have important effects on water quality in partially oxidized sulfidic mine waste under laboratory and field conditions (e.g. Simms et al., 2000; Moncur et al., 2009; Paktunc, 2013; DeSisto et al., 2017). While these studies provided useful insights into the processes involved, there are some important differences between tailings, waste rock under water-saturated conditions, and unsaturated waste rock. The sulfide oxidation process and the transport of O_2 and contaminants in waste rock dumps are much more complex than in tailings because of the greater heterogeneity with respect to physical, geochemical, and hydrological variables including the particle size distribution, porosity, and unsaturated flow (e.g. Sracek et al. 2004; Stockwell et al., 2006; Amos et al., 2015, Bailey et al., 2015; Langman et al., 2017). Since waste rock production is expected to increase greatly in the near future and more stringent requirements for mine remediation are being integrated into mine permitting and closure procedures, there is a clear need to better control element release from partially oxidized waste rock subjected to changing chemical conditions.

The Swedish mining industry is active and highly productive; in 2016, 62 Mtons of waste rock was produced by mining activities in Sweden (Swedish Geological Survey, 2017). In this study, the waste rock origin from two active open-pit mines operated by Boliden Mineral AB in northern Sweden. The aim was to assess assessing the potential mobilization of metals and metalloids from the partially oxidized waste rock upon initiation of anoxic conditions. An additional goal was to develop a suitable methodology for studying the impact of secondary

minerals. To this end, we set up unsaturated, free-draining column leaching experiments to study the release of sulfur and metals during leaching of partially oxidized waste rock with low carbonate (1%) and high (20%) sulfide contents under declining and limited O_2 conditions. The element release in these experimental systems was compared to the leaching behavior of the waste rock under atmospheric conditions, and is discussed in relation to the waste rock's geochemical and mineralogical characteristics.

4.2. Materials and methods

Partially oxidized sulfidic waste rock

Waste rock from two different mine sites was studied with greatly differ with respect to mineralogy and sulfur content, but both produce acidic metal-rich leachates (Table 4.1).

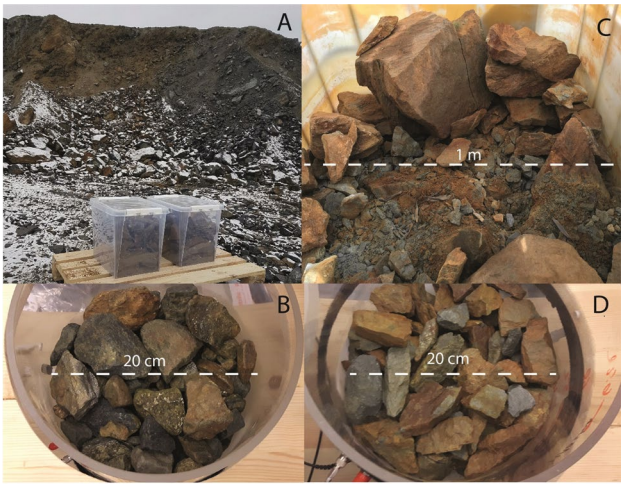

Figure 4.1. A. Top part of waste rock dump T5 at the Aitik mine, where the low sulfidic waste rock was collected. B. Low sulfidic waste rock in the column. C. One of the four pilot-scale cells in which the highly sulfidic waste rock had been leached for 5 years prior to sampling for this study. D. Highly sulfidic waste rock in the column.

The low sulfidic waste rock was supplied by Boliden Mineral AB from the Aitik Cu-Au-Ag(-Mo) mine – a low-grade porphyry copper deposit overprinted by iron oxide-copper-gold alteration (Wanhainen, 2005). It originates from the upper lift of one of the oldest waste rock dumps at the Aitik mine: T5. This dump has been used to store potentially acid-producing waste rock as well as marginal ore. The samples is not representative of the Aitik waste rock in general, but considered suitable for the present study because of its prolonged exposure to oxidative weathering. Several previous studies have examined the leaching behavior, geochemistry, and mineralogy of the Aitik waste rock (e.g., Strömberg and Banwart, 1994; 1999a,b; Eriksson and Destouni, 1997a,b). Biotite-gneiss is the main rock type of the ore deposit, while sericite to muscovite schist and skarn-banded gneiss are present in the waste rock (Strömberg and Banwart, 1994). The acid-producing waste rock gives rise to an acidic leachate with elevated concentrations of Al, Cu, and Zn because of pyrite oxidation and pH buffering due to weathering of silicate minerals, primarily biotite and plagioclase feldspar, following depletion of the calcite in the waste rock (Strömberg and Banwart, 1994; 1999a,b). O´Kane Consultants (2015) suggested that the dissolution of melanterite and jarosite-type minerals formed during waste rock weathering could profoundly impact post-closure water quality. Despite the expected limited water percolation through the cover at this mine, the increased precipitation, as a consequence of climate change, is predicted to provide enough water to flush out acidity stored in the secondary minerals, maintaining an acid pH similar to that observed today over ca. 50 years (O´Kane consultants, 2015). The possible impact on water quality by the dissolution of secondary mineral is not limited to the potential release of acidity, Fe, and S: but also to trace metals and metalloids accumulated in these phases.

Table 1.1. Selected geochemical and mineralogical characteristics of the studied waste rocks.

	Low-sulfide waste rock	**High-sulfide waste rock**
Deposit and rock type	Porphyry-type Cu-deposit with iron oxide-copper-gold overprint[a] Biotite-gneiss, sericite to muscovite schist, skarn-banded gneiss[b]	Volcanic-associated massive sulfide deposit [c] Quartz-feldspar porphyritic pumice breccia-sandstone [c]
Mined elements	Cu, Au, Ag	Cu, Zn, Au, Ag
Exposed to weathering	decades	6 years
Sulfide minerals	Pyrite, pyrrhotite, chalcopyrite, sphalerite, galena, molybdenite, bornite[b,d,e]	Pyrite, chalcopyrite, sphalerite, arsenopyrite, bournonite [e,f]
Gangue minerals	Quartz, K-feldspar, albite, anorthite, muscovite, biotite, amphibole, chlorite, epidote, magnetite, calcite, pyroxene, siderite, titanite, barite, apatite, garnet, zircon [b,d]	Quartz, muscovite, chlorite, calcite[f,g]
Leachate characteristics	Field seepage pH 4.1, 1150 mg/l SO_4, 43 mg/L Al, 288 mg/L Ca, 13.3 mg/L Cu, 6.8 mg/L Mn, 1.9 mg/L Zn [h]	pH<2, SO_4 and Fe at g/L –level, As, Cu, Zn at hundreds of mg/L level (unsaturated pilot cell)[i]
Sulfur contents [f]	Total-S: 1.2 %-TS Sulfate-S: 0.02 (<0.01) %-TS	Total-S: 20.2 %-TS Sulfate-S: 0.16 (0.09) %-TS
Carbon contents[f]	Total-C: 0.02 %-TS Carbonate-C <0.05	Total-C: 0.11%-TS Carbonate C 0.07%

[a]Wanhainen (2005); [b] Strömberg and Banwart (1994) for ore and waste rock, [c]Montelius (2005), [d]Wanhainen (2005), [e]Boliden Mineral Ab QEMSCAN on the waste rock considered in the present study [f]This study, see methods for more detailed information [g]Nyström et al. (2019), [h]O´Kane consultants (2015), [i]Alakangas et al. (2013)

The high sulfidic waste rock originates from Maurliden a Zn, Au, and Ag mine associated with massive volcanic sulfide deposit located in the Skellefte field, northern Sweden (Montelius, 2005, Table 4.1). The waste rock with a very high sulfide content (ca. 60%) has been used in various experiments within the Stop-Ox project (see e.g. chapter 2, Alakangas et al., 2013), but is not

representative of the mine's bulk waste rock. Previous studies on this high sulfide waste rock have shown that its mineralogy is dominated by pyrite and quartz, with traces of muscovite, chlorite, and calcite, as well as chalcopyrite, bournonite, sphalerite, and arsenopyrite (Nyström, et al., 2017, Table 4.1). The chemical composition of the leachate water formed from this waste rock has also been previously reported (chapter 2, Alakangas et al., 2013). The leachate had a very low pH, and high concentrations of S and Fe as well as metals and metalloids.

The waste rock used in this study had undergone ca. 6 years of weathering before sampling: first ca. one year in the field before collection and then 5 years of leaching in four pilot-scale experiments conducted under saturated and non-saturated conditions at field condition (Alakangas et al. 2013). Based on its sulfide-S and Fe contents, the waste rock subsample used in this study can estimated to consist of 38 w-%, while calcite made up to <1 w-% (0.6%) of the waste rock, based on the low amount of inorganic C (0.07%) present in the waste rock (Table 4.1). The determination of sulfate-S confirmed that S was almost completely in the form of sulfide, with only ca 1 %, of the total S being present in the form of sulfate.

For the column leaching experiments, high sulfide waste rock in the size range of 0.1-10 cm were hand-picked from four pilot scale experimental cells, while the low-sulfidic waste rock were sampled and supplied by Boliden Mineral AB. The waste rock samples were dried at room temperature, mixed, sieved to desired particle size (passing 45.5 mm sieve size, >12.5mm), and subdivided into four subsamples by coning and quartering. The partially oxidized waste rock particles were initially coated with secondary precipitates of reddish-brown and brownish red colors, characteristic for Fe(III) hydroxide and hydroxysulfate minerals that are among the most common secondary minerals forming in mine environment (Bigham and Nordstrom, 2000). One of the four subsamples was used for geochemical and mineralogical analyses listed in Table 4.2, while the other subsamples were subjected to column experiments (Figures 4.1, 4.2). To better constrain the association of various elements to the secondary minerals and to get insight into which elements may become mobilized under anoxic conditions, the samples were subjected to the 7-step sequential extraction process Dold (2003), which involves leaching with the following solutions:

Step 1: de-ionized water leach for water-soluble fractions such as metal salts, and gypsum;

Step 2: ammonium acetate leach (pH 4.5, 2h) for the exchangeable fraction and to dissolve carbonates and smectite

Step 3: cold oxalate leach in darkness (1h, pH 3) to dissolve easily reducible Fe-Mn(-Al) (hydr)oxides and hydroxysulfates

Step 4: hot oxalate extraction (80 °C, 2h, pH 3) to reduce residual Fe(-Mn-Al) (hydr)oxides.

Step 5: hot hydrogen peroxide leach to dissolve organic matter and supergene Cu-sulfides

Step 6: potassium-chlorate - hydrochloric acid followed by boiling nitric acid to dissolve primary sulfides

Step 7: four-acid leach (HCl, HF, HClO4, HNO3) to dissolve the residual fraction.

Table 4.2. Geochemical and mineralogical analyses of the waste rock samples.

Analyses	Method	Laboratory	Samples
Whole rock composition	Li-borate fusion and for 4 acid digestion (Ag, Cd, Co, Cu, Li, Mo, Ni, Pb, Sc, Zn) followed by ICP-OES and ICP-MS, ion selective electrode for F, Cl	ALS Global	Waste rock at start
Whole rock composition	NaOH-fusion followed by ICP-OES (and ICP-MS for REE, U)	SGS	Waste rock at start, highly sulfidic waste rock at the end
Sulfur and carbon contents	Carbonate-C (C-GAS05), carbonate-leachable S (S-GraO6), HCl-leachable S (S-GRa06a), total C (C-IR07)and S (S-IR08)	ALS Global	Waste rock at start
Mineralogy	QEMSCAN	Boliden Mineral AB	Low sulfidic waste rock at start
Mineralogy	Optical microscopy, XRD, Raman, SEM-EDS	LTU	Highly sulfidic waste rock (at start and selected analyses at the end, precipitates from column)
Element associated with waste rock	Sequential extraction (Dold, 2003), steps 1-4 for highly sulfidic waste rock and steps 1-4, and 5+6 for low sulfidic waste rock (see text)	SGS	Waste rock at start, highly sulfidic waste rock at the end

For the high- sulfidic waste rock, only the first four steps were performed, and the composition of the resulting extracts was compared to the composition of the whole rock determined by NaOH-fusion. For the low sulfidic waste rock, extraction steps 5 and 6 (which are intended to dissolve sulfide minerals) were also performed. Elements solubilized in steps 3 and 4 (the cold and hot oxalate leaches, respectively) are of particular interest in this work because the extracts formed in these steps are considered to represent the fraction that may be reactive under anoxic and reducing conditions. The oxalate leaches are intended to solubilize secondary Fe(III) (hydr)oxides and hydroxysulfates, and to separate the poorly crystalline phases from the more stable and crystalline ones (Dold, 2003). Step 3 has been shown to solubilize schwertmannite and the less ordered ferrihydrites (2-line), and to partially dissolve secondary jarosite and more highly ordered (e.g. 6-line) ferrihydrites (Dold, 2003). Step 4 attacks the remaining, more stable and crystalline secondary Fe(III) phases including higher ordered ferrihydrite (e.g., 6-line), goethite, secondary and primary jarosite, and primary hematite (Dold, 2003).

Together with the mineralogical information, the elemental ratios of the extracts were used to estimate which minerals were solubilized in each sequential extraction step. In this work, some Al, Mg, and in some cases K as well was extracted in steps 3 and 4. While Al is commonly

associated with Fe(III)-minerals, it is also possible that some silicates may have been dissolved by the acidic oxalate (e.g., Arshad et al., 1972). Unfortunately, the Si content of the extracts was not determined, making it impossible to assess the degree of silicate dissolution

Unsaturated column-leaching experiments

Uncrushed partially oxidized waste rock with a particle size corresponding to medium to very coarse gravel was leached in unsaturated free-draining column experiments for 12 to 15 months. The waste rock mass per column was 5.8 kg and 6.8 kg for the high and low sulfidic waste rock, respectively. The columns' design enabled operation under free-draining and anoxic conditions (Figure 4.2). The columns consisted of Perspex glass tubes with polypropylene caps and a perforated plate, and an irrigation system at the cap of the column. All experimental materials were thoroughly cleaned before the start of the experiments. The waste rock was irrigated by feeding MQ-water into the column; the water then drained through the waste rock and collected at the column base. The waste rock was supported by a perforated plate and filter (105 µm PP) located 3-4 cm above the base of the column, so the water at the bottom of the column was not in contact with the waste rock.

Column leaching experiments

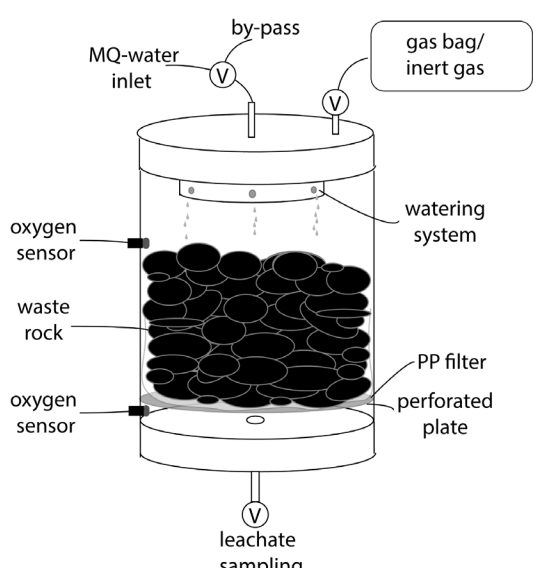

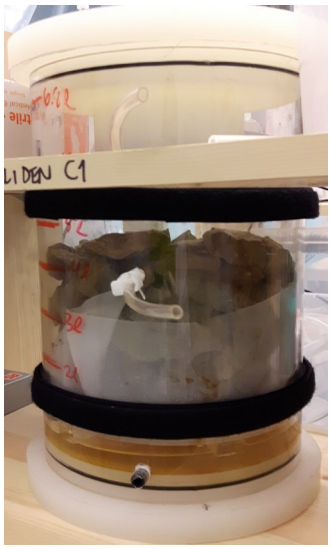

Figure 4.2. Setup for column leaching experiments.

The leachate was sampled at the base of the column ca. 4 hours after irrigation. The leachate was either drained into containers or (under limited O_2 conditions) sampled with the aid of an inert gas and transferred directly to the filtration apparatus. All the equipment used during sampling and filtration was thoroughly cleaned with acid (5% nitric acid) and soaked with MQ-water before use.

The pH, electrical conductivity (EC), and oxidation-reduction potential (ORP) of the leachates were determined immediately after sampling using electrodes (Table 4.3). Selected samples were then analyzed for over 70 major and trace elements, Fe redox speciation, and F, Cl and SO_4 concentrations (Table 4.3). For major and trace element analyses, and determination of Fe redox species concentration, samples were filtered (0.2 um) and acidified with trace metal-free (Merck, Suprapur) nitric or hydrochloric acid, respectively. Selected unfiltered samples were also analyzed. Iron redox speciation measurements for leachate samples from the low- sulfidic waste rock were terminated after the first 1-2 months due to analytical problems. The cause of these problems is unknown but is probably related to the samples' high relative content of Fe(III) and richness in Cu. Samples for fluoride determination were filtered but not further treated. Oxygen concentrations in the columns were determined using O_2-sensor spots (PreSens Precision Sensing Gmbh) placed at two different levels in the column. The sensor spots were calibrated against fully air-saturated (100 sat-%) and O_2-free water (0 sat-%). However, the data are only considered semi-quantitative because the humidity in the column was not measured and humidity is known to strongly affect O_2 saturation, and also because only a limited number of calibrations could be performed during the experimental period.

Table 4.3. Leachate water analyses.

Parameter	**Method**	**Laboratory**
pH	Glass electrode	LTU
EC	TetraCon electrode	LTU
OPR/Eh	Pt-electrode (calculated to Eh)	LTU
Fe(II), Fe_{total}	Ferrozine spectrophotometry (To et al., 1995; Stookey, 1979)	LTU
Major and trace elements	Quantitative screening with ICP-MS for over 70 elements	ALS Scandinavia
S (SO_4)	Calculated based Stot determined by ICP-MS, gravimetry, turbidimetry	ALS Scandinavia, ALS Global; LTU
F	Ion selective electrode	ALS Global
O_2	Fluorescence sensor spots (Presens)	LTU

The waste rock was leached on a weekly basis except during the first 6-10 leaching cycles, when leaching was performed twice per week. The amount of irrigation water (430 mL) was chosen based on the predicted future precipitation rates at Boliden mineral AB's Aitik mine site in northern Sweden (O´Kane consultants, 2015), with each leaching cycle being assumed to correspond to a single week. An exception was the first leach of the highly sulfidic waste rock, which was performed using 600 mL of water. Assuming that the only O_2 entering the column is that dissolved in the irrigation water, the O_2 input to the column during each cycle (ca. 0.1 mmol) is relatively similar to that estimated to enter through a well-functioning cover system

(1 mol O_2/m^2 per year, corresponding to 0.5 mmol O_2 in the column per cycle) (Boliden, 2015). Note that the development of anoxic conditions in the leaching experiments differed markedly between the low and highly sulfidic waste rocks, as discussed in sections 1.3.1 and 1.3.2.

After the first 6–10 leaching cycles, during which the pH, redox potential (Eh), and electric conductivity (EC) of the leachate water stabilized, one of the columns was made gas-tight and flushed with inert gas to remove O_2.

Geochemical and mass calculations

Geochemical calculations, including calculations of aqueous ionic activities, aqueous species distributions, and mineral saturation state, were performed using PHREEQC version 3.3.2 (Parkhurst & Appelo, 1999) with the wateq4f.dat thermodynamic database (Ball & Nordstrom, 1991). The ion imbalance for samples subjected to full chemical analysis was within ±12%, and only these samples were considered in the calculations. For the highly sulfidic waste rock, the measured Fe(II) and Fe(III) concentrations were used in the calculations, while all S was assumed to be present as sulfate. Because few measurements of the relative abundance of Fe(II) and Fe(III) in the low sulfidic rock leachate were available, all of the dissolved iron in these leachates was assumed to be present as Fe(III), in accordance with the limited analytical data and the measured Eh values. For calculations involving Fe(III) minerals, thermodynamic data for Fe(III) mineral solubility was taken from the literature. A range of solubility products have been reported for ferrihydrite, which appear to depend on its degree of ordering and to reflect the rate of hydrolysis resulting in its formation (Schwertmann et al., 1999). Here, we used the values for freshly precipitated ferrihydrite, goethite, and jarosite as recorded in the Wateq4f database (Ball and Nordstrom, 1991). The solubility constants of the more ordered ferrihydrites, namely 2- and 6-line ferrihydrites, were those compiled and reported by Stefánsson (2007), while the solubility constants used for schwertmannite were taken from Majzlan et al. (2004), who integrated results reported by Bigham et al. (1996), Yu et al. (1999), and Kawano and Tomita (2001).

The rates of solute release during the experiments were estimated by computing the average release rate (moles per kg of waste rock per cycle) over the first 30 cycles for both waste rock types under two experimental conditions. For the highly acidic waste rock, these rates represent the solute release under conditions where the O_2 input to the column is limited to that supplied with the ingoing water, which remained constant throughout the experiment. In the case of the low sulfidic waste rock, however, O_2 levels declined between cycles 30–52 because of the conditions developing within the column (see sections 1.3.1, 1.3.2). The total mass released during the experiment was assessed by weighing the leachates and considering their chemical composition. Because elemental compositions were only determined for a subset of the leachate samples, concentrations for samples lacking analytical data were estimated by assuming linear concentration changes. Therefore, the reported total mass release values are estimates with uncertainties. However, they are sufficient to enable comparisons between the total element composition of the leachate and the sequential extraction results for the waste rock.

4.3. Main results

Waste rock characteristics

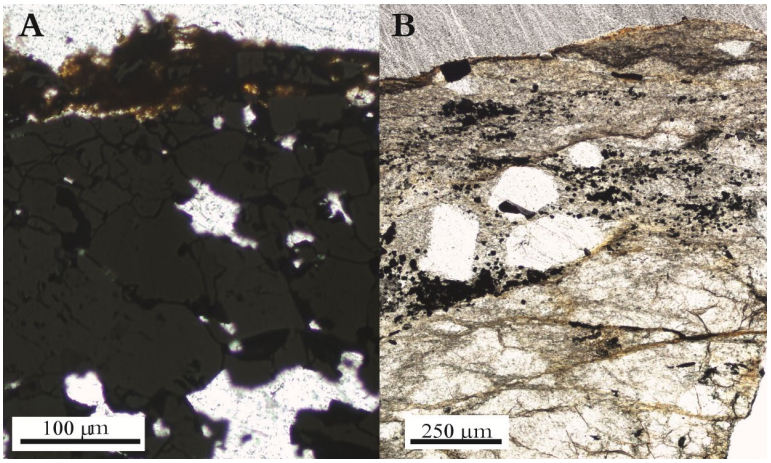

Figure 4.3. Optical microscopic images of highly sulfidic waste rock. A. Sulfide-rich particle surrounded by Fe precipitates. B. Silicate particle stained with Fe.

Despite its intense coloration, both the mineralogical and geochemical analyses of the partially oxidized highly sulfidic waste rock indicated that it exhibited only limited accumulation of secondary minerals. Optical microscopy revealed that pyrite grains in the sulfide-rich waste rock were largely unaltered (Figure 4.3A), but were typically surrounded by a thin reddish-brown layer, while silicate-rich waste rock particles were stained with a reddish-brown color (Figure 4.3B). The sequential extraction data indicated that less than 3% of the Fe and Al and 1.6% of the S in this rock was associated with secondary minerals (Table 1, Table 4). This is consistent with the high solubility of Fe, S, and Al under acidic conditions, which would be the predominant conditions under which the waste rock weathered prior to the experiments. Moreover, the formation of secondary minerals was likely limited by the surface area of the relatively large waste rock particles used in this study.

The secondary minerals identified using XRD, Raman spectroscopy, and SEM-EDS at the start of the experiments included gypsum, schwertmannite, ferrihydrite and goethite. Additionally, the sequential extraction data suggest that other phases such as Al-hydroxysulfates and jarosite may also have been present. The solubilization of Ca during extraction steps 1 and 2 is consistent with the presence of gypsum in the waste rock. In addition to gypsum, small quantities of other easily soluble salts may have also been present given that small quantities of Na, Mg and Mn were solubilized in step 1 of the sequential extraction. This hypothesis is also supported by the release of several elements (Fe, S, and many metals and metalloids) into the leachate during the first three leaching cycles (Figures 4.2, 4.3); such releases are commonly observed in humidity cell tests and are thought to arise from the dissolution of soluble salts (e.g. Sapsford et al., 2009; Maest and Nordstrom, 2017). In addition to Ca, several other elements including Al, Fe, S, Mn, Zn, and rare earth elements (REE) were solubilized in step 2, representing the weakly adsorbed and exchangeable metals. In addition to the exchangeable fraction, calcite and clays may dissolve during this step (Dold, 2003). The level of extracted Ca is consistent with the calcite content estimated based on the carbon concentration of the waste rock, which was observed to be associated with kaolinite (Nyström, unpublished data). The existing data are insufficient to determine whether the elements solubilized during step 2 are adsorbed or associated with the calcite and/or the clay. However, their release may be of concern under acidic conditions.

The fraction extracted during sequential extraction step 3 is considered to be that most prone to dissolution under declining O_2 conditions, so the release of experiments associated with this step was of particular concern. Trace elements released in this step - As, Cu, and Pb, along with Mn and Zn – are considered to be those most prone to dissolution under declining O_2 conditions. Of these elements, Cu, Pb, Mn, and Zn were also released during step 4. However, highly reducing conditions are required for the dissolution of this fraction. Previous experimental studies have shown that these metals differ in their affinity for Fe(III) minerals and adsorb at different pH values (e.g., Lee et al., 2002, Sidenko and Sheriff, 2005; Nagano et al., 2011). For example, Zn was found to accumulate to schwertmannite, while Cu has a higher overall affinity to accumulates into crystalline phases such as goethite (Sidenko and Sheriff, 2005). This is consistent with results obtained in the present study.

Table 4.4. Summary of elements' association with secondary mineral phases and elements identified to be of major concern under changing chemical conditions.

	Low-sulfide waste rock	**High-sulfide waste rock**
Fraction of elements in extraction steps 1-4	Fe (22%), S (<6%), Al (3.8%)	Fe (2.6%), S (1.6%), Al (2.6%),
Secondary minerals identified	Ferrihydrite, goethite, schwertmannite, siderite, kaolinite	Ferrihydrite, goethite, schwertmannite, gypsum, kaolinite
Metal(loid)s associated with extraction step 3	Fe, Al , Cu, Mn, Zn, REE	Fe, Al, As, Cu, Mn, Zn, Pb
Metal(loid)s associated with extraction step 2	Fe, Al, Mn, Cu, Zn, Pb	Fe, Al, Zn, Mn, REE
Metal(loid) at moderately to very high level in leachate (SEPA, 2000) under atmospheric conditions (after cycle 30)	Cd, Cu, Ni, Zn, Pb	As, Cd, Cu, Zn

Based on the sequential extraction data, we anticipated that As, Cu, and Pb, together with Zn and Mn and the major elements Fe, S, and Al would become mobilized in the experiments conducted under limited O_2 conditions. However, the residual fraction (which includes sulfide and silicate minerals) was particularly rich in Cu, Zn, Pb, and especially As, in agreement with its high content of unoxidized sulfide minerals. All these elements are commonly present in pyrite (Abraitis et al., 2004), but arsenopyrite, chalcopyrite, bournonite, and sphalerite have previously been identified in the studied waste rocks (Nyström et al., 2019). Therefore, an overall improvement of water quality is expected if the waste rock is stored under anoxic conditions that limit sulfide dissolution.

Development of anoxic conditions

In the case of the highly sulfidic waste rock, an inert gas was used to reduce the O_2 concentration below 60 sat-%. When this was done, the O_2 concentration decreased rapidly without further intervention, presumably due to consumption by sulfide oxidation, and the O_2 concentration fell from 100 sat-% to 0 sat-% within 10 cycles of the column's sealing (Figure 4.4). During the 12 months of leaching, no effort was made to remove O_2 from the ingoing MQ water, so O_2 dissolved in MQ-water entered the column during each leaching cycle (Figure 4.4). Rough calculations based on the O_2 sensor data indicate that the amount of O_2 entering the column may have been 5-10x higher than initially expected (see section 1.2.2), corresponding to ca. 0.5-1 mmol O2 per cycle. The rate of oxygen ingress thus closely matched that expected for a typical real-world cover system. The O2 introduced in each leaching cycle was quickly (within 1-2 days) consumed in the column, presumably by sulfide oxidation (Figure 4.4). Therefore, O_2 availability was limtied between cycles 20 and 50. After 12 months of leaching (from cycle 50 onwards), the incoming MQ water was degassed by bubbling with inert gas for 20 minutes before irrigation to minimize the amount of O_2 entering the column. Despite this, traces of O_2 were detected in the continuous measurements (Figure 4.4).

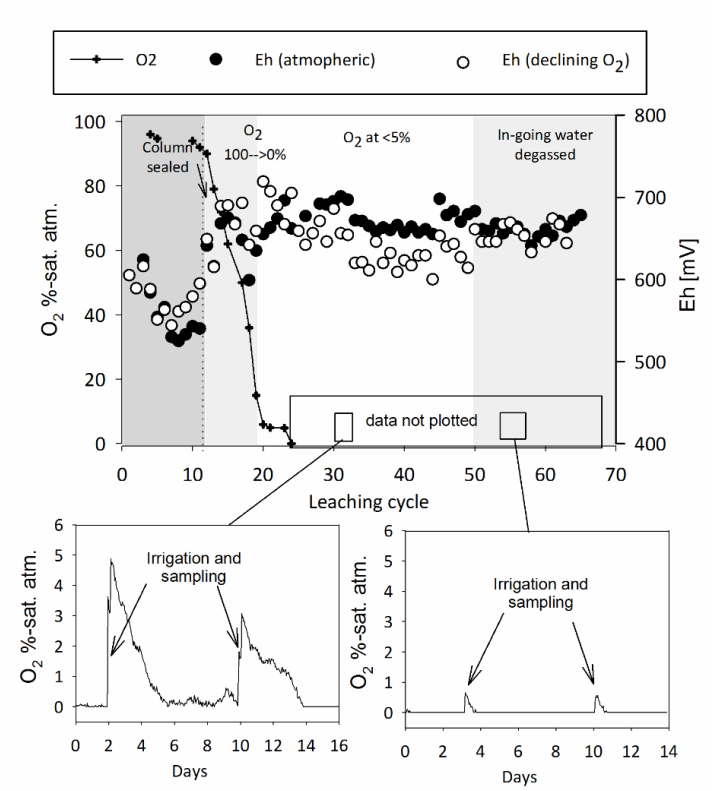

Figure 4.4 Declining O_2 concentrations and the development of anoxic conditions during the experiment using highly sulfidic waste rock. The leachate water redox potential (Eh) (closed and open circles, respectively) measured with a Pt-electrode was similar under atmospheric and declining/limited O_2 conditions, and was clearly decoupled from the O_2 concentration. The small figures illustrate the ingress and gradual disappearance of O_2 upon irrigation and sampling of the leachate.

Leachate chemistry

The evolution of the pH, EC, and S and Fe contents of the leachates from the two experiments using the highly sulfidic waste rock are shown in Figure 4.5. During the first 11 leaching cycles, both columns were leached under atmospheric conditions. The leachate chemistry mirrors that typically observed during the initial leaching of previously weathered sulfidic material in humidity cell tests, with an "early flush" due to the dissolution of soluble salts prior to the start of sulfide oxidation (e.g., Sapsford et al., 2009; Maest and Nordstrom, 2017). During this period, the leachate has a low pH, high EC, and elevated solute concentrations. The early flush is followed by an increase in pH and a decrease in EC and solute concentrations that persists until cycle 10 (Figure 4.5). After cycle 11, one of the columns was made gas-tight, limiting the availability of O_2, while the other was left open to the atmosphere.

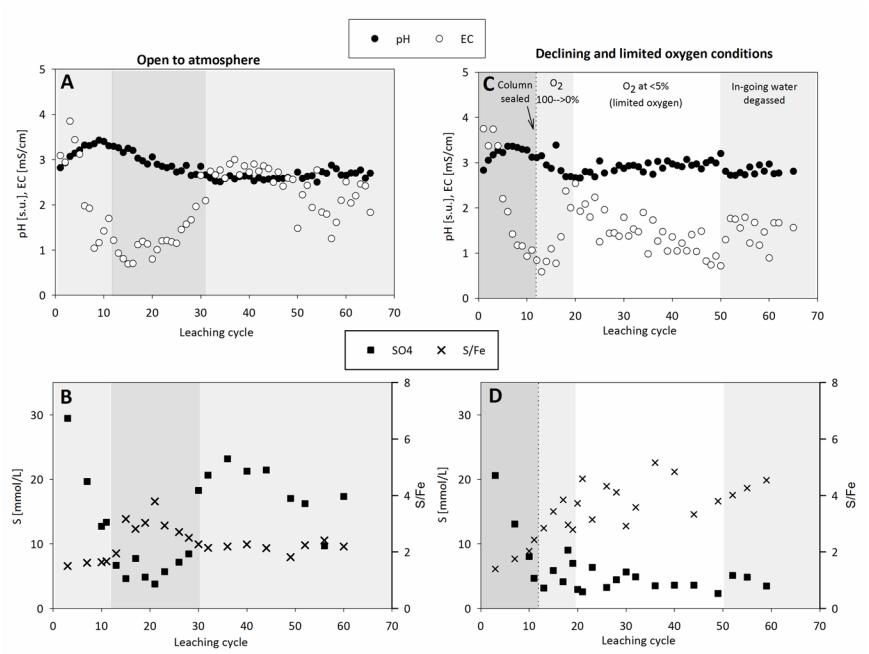

Figure 4.5. Evolution of the pH, EC, Eh, SO_4 concentration, and S/Fe molar ratio of the leachates formed from the highly sulfidic waste rock under atmospheric O_2 conditions (A, B) and under limited and declining O_2 conditions (C,D).

When leaching was performed under atmospheric conditions, the leachate's pH continued to decrease while its EC and concentrations of Fe, SO_4, and many metals and metalloids continued to increase until cycle 30–40 (Figures 4.5, 4.6), when the leachate's Eh reached 600 mV (not shown). Under these conditions, the leachate's S/Fe ratio closely approached that in pyrite (S/Fe=2) after cycle 30 (Figure 4.5). These events indicate the start of sulfide oxidation and acidity production, as previously described by several authors (e.g., Sapsford et al., 2009; Maest and Nordstrom, 2017).

Upon leaching of waste rock under atmospheric conditions, the concentrations of most solutes initially increased, peaking between leaching cycles 30 and 50 (i.e. after ca. 9-12 months' leaching), but then leveled off or started slowly decreasing. Additionally, there was a minor increase in solute concentrations during cycles 12-20, which coincided with decreasing pH. The release of sulfur and metals upon leaching of partially oxidized waste rock appears to be largely dominated by pyrite oxidation, as indicated by the Fe/S ratio closely approaching that of pyrite (Figure 4.5). The concentrations of metals and metal(loid)s appear to increase overall, and their maxima appear to coincide with the peak of the sulfide oxidation rate. Sulfide oxidation thus seems to be the main process responsible for metal(loid) release under atmospheric conditions, either because of the direct association of these elements with the sulfides or due to the dissolution of gangue minerals under the acidic conditions generated by sulfide oxidation.

The concentrations of some metals, including Cu, Zn, and Mn rose modestly between cycles 12 and 25 (Figure 4.6) before peaking around cycle 30, when the S/Fe ratio (ca. 2.5-4) differed appreciably from that of pyrite (2), which was approximately equal to the S/Fe ratio observed during the remainder of the experiment (Figure 4.5). This indicates that sulfide oxidation was not the only process causing the release of metal(loid)s. Other processes that may have contributed to the observed release include the dissolution of secondary or primary minerals and/or desorption from mineral surfaces caused by a decrease in the pH or a change in the waste rock surface area due to mineral dissolution. Indeed, geochemical calculations suggest that

dissolution of secondary Fe(III) minerals such as schwertmannite occurred briefly around cycle 20. These calculations, which are based on the levels of aqueous Fe(II) and Fe(III) in the leachate and observed Fe(III) minerals (data not shown), also indicate that Fe(III) mineral solubility may limit the release of Fe and that of other solutes under these conditions, and may control the leachate pH (Kaasalainen et al., 2019). This would be consistent with the conclusions of several earlier studies (e.g., Bigham et al., 1996; Bigham and Nordstrom, 2000). However, the mass of Fe mass released during the experiment as a whole appeared to be largely independent of these considerations because the overall S/Fe ratio closely matched that of pyrite. This is consistent with high mobility of Fe under acidic conditions.

A different pattern was observed in the leachate formed under declining and limited O_2 conditions. After sealing the column on cycle 11, the concentrations of all solutes peaked around cycle 20, coincidentally with a decline in O_2 levels from 100 to <5 sat-%. The solute concentrations then fell to a relatively low level and decreased slowly until cycle 50, at which point they started increasing slightly when degassing of the ingoing water was initiated. These changes are reflected in the leachate EC, which is a general indicator of leachate quality (Figure 4.5), and also in the leachate's measured concentrations of As, S and Zn over time (Figures 4.5, 4.6). The leachate remained strongly acidic throughout the experiment, but it exhibited a slightly increasing trend in pH until cycle 50. The leachate's Eh (measured with the Pt electrode) remained above 600 mV throughout the experiment (Figure 4.4) and was clearly decoupled from the O_2 concentrations but was very similar to the value expected based on its aqueous Fe(II) and Fe(III) contents (Kaasalainen et al., 2019). The leachate's S/Fe ratio differed from that observed under atmospheric conditions and that in pyrite (S/Fe=2), indicating significant release from other sources or Fe uptake to secondary minerals (Figure 4.5).

Figure 4.6 shows the measured concentrations of the metal(loid)s As and Zn in the leachate under two experimental conditions over time. Of the metals and metalloids, As and Cu exhibited the clearest concentration peaks, but their concentrations only remained near the peak levels for a few cycles under declining O_2 conditions before falling rapidly. Aluminum, Mn, and Zn were also released, albeit to a lesser extent, and the subsequent decrease in concentrations was less pronounced than for As, and Cu. This pattern of a brief release of these elements was replicated towards the end of the experiment, when the O_2 input to the column was reduced further by degassing the ingoing MQ-water (from cycle 50 onwards).

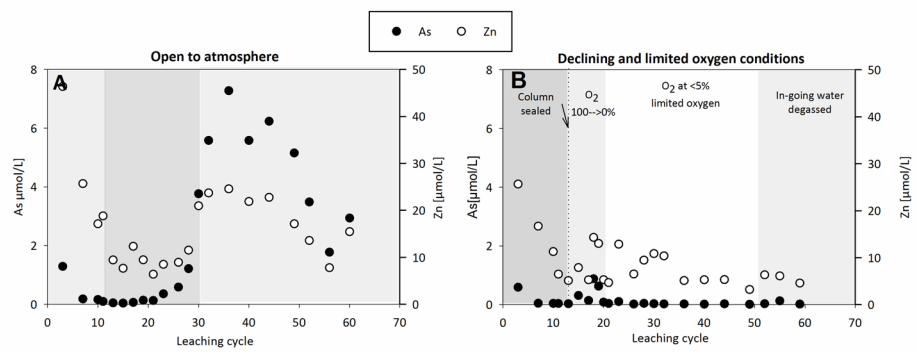

Figure 4.5. Arsenic and Zn concentrations in the leachate formed by leaching of the highly acidic waste rock under atmospheric (A) and declining and limited O_2 conditions (B).

Sulfide oxidation was partially suppressed under limited O_2 conditions, which was assumed to be the primary reason for the reduced solute release under these conditions. The sulfate release observed after cycle 30 agrees reasonably well with the amount that would be expected to result from sulfide oxidation based on the estimated availability of O_2. However, the leachate's S/Fe ratio differed markedly from that observed under atmospheric conditions and that of pyrite, indicating that low oxygen levels resulted in the preferential release of sulfate and the immobilization of Fe. This was attributed to the dissolution of schwertmannite, which would release SO_4 and Fe into the leachate, with the Fe subsequently being immobilized into Fe(III) hydroxide minerals (goethite, ferrihydrite). This hypothesis is supported by both thermodynamic calculations and mineralogical observations (Kaasalainen et al. 2019).

The transformation of schwertmannite into goethite or an S-poor Fe(III) phase accompanied by S release has been discussed extensively in the scientific literature and observed to occur upon aging of schwertmannite, under anoxic conditions, and in the presence of Fe(II) (e.g. Bigham et al., 1996; Acero et al., 2006; Burton et al., 2008). Therefore, the decrease in the sulfate concentration of the leachate caused by the suppression of sulfide oxidation is likely to be buffered by the schwertmannite dissolution. Such buffering by the Fe-system may partly explain why the leachate's pH remained low while its Eh (measured using a Pt-electrode) remained high (ca. 600 mV) throughout the experiment, in agreement with the measured Fe(II) and Fe(III) concentrations (Kaasalainen et al., 2019). However, the Fe concentrations formed upon leaching of partially oxidized waste rock under limited O_2 conditions were 89% lower than those formed under atmospheric conditions, with Fe(III) concentrations exhibiting a particularly pronounced decline. The limited mobility of Fe has important implications because Fe(III) is considered to be a major oxidant of pyrite at low pH. In the long term, it seems likely that the pH would continue rising if sulfide oxidation (which is the main source of acidity) were suppressed for an extended period, once the Fe(III) minerals that buffer the low pH were depleted. The small amount of neutralizing minerals present in the waste rock, however, will not provide significant buffering on its own, meaning that acid production must be actively prevented.

Effect of declining and limited O_2 conditions on metal(loid) release

The overall leachate quality formed under limited O_2 conditions during the final months of the experiments was clearly superior to that of the leachate formed under atmospheric conditions, despite the limited improvement in pH. The release rates of Fe, As, Cu, SO_4, Al, Mn, Zn, and Pb, to a lesser extent, were all clearly lower under the limited O_2 conditions than under atmospheric conditions (Figure 4.7). Additionally, the maximum concentrations reached under the declining O_2 conditions were typically lower than those observed under atmospheric conditions (e.g., Figure 4.6). Despite these important reductions in the release of metals and metalloids, however, As, Cu and Zn were still released at concentrations considered moderately or very high according to the SEPA (2000) standards.

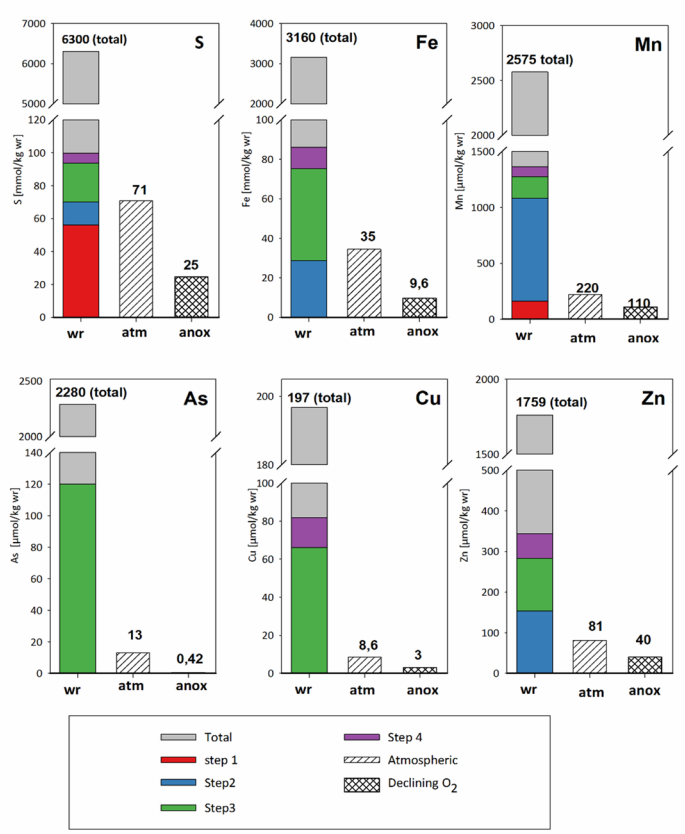

Figure 4.7. Comparison of the elements solubilized in the sequential extractions, and the estimated total mass of each element leached during the 15-month leaching experiment under atmospheric and declining O_2 conditions for highly sulfidic waste rock.

Despite the overall decrease in the release rate, the concentrations of many metals (As, Al, Cu, Mn, Zn) peaked briefly under the declining O_2 conditions before falling to a lower level (e.g., Figure 4.6). Reducing the O_2 concentration further caused another (smaller) peak in solution concentrations, indicating that further changes in environmental conditions could trigger additional releases. The released elements were detected at high concentrations in the step 3 extracts during the sequential extraction process. The step 3 extraction dissolves minerals such as schwertmannite, suggesting that these minerals also begin dissolving when the O_2 concentration declines, which is not unexpected. The observed solute concentration peaks can be attributed to remobilization of these elements from the secondary minerals due to this dissolution and/or the resulting decrease in the surface area available for adsorption. However, the extent of this metal(loid) mobilization appears to be limited, probably because the released elements are incorporated (to at least some degree) into the Fe(III) oxyhydroxide phase formed under limited O2 conditions (Kaasalainen et al., 2019). Unfavorable electrostatic attractions will limit the adsorption of the cationic metals Al, Mn and Zn on the Fe(III) mineral surface, which is positively charged under acidic conditions. Moreover, the low pH means that these metals may continue to be released from gangue minerals, or possibly from the exchangeable/carbonate fraction. The differences in the release of various metal(loid)s are thought to arise from differences in aspects of their geochemical behavior such as their aqueous speciation, their association both initially and during the

experiment with the secondary phases (including both their incorporation into secondary minerals and their sorption behavior), and their differing origins.

Figure 4.7 shows that the total mass of metal(loid)s, Fe, and S released during the experiments can be explained by their mobilization from the water soluble, exchangeable, and reducible fractions that are solubilized during steps 1-4 of the sequential extraction process. Since sulfide oxidation clearly affects the leachate composition, only a fraction of the elements associated with these phases was released during the 15-month experiment; this was at least partly due to the limited contact time between the water and the waste rock in these experiments.

Low-sulfidic waste rock

Waste rock characteristics

The low sulfidic waste rock had a total S content of 1.2% TS, and sulfate sulfur only accounted for 0.02% TS (Table 1). As much as 22% of its total Fe was associated with the step 3 and 4 extracts from the sequential extraction, which represent various secondary Fe(III) hydroxysulfates and (hydr)oxide minerals (Table 4). Additionally, 0.6% and 3.3% of the total Fe was solubilized in steps 1 and 2. Around 25% of the total Fe was associated with the sulfide fraction, with the remainder presumably existing as silicates such as chlorite. The relatively high mass of Fe present as secondary Fe(III) (hydr)oxides agrees well with the relatively low concentration of Fe in the seepage water at the mine site, which has a pH of around 4. The absence of S in the step 3 and 4 extracts is notable, indicating that the waste rock used in this work contains only small quantities of Fe(III)-sulfate phases such as schwertmannite or jarosite. In keeping with this conclusion, the QEMSCAN data indicate that the rock contains ferrihydrite, small amounts of schwertmannite, and goethite, which dissolve in extraction steps 3 and 4, respectively (Table 4). However, no metal sulfate salts or jarosite were detected. Siderite was observed, and is probably the source of the Fe solubilized in extraction step 2. Based on the siderite mass from the QEMSCAN analyses and the total carbon content (0.02%TS) determined for the waste rock (Table 1), siderite appears to be the main carbonate present in the waste rock. The low calcite content is consistent with the results of field, laboratory, and modeling studies (e.g., Stromberg and Banwart 1994) suggesting that calcite becomes depleted within a few years. The sulfide minerals include pyrite as the most abundant sulfide, and pyrrhotite and chalcopyrite along with traces of sphalerite, galena and molybdenite. The sequential extraction results indicate the presence of both primary (42%) and supergene (39%) material, but no supergene S minerals were identified in the QEMSCAN. The step 1 extract contained 3.4% of the total S, which is in fair agreement with the sulfate sulfur analyses. The major cation-forming elements extracted in step 1 were K, Al, Fe, and Ca, along with Cu and Zn and some other trace elements. This suggests that some soluble salts may be present despite not being identified by QEMSCAN. In extraction steps 2, 3 and 4, some Al, K and Mg were solubilized in addition to Fe and S, indicating that minerals other than those discussed above may have dissolved during these extractions, such as clays, gibbsite and Al-sulfate-minerals, and/or possibly other silicates such as chlorite (see section 1.2.1).

Based on the sequential extractions, both Cu and Zn in the waste rock were predominantly associated with the sulfide fractions, which held 90% and 55% of the total Cu and Zn,

respectively. Copper was also detected in the step 1 (1.7% of Cu), 2 (3.6%), and 3 (0.8%) extracts, while Zn was detected in all four extracts (2.8% in step 1, 3.2% in step 2, 3.2% in step 2, and 6.4% in step 4). Therefore, the most soluble fractions, i.e. the water soluble (step 1) and exchangeable (step 2) fractions, have appreciable contents of both metals, as do the Fe(III) minerals (step 3 and 4). It should however be noted that Zn is more abundant in the more crystalline phases (represented by the step 4 extracts) than Cu. Like Zn, Mn is found in the step 1-4 extracts and is more abundant in the step 4 extract than the other three. However, it predominantly occurs in the silicate fraction.

These results suggest that the Fe, Al, Cu, Mn, and Zn associated with sequential extraction step 3 may remobilize as O_2 levels fall (Table 4). However, since a majority of the S, Cu, and Zn, together with a significant fraction of the Fe remain associated with sulfides, water quality may improve as a result of the suppression of sulfide oxidation under conditions that limit O_2 availability.

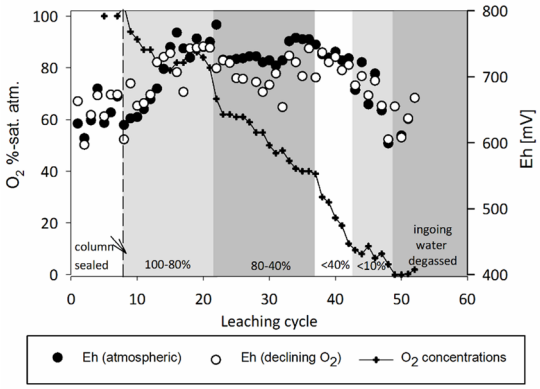

Figure 4.8. Declining O_2 concentrations and the development of anoxic conditions during the experiment using low sulfidic waste rock. The leachate water redox potential (Eh) formed under atmospheric and declining O_2 conditions is similar, and is decoupled from the O_2 concentrations.

Development of anoxic conditions

In the low sulfidic waste rock system, the O_2 concentrations decreased much more slowly than in the highly sulfidic system, and only minor or no decrease occurred before the introduction of inert gas. Inert gas was introduced into the column slowly to avoid missing a possible release of contaminants under declining O_2 conditions, but achieving the anoxic conditions was challenging. The oxygen levels finally fell to <2-3% after 50 leaching cycles, at which point degassing of the incoming MQ water began (Figure 4.8). Therefore, taken as a whole, the experiment demonstrates the effect of gradually reducing the O_2 level from 100 to 0 sat-%.

Leachate chemistry

Leachates originating from partially oxidized low-sulfidic waste rock are characterized by acidic pH values that are typically in the range of 3.1-4.0, and EC in the range of 0.2-0.8 mS/cm (Figure 4.9). According to the SEPA (2000) classifications, the concentrations of Cu, Pb, and Zn in the leachates formed under atmospheric conditions were very high, while those of Cd and Ni were high. This is despite the large particle

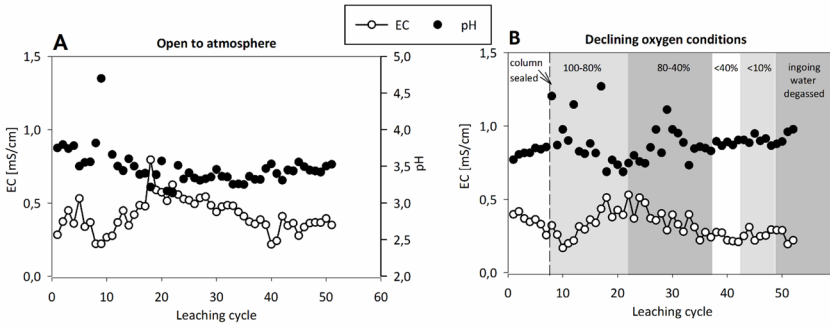

Figure 4.9. EC and pH values of leachates formed from low sulfidic waste rock under atmospheric (A) and declining O_2 conditions (B). The O_2 levels under the declining O_2 conditions are indicated by the background colour (see Figure 4.6).

size (and thus limited surface area) of the tested waste rock and the short contact time between the waste rock and water in these experiments. The leachate also contains some rare earth elements including Ce and La at concentrations of ~1–10 µmol/L. For some elements including Cu and Pb, there appears to have been a difference in overall concentration between the two columns, as indicated by the different concentrations measured during the first 10 weeks of leaching (Figure 4.10). These differences likely arise from the heterogeneous distribution of host minerals such as chalcopyrite and galena in the waste rock and the experimental columns, as well as preferential flow. Therefore, findings relating to these elements (and possibly some others) should be interpreted with care.

Elevated concentrations of several solutes including S and metal(loid)s, occurred during the initial few leaching cycles in both columns. This was attributed to the washing out of pore water that had dried on the material's surface, and the dissolution of soluble salts (e.g., Maest and Nordstrom, 2017; Sapsford et al., 2009). The leachate's pH was relatively stable despite a few outlier values that were clearly higher than the other measurements and are most likely erratic. The leachate formed under atmospheric conditions exhibited a modest decrease in pH from the start of the experiment, reaching a minimum of 3.1 around cycle 20. Its pH then rose slowly to ~3.5. The leachate's EC and solute concentrations exhibited opposing trends: they both increased from minima in cycles 10–11 to maxima in cycles 20–22 before decreasing again. Similar patterns were observed under both experimental conditions. However, in the declining O_2 case, the peak concentrations were reached a few cycles earlier (cycle 18), the element concentrations were somewhat lower overall, and the pH was slightly higher, with a local maximum around cycle 30 (Figure 4.9). The buffering of the pH in this range is thought to be due to the dissolution of Fe and Al (hydr)oxides (Blowes and Ptacek, 1994) together with silicate dissolution and acid production by sulfide oxidation and other processes.

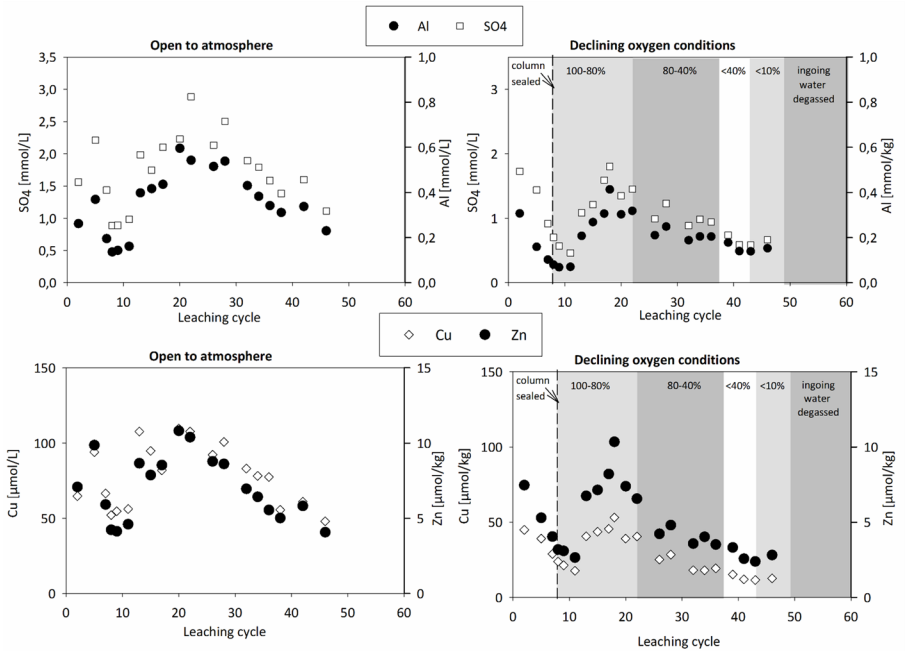

Figure 4.10. Examples of the concentrations of selected elements upon leaching of low sulfidic waste rock under atmospheric and declining O_2 conditions.

Effect of declining O_2 conditions on water quality.

The average release rates (solute release per kg of waste rock per cycle) under the atmospheric and declining O_2 conditions after 30 cycles were compared to assess the effect of declining O_2

levels on leachate quality. An overall improvement was observed, with an increase in leachate pH and a decrease in leachate EC, which is an indicator of overall leachate quality (Figure 4.9). The release rates of S, Fe, Ca, Mg. K, Al, Cd, Co, Mn, Ni, Th, U, Zn were lower under the declining O_2 conditions. However, the magnitude of the decrease differed between elements (Figure 4.11), ranging from over 90% to only 14-15%; it fell in the order Fe>Co>Al>SO4>K>Cd> Ni>Zn>Ca>Mg>Mn>Ce>La. In addition to lower overall release rates, the declining O_2 conditions also yielded lower maximum concentrations of these elements in the leachate.

Copper and Pb were among the elements exhibiting the greatest decreases. However, as discussed above, this may have been partly due to differences in their initial concentrations in the two columns. Therefore, the results for these elements should be interpreted with care.

Despite the overall better leachate quality under declining O_2 conditions and the potential differences between the columns, the leachates' Cu concentrations fall into the very high range according to the SEPA standards (2000), and the Cd, Ni, and Zn concentrations are in the moderately high to high range. Under declining O_2 conditions, the Pb concentrations fell into the low range but remained close to the moderately high range. However, the reliability of the results for this element is unclear because of the initial concentration differences between the columns.

The difficulty of achieving anoxic conditions in the sealed column, which is presumably due to low O_2 consumption, suggests that limited sulfide oxidation occurs in the low sulfide waste rock. However, leaching of this waste rock produces an acidic leachate rich in SO_4, Al, Cu, and Mn, among other ions. Sulfide oxidation is not the only possible source of leachate solutes; other potential sources include the dissolution of silicates and various other minerals such as those solubilized in the sequential extractions (Figure 4.9). For example, dissolved S may originate from the minerals solubilized in sequential extractions steps 1 (water soluble) and 2 (exchangeable), as well as the minor schwertmannite detected in the waste rock (Table 4.4, Figure 4.9), in addition to sulfides. Geochemical calculations also suggested the potential dissolution of gypsum, alunite, and melanterite-type minerals. While these minerals were not observed in association with the waste rock during this study, they often occur in mine environments (see e.g, Bigham and Nordstrom, 2000) and some of them have been associated with Aitik waste rock specifically (O´Kane Consultants, 2015). Moreover, due to the difficulty of detecting secondary minerals present in small quantities in the complex mineralogical matrix of waste rock, their presence cannot be excluded. However, identifying the sources of different solutes is outside the scope of this work;

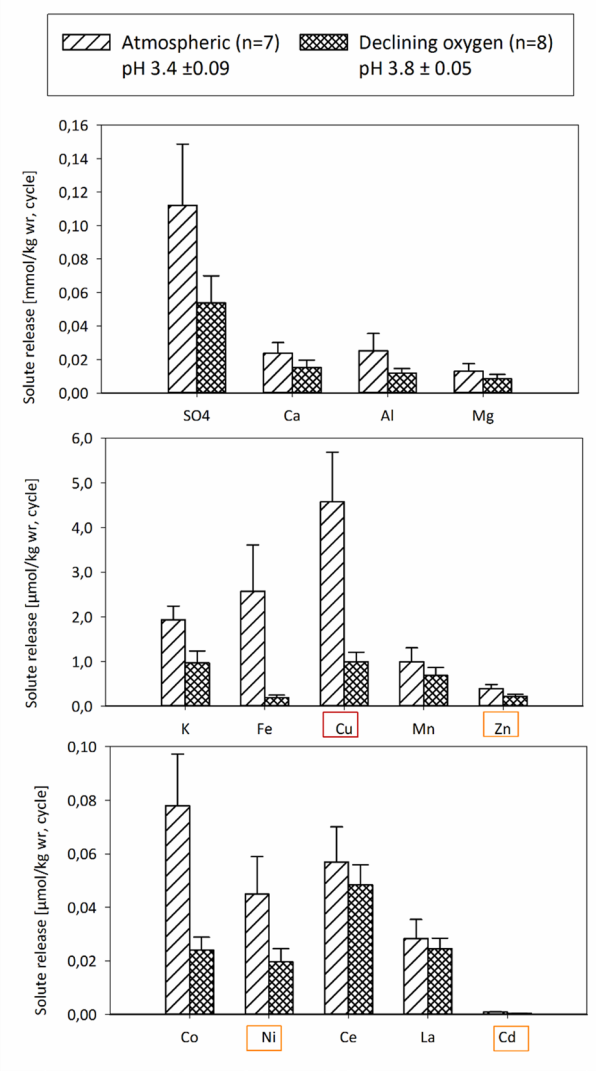

Figure 4.11. Solute release rates from the low sulfidic waste rock under atmospheric and declining O_2 conditions calculated based on the leachate's composition after cycle 30. The average pH and number of samples are given in the top part of the figure. The coloured squares indicate elements for which SEPA (2000) provides concentration standards (red – very high; orange – moderately high to high green – low). The results for Cu should be interpreted with care due to apparent differences in initial

achieving it would require a multielement approach together with a detailed understanding of each element's association with primary and secondary minerals.

A rough calculation of the total mass leached during the year-long experiment together with comparisons to the sequential extraction data (Figure 4.12) revealed that the total leached mass of the studied elements could have originated solely from the washing out of soluble salts

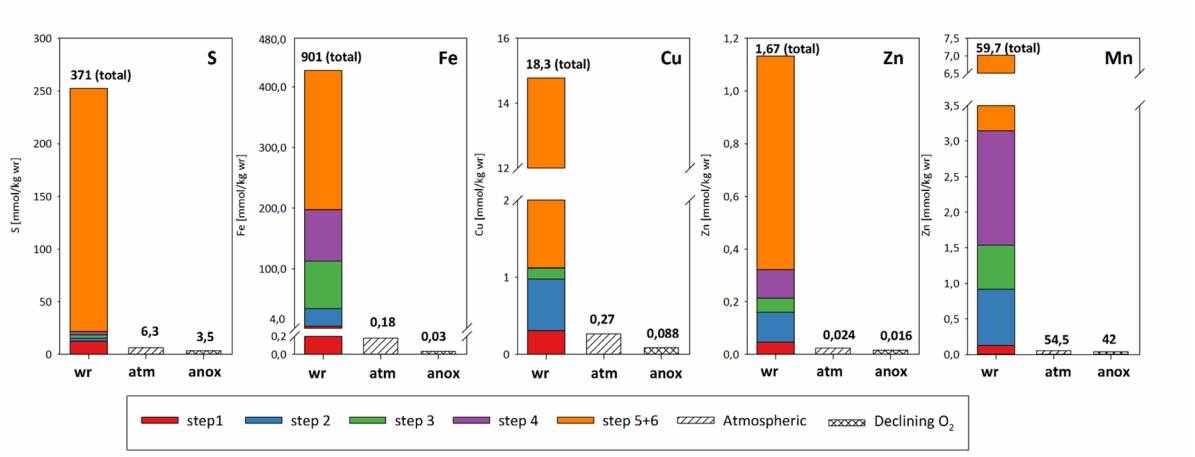

Figure 4.12. Elements solubilized in the sequential extractions, and the estimated total masses of each element leached from the low sulfidic waste rock during the one-year leaching experiment under atmospheric and declining O_2 conditions.

(including dried pore water), possibly together with other sources. The leachates produced under the two experimental conditions exhibited similar compositions, as would be expected if their solute content came primarily from dried pore water and soluble salts. The observed increase in leachate pH and the comparatively low concentrations of elements such as Co, Ni, Cu, and (to a lesser extent) S under the declining O_2 conditions may indicate a lower rate of sulfide oxidation. However, an uneven distribution of sulfide minerals and/or preferential flow causing somewhat different initial concentrations of Cu and Pb could also play a role.

The low concentrations of Fe released to the leachate under declining O_2 conditions suggest that Fe(III) in the waste rock is largely immobile, which is consistent with the leachate pH being in the range 3.5–4. The difference in Fe release between the two columns is consistent with the difference in leachate pH, and geochemical calculations indicate that the leachate formed under atmospheric conditions is supersaturated with respect to Fe(III) (hydr)oxides and hydroxysulfates, while that formed under declining O_2 conditions is supersaturated with respect to Fe(III) hydroxides. Higher leachate pH values create conditions that are more favorable for the adsorption of cationic elements to Fe(III) secondary minerals. In the low sulfidic waste rock, the 12 month leaching process did not include prolonged leaching under low or fully anoxic conditions. Rather, the O_2 concentration was gradually reduced from 100 to 0 %-sat. Therefore, the fate of secondary minerals, including Fe(III) phases, and the associated metal(loid)s under such conditions remains unexplored.

Limitations and future considerations

The experimental setup used in this work was designed to enable monitoring of leachate quality during the leaching of partially oxidized waste rock under unsaturated, free-draining conditions, with different O_2 levels, including anoxic conditions. Accordingly, it differs from standard methods such as those used in humidity cell tests. The approach included leaching of waste rock and monitoring of leachate composition, so the waste rock was irrigated with MQ-water. However, a dry cover on a waste rock dump will both limit O_2 ingress to the waste and also reduce water percolation and thus the transport of solutes from the reaction site. The waste rock particle size used in this study (medium coarse to very coarse gravel) is not optimal for the column size, and was a compromise between material availability and the desire to use uncrushed waste rock particles to avoid exposing fresh surfaces. In the experimental columns, the vertical dimension of transport is much more limited than it would be under field conditions. For these reasons (and others), the contact time between water and waste rock in the experimental system will differ significantly from that in the field.

The waste rock used in the study was chosen based on previous experimental results and its prolonged exposure to weathering (in the case of the low sulfidic waste rock), in order to provide insights into the leaching behavior of partially oxidized waste rock in a changing chemical environment under unsaturated conditions. Upscaling and making mine-scale predictions were not among the study's objectives. Leachate chemistry is governed by complex hydrological-geochemical-microbiological interactions that cannot be fully reproduced in the laboratory. Experimental studies can, however, address specific questions such as some raised during this study. One such question concerns the relationship between particle size, the mass of secondary minerals, and their effect on leachate quality in changing chemical environments. The finest particles, which have the highest specific surface area, are considered to be the most reactive size fraction in waste rock dumps (Langman et al., 2015; Strömberg and Banwart, 1999c), and the formation of secondary minerals on particle surfaces implies that smaller particles may accumulate higher relative quantities of secondary minerals. This possibility could be tested systematically using experiments of the sort presented here. However, the field scale transport of solutes and the precipitation of secondary minerals in waste rock dumps remains largely unexplored and poorly understood, particularly at high altitudes where freeze-thaw cycles have significant effects (e.g., Langman et al., 2017).

This work included experiments lasting for 15 months at most, 12 of which were performed under limited O_2 conditions. As such, it can only provide a short time lapse picture of the leaching behavior of partially oxidized waste rock. In the case of low-sulfidic waste rock, only declining O_2 conditions were examined in detail, and the water quality under limited O_2 conditions and fully anoxic conditions were not studied. However, in both cases, the O_2 concentration was clearly decoupled from the Eh (determined using a Pt-electrode), which remained high throughout the experiment and is assumed to be governed by interactions with aqueous Fe species. The low Fe mobility observed during these experiments indicates limited availability of aqueous Fe(III), which is an effective oxidant of pyrite, and suggests that the accumulation of Fe(III) minerals may be enhanced under anoxic conditions. However, the small amounts of O_2 entering the experimental system may have influenced these results. Moreover, it is not clear to what extent Fe was mobilized and then re-precipitated, where in the system that may have occurred, and if or how such a process would occur in the field. While this study

cannot address these issues, the results obtained do highlight some questions relating to water quality that should be examined in future. In particular, there is a need to characterize the evolution of the redox conditions associated with partially weathered waste rock, and to determine how the intensity of anoxic or reducing conditions affects leachate composition. The identity of the Fe(III) minerals should also be determined because of the high resistance to environmental change (i.e. changes in pH and redox conditions) of crystalline Fe(III) hydroxides such as goethite, which are proposed to form under anoxic conditions and are associated with highly sulfidic waste rock. This is also important for overall risk assessments of potential remediation methods. Organic amendments may be desirable to promote anoxic conditions, but intensely reducing conditions may not be beneficial for water quality if they destabilize Fe(III) phases. For example, increased Fe and As mobility has been observed in tailings covered with biosolids or amended with organic material (Lindsay et al., 2011; Paktunc, 2013), while covering tailings with a low-organic cover did not produce reducing conditions in a recent experiment, and As was not mobilized (DeSisto et al., 2017).

To evaluate the effect of secondary mineral dissolution and transformations of leachate quality, it is critical to gain reliable information on the identity and the quantity of different minerals in the waste rock, and on the metal(oid)s associated with each mineral. Sequential extractions provide rough insights into the quantity and stability of these minerals and the associated metal(loid)s under changing chemical conditions, but rely on aggressive chemical treatment to fully solubilize each fraction. In the field, where less extreme conditions prevail, the solubilization of the different fractions may be incomplete. While several studies have addressed the stability and transformation of, e.g., Fe(III) minerals such as schwertmannite both experimentally and in the field, most such works have focused on pure minerals formed in the drainage environment or settings other than waste rock dumps (such as acid sulfate soils, sediments with high organic content, and water-saturated systems). Therefore, other methods such as the column experiments presented here can provide complementary information on metal(loid) leachability under more relevant conditions.

Here we have presented an experimental approach for studying these interactions in waste rock under unsaturated conditions. This method could be used to systematically study particles of different sizes and the relative importance of secondary minerals in a waste rock, their behavior under systematically controlled and forced O_2 conditions, and their response to floating conditions. However, a key unaddressed challenge is to translate and upscale laboratory experiments so as to make their results applicable in real-world waste dumps featuring complex hydrological-geochemical-microbiological interactions.

4.4. Conclusions

The aim of this study was to assess the impact of anoxic conditions on the release of sulfur, metals, and metalloids from partially oxidized waste rock. To this end, waste rock samples with low (1%) and high (20%) sulfide contents were leached in undersaturated column experiments under atmospheric conditions and under declining and limited O_2 conditions.

The main findings obtained for partially oxidized highly sulfidic waste rock were that:

Anoxic conditions were quickly achieved after sealing the column, and any O_2 entering the column was quickly consumed, presumably by sulfide oxidation.

Despite a limited increase in pH, the leachate remained acidic (pH ~3) after a year of leaching with O_2 availability similar to that expected under a cover system. The properties of the leachate from the partially oxidized waste rock clearly improved under the limited O_2 conditions because the release of solutes from the waste rock was reduced, probably because of a reduced sulfide oxidation rate. Despite this improvement, the concentrations of several metal(loid)s in the leachate are high according to classification by SEPA (2000).

The concentrations of As, Cu, and (to lesser extents) Al, Pb, Mn, Zn peaked under the declining O_2 conditions. Their peak concentrations persisted only briefly (for a few cycles) and were generally lower than the maximum concentrations produced under atmospheric conditions, so the negative impact of the declining O_2 conditions was considered to be limited.

The magnitude of the reduction in the release of solutes under the declining O_2 conditions varied between elements. However, the reductions were generally consistent with previous observations on the associations between trace elements, secondary minerals, and the initial waste rock. Arsenic was the element whose release was most significantly reduced (99%), and also exhibited the clearest mobilization under declining O2 conditions. Additionally, anoxic conditions resulted in low Fe availability, and particularly low Fe(III) availability.

Schwertmannite dissolution appears to buffer the SO_4 concentrations and helps to maintain acidic pH (~3), possibly together with sulfide oxidation.

The main findings relating to partially oxidized low sulfidic waste rock were:

Oxygen concentrations decreased very slowly and exhibited only negligible or minor reductions in the absence of inert gas treatment, suggesting limited consumption of O_2 by sulfide oxidation. Because of this, the results of the experiment illustrate the effects of gradually reducing the O_2 concentration from 100 to <1 %-sat. Similar difficulties with achieving truly anoxic conditions may also occur under field conditions.

Acidic (pH~3.1-4.0) leachates with elevated levels of SO_4, Al, Cu, Zn, and other solutes are formed under both atmospheric and declining O2 conditions.

The solubilization of key elements (including S, Fe, Cu, and Zn) during the one-year experiment can be explained entirely by the dissolution of the water-soluble fraction (which consists of readily soluble minerals and dried pore water) extracted from the waste rock in step 1 of the sequential extraction process.

The quality of the leachate formed under declining O2 conditions during the final months of the year-long experiment was superior to that of the leachate formed under atmospheric conditions. The low oxygen conditions increased the leachate pH from 3.4 to 3.8 while reducing the release rates of solutes such as Fe, Co, Al, SO4, Cd, Ni, Zn. The most likely reason for this is decreased sulfide oxidation and the resulting increase in pH.

The release of Cu and Pb was also suggested to decrease significantly. However, the overall concentration level differed between the two columns at the start, in particular for Pb, and these elements need to be interpreted with care.

Despite the decreases in concentrations, Cu, Cd, Ni and Zn remain at moderately to very high level according to SEPA (2000).

4.5. References

Abraitis, P.K., Pattrick, R.A.D., Vaughan, D.J. (2004) Variations in the compositional, textural and electrical properties of natural pyrite: a review. International Journal of Mineral Processsing 74, 41-59.

Acero, P., Ayora, C., Torrentó, C., Nieto, J-M. (2006) The behavior of trace elements during schwertmannite precipitation and subsequent transformation into goethite and jarosite. Geochimica et Cosmochimica Acta 70, 4130-4139.

Alakangas, L., Andersson, E., Mueller, S. (2013). Neutralization/prevention of acid rock drainage using mixtures of alkaline by-products and sulfidic mine wastes. Environ Sci Pollut Res 20, 7909-7916.

Amos, R.T., Blowes, D:W., Bailey, B.L., Sego, D.C., Smith, L., Ritchie, A.I.M. (2015) Waste-rock hydrogeology and geochemistry. Applied Geochemistry 57, 140-156.

Bailey, B., L., Blowes, D.W., Smith, L., Sego, D.C. (2015). The Diavik waste rock project: geochemical and microbiological characterization of drainage from low –sulfide waste rcok: active zone field experiments. Applied Geochemistry 62, 18-34.

Arshad, M.A., Arnaud, P.J., St., Huang, P.M. (1972) Dissolution of trioctahedral layer silicates by ammonium oxalate, sodium dithionite-citrate-bicarbonate, and potassium phyrophospate. Canadian Journal of Soil Science 52, 19-26.

Ball, J.W., Nordstrom, D.K. (1991) User´s manual for WATEQ4F with revised thermodynamic data base and test cases for calculating speciation of major, trace and redox elements in natural waters. Pp. 91-183, 189. U.S. Geological Survey Open-file report.

Bigham, J.M., Nordstrom, D.K. (2000) Iron and aluminum hydroxysulfates from acid sulfate waters. In Alpers, C.N, Jambor, J.L., Nordstrom, D.K. (Eds) Sulfate minerals: Crystallography, geochemistry, and environmental significance. Reviews in Mineralogy and Geochemistry 40, 351-403.

Bigham, J.M., Schwertmann, U., Traina, S.J., Winland, R.L., Wolf, M. (1996a) Schwertmannite and the chemical modeling of iron in acid sulfate waters. Geochim. Cosmochim. Acta 60, 2111-2121.

Bigham, J.M., Schwertmann, U., Pfab, G. (1996b) Influence of pH on mineral speciation in a bioreactor simulating acid mine drainage. Applied Geochemistry 11, 845-849.

Burton, E.D., Bush, R.T., Sullivan, L.A., Mitchell, D.R.G. (2008) Schwertmannite transformation to goethite via the Fe(II) pathway: reaction rates and implications for iron-sulfide formation 72, 4551-4564.

DeSisto, S.L., Jamieson, H.E., Parsons, M.B. (2017) Arsenic mobility in weathered gold mine tailings under a low-organic soil cover. Environmental Earth Science 76, 773.

Dold, B. (2003) Speciation of the most soluble phases in sequential extraction procedure adapted for geochemical studies of copper sulfide mine waste. Journal of Geochemical Exploration 80, 55–68.

Eriksson, N., Destouni, G. (1997a) Combined effects of dissolution kinetics, secondary mineral precipitation, and preferential flow on copper leaching from mining waste rock. Water Resources Research 33, 471–483.

Eriksson, N., Gupta, A., Destouni, G. (1997b) Comparative analysis of laboratory and field tracer tests for investigating preferential flow and transport in mining waste rock. Journal of Hydrology194, 143–163.

Langman, J.B., Blowes, D.W., Sinclair, S.A., Krentz, A., Amos, R.T., Smith, L., Pham, H.N., Sego, D.C., Smith, L. (2015) Early evolution of weathering and sulfide depletion of a low-sulfur, granitic, waste rock in an Arctic climate: a laboratory and field site comparison. Journal of Geochemical Exploration 156, 61–71.

Langman, J.B., Blowes, D.W., Amos, R.T., Atherton, C., Wilson, D., Smith, L., Sego, D.C., Sinclair, S.A. (2017) Influence of a tundra freeze–thaw cycle on sulfide oxidation and metal leaching in a low sulfur, granitic waste rock. Applied Geochemistry 76, 9–21.

Kaasalainen, H., Lundberg, P., Aiglsperger, T., Alakangas, L. (2019) Impact of declining oxygen conditions on metal(loid) release from partially oxidized waste rock. Environ Sci Pollut Res. https://doi.org/10.1007/s11356-019-05115-z

Kawano M. and Tomita K. (2001) Geochemical modeling of bacterially induced mineralization of schwertmannite and jarosite in sulfuric acid spring water. Am. Miner. 86, 1156–1165.

Lee, G., Bigham, J.M., Faure, G. (2002) Removal of trace metals by coprecipitation with Fe, Al and Mn from natural waters contaminated with acid mine drainage in the Ductown Mining District, Tennessee. Appl. Geochem. 17, 569–581.

Maest, A., Nordstrom, D.K. (2017) A geochemical examination of humidity cell tests. Applied Geochemistry 81, 109–131.

Majzlan, J., Navrotsky, A., Schwertmann, U. (2004) Thermodynamics of iron oxides: Part III. Enthalpies of formation and stability of ferrihydrite (~$Fe(OH)_3$), schwertmannite (~$FeO(OH)_{3/4}(SO_4)_{1/8}$), and ε-$Fe_2O_3$. Geochim. Cosmochim. Acta 68, 1049–1059.

Moncur, M.C., Jambor, J.L., Ptacek, C.J., Blowes, D.W. (2009) Mine drainage from the weathering of sulfide minerals and magnetite. Applied Geochemistry 24, 2362–2373.

Montelius, C. (2005). The genetic relationship between rhyolitic volcanism and Zn-Cu-Au deposits in the Maurliden volcanic centre, Skellefte district, Sweden : volcanic facies, lithogeochemistry and geochronology. Doctoral thesis, Luleå tekniska universitet, p. 15.

Nagano, T., Yanase, N., Hanzawa, Y., Takada, M., Mitamure, H., Sato, T., Naganawa, H. (2011) Evaluation of the affinity of some toxic elements to schwertmannite in natural streams contaminated with acid mine drainage. Water Air Soil Pollut 216, 153–166.

Nyström, E., Kaasalainen, H., Alakangas, L. (2019) Prevention of sulfide oxidation in waste rock by the addition of lime kiln dust. Environ Sci Pollut Res. https://doi.org/10.1007/s11356-019-05846-z

O´Kane Consultants Inc (2015) Aitik Mine Closure project waste rock storage facility: cover system design, prediction of geochemistry and discharge water quality. Report prepared for Boliden, nro 771/9-01.

Paktunc, D. (2013) Mobilization of arsenic from mine tailings through reductive dissolution of goethite influenced by organic cover. Applied Geochemistry 36, 49-56.

Parkhurst, D.L., Appelo, C.A.J. (1999) User´s guide to PHREEQC (Version 2) – A computer program for speciation, batch-reaction, one-dimensional transport, and inverse geochemical calculations pp. 99-4259. U.S. Geological Survey Water-Resour. Invest. Rep, Denver Colorado.

Sapsford, D. J., Bowell, R.J., Dey, M., Williams, K.P. (2009) Humidity cell tests for the prediction of acid rock drainage. Minerals Engineering 22, 25-36.

Schwertmann, U., Friedl, J., Stanjek, H. (1999) From Fe(II) to Ferrihydrite and then to hematite. Journal of Colloid and Interface Science 209, 215-223.

Sidenko, N.V., Sherriff, B.L. (2005) The attenuation of Ni, Zn and Cu by secondary Fe phases of different crystallinity from surface and ground water of two sulfide mine tailings in Manitoba, Canada. Appl. Geochim. 20, 1180-194.

Simms, P.H., Yanful, E.K., St-Arnaud, L., Aubé, B. (2000) A laboratory evaluation of metal release and transport in flooded pre-oxidized mine tailings. Applied Geochemistry 15, 1245-1263.

Sracek, O., Choquette, M., Gélinas, P., Lefebvre, R., Nicholson, R.V (2004) Geochemical characterization of acid mine drainage from a waste rock pile, Mine Doyon, Québec, Canada. Journal of Contaminant Hydrology 69, 45-71.

Stefánsson, A. (2007) Iron(III) hydrolysis and solubility. Environ. Sci. Technol. 41, 6117-6123.

Stockwell, J., Smith, L., Jambor, J.L., Beckie, R. (2006) The relationship between fluid flow and mineral weathering in heterogeneous unsaturated porous media: a physical and geochemical characterization of waste rock pile. Applied Geochemistry 21, 1347-1361.

Stookey, L.L. (1970) Ferrozine – a new spectrophotometric reagent for iron. Analytical Chemistry 42, 779-781.

Strömberg, B., Banwart, S.A. (1994) Kinetic modelling of geochemical processes at the Aitik mining waste rock site in northern Sweden. Applied Geochemistry 9, 583-595.

Strömberg, B., Banwart, S.A. (1999a) Experimental study of acidity-consuming processes in mining waste rock: some influences of mineralogy and particle size. Applied Geochemistry 14, 1-16.

Strömberg, B., Banwart, S.A. (1999b)Weathering kinetics of waste rock from the Aitik copper mine, Sweden: scale dependent rate factors and pH controls in large column experiments. Journal of Contaminant Hydrology 39, 59-89.

Strömberg, B., Banwart, S.A. (1999c) Experimental study of acidity-consuming processes in mining waste rock: some influences of mineralogy and particle size. Applied Geochemistry 14, 1-16.

Swedish Agency for Marine and Water Management ((HVMFS) (2013) Havs- och vattenymyndighetens föreskrifter om klassificering och miljökvalitestnormer avseende ytvatten (in Swedish). HVMFS2013:19. https://www.havochvatten.se/hav/vagledning--lagar/foreskrifter/register-vattenforvaltning/klassificering-och-miljokvalitetsnormer-avseende-ytvatten-hvmfs-201319.html (accessed 16th April 2018)

Swedish Geological Survey (2017). Bergverksstatistik 2016. Statistics of the Swedish Mining Industry 2016). Periodiska publikationer 2017:1. (http://resource.sgu.se/produkter/pp/pp2017-1-rapport.pdf (accessed 13th March.2018).

Swedish Environmental Protection Agency, SEPA (2000). Environmental quality criteria – lakes and watercourses. Report 5050. Kalmar, Sweden. Lenanders.

To, T.B., Nordstrom, D.K., Cunningham, K.W., Ball, J.W., McCleskey, R.B. (1999) New method for the direct determination of dissolved Fe(III) concentration in acid mine waters. Environ. Sci. Technol., 33, 807-813.

Yu J.-Y., Heo B., Choi I.-K., Cho J.-P., and Chang H.-W. (1999) Apparent solubilities of schwertmannite and ferrihydrite in natural stream waters polluted by mine drainage. Geochim. Cosmochim. Acta **63,** 3407–3416.

Acknowledgements

Boliden Mineral AB is thanked for their collaboration and support for the project, including supplying the waste rocks for the present study. Dr. Thomas Aiglsperger is thanked for his help with secondary minerals, Lina Hällström for optical microscope images and Paula Lundberg and Lovisa Renberg for their contributions in setting up and running the experiments and water sampling and analyses.

5. PUBLICATIONS WITHIN STOPOX PROJECT

5.1. Peer-reviewed journal articles

Kaasalainen, H., Lundberg, P., Aiglsperger, T., Alakangas, L. (2019) Impact of declining oxygen conditions on metal(loid) release from partially oxidized waste rock. Environ Sci Pollut Res. https://doi.org/10.1007/s11356-019-05115-z

Nyström, E., Kaasalainen, H., Alakangas, L. (2019) Suitability study of secondary raw materials for prevention of acid rock drainage generation from waste rock. J Clean Prod. https://doi.org/10.1016/j.jclepro.2019.05.130

Nyström, E., Kaasalainen, H., Alakangas, L. (2019) Prevention of sulfide oxidation in waste rock by the addition of lime kiln dust. Environ Sci Pollut Res. https://doi.org/10.1007/s11356-019-05846-z

5.2. Peer-reviewed conference proceedings:

Nyström, E., Kaasalainen, H., Alakangas, L. (2017) Prevention of sulfide oxidation in waste rock using by-products and industrial remnants: A suitability study. Paper presented at the 13th International Mine Water Association Congress – "Mine Water & Circular Economy – A Green Congress", Lappeenranta, Finland, 25-30 June 2017. 1170-1178

5.3. Peer-reviewed conference abstracts:

Nyström, E., Alakangas, L. (2015) Prevention of sulfide oxidation in sulfide-rich waste rock. Abstract presented at the European Geosciences Union - General Assembly 2015, Vienna, Austria, 12-17 April 2015.

Nyström, E., Alakangas, L. (2019) The occurrence of As, Hg, Sb and Tl in pyritic waste rock and the ability to prevent their release. Abstract presented at the Goldschmidt Conference 2019, Barcelona, Spain, 18-23 August 2019.

5.4. Abstracts and presentations

Kaasalainen, H. (2018) Sulfur and metal mobility in dynamic aqueous environments. Keynote presentation in AURA Symposium, University of Turku & Åbo Akademi, Turku, Finland, 24-26 April, 2018.

Kaasalainen, H. (2016) Weathered waste rock under changing chemical conditions: metal(loid) mobility. Presentation in the WELCAMM workshop by Luleå University of Technology Centre of Advanced Mining and Metallurgy (CAMM), October 2016.

5.5. Theses

Nigéus, S. (2018) Green liquor dregs-amended till to cover sulfidic mine waste (licentiate thesis), Luleå, Sweden. Retrieved from http://ltu.diva-portal.org/smash/record.jsf?pid=diva2%3A1204180&dswid=7226

Nyström, E. (2018) Suitability of Industrial Residues for Preventing Acid Rock Drainage Generation from Waste Rock (licentiate thesis), Luleå, Sweden. Retrieved from http://ltu.diva-portal.org/smash/record.jsf?pid=diva2%3A1200782&dswid=7226

Lundberg, P. (2017) Geochemical processes in mine waste subjected to a changing chemical environment: Fe speciation in leachate water from column experiments. Degree project, Natural Resources Engineering, Luleå University of Technology.